EFFECTS OF AEROSOLS ON THE TROPOSPHERIC GAS-PHASE REACTIONS OF THE HYDROXYL RADICAL WITH ORGANIC COMPOUNDS

By

SE WON OH

A DISSERTATION PRESENTED TO THE GRADUATE SCHOOL
OF THE UNIVERSITY OF FLORIDA IN PARTIAL FULFILLMENT
OF THE REQUIREMENTS FOR THE DEGREE OF
DOCTOR OF PHILOSOPHY

UNIVERSITY OF FLORIDA

2001

ACKNOWLEDGMENTS

I would like to express my sincere appreciation and gratitude to Dr. Jean M. Andino, my advisor and the chairperson of my supervisory committee, for her invaluable guidance, support, and inspiration throughout the course of this research. I also would like to thank Dr. Dale A. Lundgren, Dr. Brij M. Moudgil, Dr. Chang-Yu Wu, and Dr. Matthew M. Booth for their interest and guidance and for residing on my supervisory committee.

I express my gratitude to my fellow air pollution graduate students for their assistance.

I would like to thank the National Science Foundation for its financial support to perform this research.

Finally, I sincerely thank my parents and my wife, Hyunjoo Chae, for their support and encouragement.

TABLE OF CONTENTS

page

ACKNOWLEDGMENTS ii

LIST OF TABLES v

LIST OF FIGURES vi

ABSTRACT ix

CHAPTERS

1 INTRODUCTION 1

2 EXPERIMENTAL SYSTEM 10

System Description 10
Aerosol Loss Studies 16
Organic Reactant Loss Studies 31

3 EFFECTS OF AMMONIUM SULFATE AEROSOLS ON THE GAS-PHASE REACTIONS OF THE HYDROXYL RADICAL WITH ORGANIC COMPOUNDS 33

Background 33
Experimental Methods 33
  Purely Gas-Phase Study 36
  Study in the Presence of Aerosols 37
Results and Discussion 43
  Reactions in the Absence of Aerosols 43
  Reactions in the Presence of Aerosols 47
  Implications for Tropospheric Chemistry Modeling 48

4 EFFECTS OF AMMONIUM SULFATE AEROSOLS ON THE GAS-PHASE REACTIONS OF THE HYDROXYL RADICAL WITH C_1-C_6 ALIPHATIC ALCOHOLS 51

Background 51
Experimental Methods 52
  Ethanol, 1-Butanol, 1-Pentanol and 1-Hexanol Study 54

Methanol Study 56
Results and Discussion 58
Reactions in the Absence of Aerosols 58
Reactions in the Presence of Aerosols 68
Discussion 69

5 EFFECTS OF AEROSOL COMPOSITION ON THE ·OH RATE CONSTANT OF A SELECTED ALCOHOL 73

Background 73
Experimental Methods 74
Results and Discussion 75
Reactions in the Presence of Aerosols 75
Implications for Tropospheric Chemistry 90

6 EFFECTS OF INORGAINIC AEROSOLS ON THE GAS-PHASE REACTIONS OF THE HYDROXYL RADICAL WITH SELECTED ALIPHATIC ALKANES 92

Background 92
Experimental Methods 93
Results and Discussions 95
Reactions in the Absence of Aerosols 95
Reactions in the Presence of Aerosols 106

7 CONCLUSIONS AND RECOMMENDATIONS 110

APPENDICES

A CALIBRATIONS 115

Calibrations of Gas Flow Rate Measuring Devices 115
GC-MS Calibrations 119

B CHROMATOGRAMS 133

C EXPERIMENTAL PROCEDURES 148

Methyl Nitrite Synthesis 148
Kinetic Study 151

LIST OF REFERENCES 155

BIOGRAPHICAL SKETCH 161

LIST OF TABLES

Table Page

1-1. Typical concentrations of tropospheric aerosols. 6

1-2. Typical compositions of tropospheric aerosols. 8

1-3. Mean concentrations and percents of species groups for overall summer and fall surface data from the Southern California Air Quality Study....9

2-1. Distribution of charge on aerosol particles at Boltzmann Equilibrium. 15

2-2. Normalized number concentrations of particles as a function of time ($N(t)/N_o$) due to deposition losses for monodisperse particles. 25

2-3. Aerosol concentrations in the Tedlar® bag as a function of time. 31

4-1. Initial aerosol characteristics in the bag for aerosol conditions I and II. 56

4-2. Relative rates (k_s/k_r) for the reactions of OH radical with aliphatic alcohols in the absence and presence of aerosols....64

4-3. Gas-phase relative rates (k_s/k_r) and rate constant (k_s) for the reactions of OH radical with aliphatic alcohols and p-xylene. 66

5-1. Relative rates of the 1-propanol/$^\cdot$OH reaction versus the p-xylene/$^\cdot$OH reaction in the absence and presence of aerosols. 81

5-2. Rate constants and disappearance rates of the organics in the system for the organics/$^\cdot$OH reactions and the organics/Cl reaction. 84

6-1. Gas-phase relative rates (k_s/k_r) and rate constant (k_s) for the reactions of OH radical with the alkanes using p-xylene as a reference compound. 105

6-2. Relative rates of the alkane/$^\cdot$OH reactions versus the p-xylene/$^\cdot$OH reaction in the absence and presence of aerosols. 107

LIST OF FIGURES

Figure Page

1-1. Typical aerosol size distributions in an urban area. 7

2-1. Schematic of the experimental apparatus. 11

2-2. Spectral distribution of a typical black lamp. 12

2-3. A schematic of a Collison atomizer. 14

2-4. Normalized number concentrations of particles as a function of time due to coagulation for monodisperse particles. 19

2-5. Normalized number concentrations of particles as a function of time ($N(t)/N_o$) by deposition for monodisperse particles. 27

2-6. Size distributions of the aerosols in the bag at different times. 28

3-1. Size distributions of the aerosols in the bag. (A) Number (B) Surface area (C) Volume 39

3-2. Plots of $\ln[(Reactant_1)_o/(Reactant_1)_t]$ vs. $\ln[(Reactant_2)_o/(Reactant_2)_t]$ in the absence of aerosols (○: in the absence of NO, □: in the presence of NO) and the presence of $(NH_4)_2SO_4$ aerosols (●: in the absence of NO, ■: in the presence of NO) 44

3-3. Estimated ozone concentrations obtained from the atmospheric reactions of 1-propanol using the recommended rate constant (······) and the new rate constant (——) of the 1-propanol/OH radical reaction. 50

4-1. Surface area distributions of the aerosols in the bag. 57

4-2. Plots of $\ln[(Reactant)_o/(Reactant)_t]$ vs. $\ln[(p\text{-}Xylene)_o/(p\text{-}Xylene)_t]$ in the absence of aerosols (○: 1-butanol, ●: 1-pentanol) and the presence of $(NH_4)_2SO_4$ aerosols (□: Aerosol Condition I, △: Aerosol Condition II for 1-butanol and ■: Aerosol Condition I, ▲: Aerosol Condition II for 1-pentanol). 60

4-3. Plots of $\ln[(1\text{-}Hexanol)_0/(1\text{-}Hexanol)_t]$ vs. $\ln[(p\text{-}Xylene)_0/(p\text{-}Xylene)_t]$ in the absence of aerosols (□) and the presence of $(NH_4)_2SO_4$ aerosols (■:Aerosol Condition I, ▲: Aerosol Condition II). 61

4-4. Plots of $\ln[(Ethanol)_0/(Ethanol)_t]$ vs. $\ln[(p\text{-}Xylene)_0/(p\text{-}Xylene)_t]$ in the absence of aerosols (□) and the presence of $(NH_4)_2SO_4$ aerosols (■:Aerosol Condition I, ▲: Aerosol Condition II). 62

4-5. Plots of $\ln[(Methanol)_0/(Methanol)_t]$ vs. $\ln[(Ethanol)_0/(Ethanol)_t]$ in the absence of aerosols (□) and the presence of $(NH_4)_2SO_4$ aerosols (■:Aerosol Condition I, ▲: Aerosol Condition II). 63

4-6. Plots of $\ln[(Reference)_0/(Reference)_t]$ vs. $\ln[(p\text{-}Xylene)_0/(p\text{-}Xylene)_t]$ in the absence of aerosols using n-octane as a reference compound (□) and cyclohexane as a reference compound (●). 65

5-1. Plots of $\ln[(1\text{-}Propanol)_0/(1\text{-}Propanol)_t]$ vs. $\ln[(p\text{-}Xylene)_0/(p\text{-}Xylene)_t]$ in the absence of aerosols (○) and the presence aerosols (■:Aerosol Condition I, ▲: Aerosol Condition II). 77

5-2. Schematic of the reactions at the surface of NaCl aerosols. 82

5-3. Plots of $\ln[(1\text{-}Propanol)_0/(1\text{-}Propanol)_t]$ vs. $\ln[(p\text{-}Xylene)_0/(p\text{-}Xylene)_t]$ for the 1-propanol / p-xylene / CH_3ONO system (○) and 1-propanol / p-xylene / CH_3ONO / NH_3 system(■). 89

6-1. Plots of $\ln[(Reactant)_0/(Reactant)_t]$ vs. $\ln[(p\text{-}Xylene)_0/(p\text{-}Xylene)_t]$ in the absence of aerosols (○: n-butane, □: n-pentane) and the presence of aerosols (●: Aerosol Condition I, ▲: Aerosol Condition II for n-butane and ■: Aerosol Condition I, ◆: Aerosol Condition II for n-pentane). 96

6-2. Plots of $\ln[(Reactant)_0/(Reactant)_t]$ vs. $\ln[(p\text{-}Xylene)_0/(p\text{-}Xylene)_t]$ in the absence of aerosols (○: n-octane, □: n-decane) and the presence of aerosols (●: Aerosol Condition I, ▲: Aerosol Condition II for n-octane and ■: Aerosol Condition I, ◆: Aerosol Condition II for n-decane). 99

6-3. Plots of $\ln[(n\text{-}Hexane)_0/(n\text{-}Hexane)_t]$ vs. $\ln[(p\text{-}Xylene)_0/(p\text{-}Xylene)_t]$ in the absence of aerosols (○) and the presence of aerosols (■: Aerosol Condition I, ▲: Aerosol Condition II). 102

A-1. Calibration curve of the rotameter. 116

A-2. Calibration curve of the orifice meter. 118

A-3. GC-MS calibration curve for methanol. 120

A-4. GC-MS calibration curve for ethanol. 121

A-5. GC-MS calibration curve for 1-propanol.....122

A-6. GC-MS calibration curve for 1-butanol.....123

A-7. GC-MS calibration curve for 1-pentanol.....124

A-8. GC-MS calibration curve for 1-hexanol.....125

A-9. GC-MS calibration curve for n-butane.....126

A-10. GC-MS calibration curve for n-pentane.....127

A-11. GC-MS calibration curve for n-hexane.....128

A-12. GC-MS calibration curve for n-octane.....129

A-13. GC-MS calibration curve for n-decane.....130

A-14. GC-MS calibration curve for p-xylene.....131

A-15. GC-MS calibration curve for cyclohexane.....132

B-1. Typical chromatograms of samples from a bag containing a mixture of 1-propanol / n-hexane / p-xylene / methyl nitrite.....134

B-2. Typical chromatograms of samples from a bag containing a mixture of ethanol / p-xylene / methyl nitrite.....136

B-3. Typical chromatograms of samples from a bag containing a mixture of 1-butanol / 1-pentanol / p-xylene / methyl nitrite.....138

B-4. Typical chromatograms of samples from a bag containing a mixture of 1-hexanol / p-xylene / methyl nitrite.....140

B-5. Typical chromatograms of samples from a bag containing a mixture of methanol / ethanol / methyl nitrite.....142

B-6. Typical chromatograms of samples from a bag containing a mixture of n-butane / n-pentane / p-xylene / methyl nitrite.....144

B-7. Typical chromatograms of samples from a bag containing a mixture of n-octane / n-decane / p-xylene / methyl nitrite.....146

C-1. Schematic of the apparatus used to synthesize methyl nitrite.....149

C-2. Schematic diagram of the glass manifold system.....151

Abstract of Dissertation Presented to the Graduate School
of the University of Florida in Partial Fulfillment of the
Requirements for the Degree of Doctor of Philosophy

EFFECTS OF AEROSOLS ON THE TROPOSPHERIC GAS-PHASE REACTIONS OF THE HYDROXYL RADICAL WITH ORGANIC COMPOUNDS

By

Se Won Oh

May 2001

Chairperson: Jean M. Andino, Ph.D., PE
Major Department: Environmental Engineering Sciences

The effects of inorganic aerosols on the kinetics of the hydroxyl radical reactions with organic compounds have been investigated using the relative rate technique. The relative rates in the absence and presence of aerosols were determined for C_1-C_6 aliphatic alcohols and selected alkanes including n-butane, n-pentane, n-hexane, n-octane, and n-decane. P-xylene was used as a reference compound for all of the studies, with the exception of the methanol study. Ethanol was used as a reference compound for the methanol study. Inorganic aerosols including $(NH_4)_2SO_4$, NH_4NO_3, NaCl, Na_2SO_4 and NH_4Cl aerosols at two different aerosol concentration that are typical of polluted urban conditions were tested. Total surface areas of aerosols were 1400 μm^2 cm^{-3} (Condition I) and 3400 μm^2 cm^{-3} (Condition II).

Results indicate that the aerosols promote the 1-propanol/$^{\cdot}$OH, ethanol/$^{\cdot}$OH, and methanol/$^{\cdot}$OH reactions versus the p-xylene/$^{\cdot}$OH reaction, and the extents of the promoting effects depend on the aerosol composition and concentration. For the 1-propanol study, increases in the relative rates of the 1-propanol/$^{\cdot}$OH reaction versus the p-xylene/$^{\cdot}$OH reaction were only observed for $(NH_4)_2SO_4$ aerosol conditions I and II, and NH_4NO_3 aerosol condition II. In addition, Na_2SO_4 and NH_4Cl aerosols showed an increase of the relative rates of the 1-propanol/$^{\cdot}$OH reaction versus the p-xylene/$^{\cdot}$OH reaction only for NH_4Cl aerosol condition II. These results indicate that NH_4^+ is the species promoting the 1-propanol/$^{\cdot}$OH reaction and suggest the possibility of a strong interaction between NH_4^+ and 1-propanol that can change the transition state energy of the initial $^{\cdot}$OH attack. However, significant changes in the relative rates in the presence of aerosols were not observed for the 1-butanol/$^{\cdot}$OH, 1-pentanol/$^{\cdot}$OH, and 1-hexanol/$^{\cdot}$OH reactions versus p-xylene/$^{\cdot}$OH reaction. The results indicate that the size of the alcohol molecule also determines the promoting effects of aerosols on the alcohols. For the alkane studies, effects of aerosols on the kinetics of the alkanes/$^{\cdot}$OH reactions versus the p-xylene/$^{\cdot}$OH reaction were not observed, suggesting that the promoting effects also depend on the nature of the organic compounds.

CHAPTER 1
INTRODUCTION

The troposphere is the lowest layer of the atmosphere, extending from the ground to an altitude of 10 to 15 km. It is the region where most weather processes occur. Because the temperature in the troposphere decreases with altitude, the troposphere is an unstable region characterized by rapid vertical mixing. A characteristic time for mixing up to the stratosphere, the layer lying on the top of the troposphere, is on the order of 10 to 30 days (Seinfeld et al. 1994). Air quality issues in the troposphere have been the primary concerns for human health because most human activities take place in this region. Various chemical compounds are emitted to the troposphere from both anthropogenic and natural sources, and these chemicals can undergo chemical reaction leading to the formation of new compounds which are not directly emitted from any sources. These compounds are in either gaseous or particulate form. The U.S. Environmental Protection Agency (EPA) set National Ambient Air Quality Standards (NAAQSs) for various atmospheric gases and particles, and set industrial process and motor vehicle emission limits to help control the ambient air concentration of pollutants.

Compounds such as CO, SO_2, NO_x, O_3, and hydrocarbons are major gaseous pollutants in the troposphere. Hydrocarbons are emitted into the troposphere from various anthropogenic and biogenic sources. Alkanes, alkenes, aromatics, and oxygen-containing organics such as aldehydes, ketones, ethers, acids, and alcohols are important hydrocarbons in the troposphere (Graedel et al. 1986).

Organic compounds in the troposphere are capable of reacting with O_3, OH radicals, and NO_3 radicals. Using average tropospheric concentrations for O_3, OH radical, and NO_3 radical of 7×10^{11}, 1.5×10^{6}, and 5×10^{8} molecules cm^{-3}, respectively, in conjunction with the available rate constant data for selected hydrocarbons, it is evident that the major gas-phase loss process for hydrocarbons in the troposphere is reaction with OH radicals (Seinfeld et al. 1994). In combination with sunlight and oxides of nitrogen, these hydrocarbons react with OH radicals to produce ozone, a nationally regulated air pollutant and a component of photochemical smog in urban areas. When NO and NO_2 are present in sunlight, ozone formation occurs as a result of the photolysis of NO_2 at wavelengths less than 424 nm,

$$\mathrm{NO_2} + h\nu \rightarrow \mathrm{NO} + \dot{\mathrm{O}} \tag{1.1}$$

$$\dot{\mathrm{O}} + \mathrm{O_2} \xrightarrow{M} \mathrm{O_3} \tag{1.2}$$

$$\mathrm{O_3} + \mathrm{NO} \rightarrow \mathrm{NO_2} + \mathrm{O_2} \tag{1.3}$$

where M represents N_2 or O_2 or another third molecule that absorbs the excess vibrational energy and thereby stabilizes the O_3 molecules formed. The steady-state O_3 concentration is given by:

$$[\mathrm{O_3}]_{ss} = \frac{k_{1.1}[\mathrm{NO_2}]}{k_{1.3}[\mathrm{NO}]} \tag{1.4}$$

where $k_{1.1}$ is the photolysis constant of NO_2, and $k_{1.3}$ is the rate constant of reaction (1.3). Thus, in the absence of hydrocarbons the O_3 concentration is dependent on the intensity of solar radiation and the ratio of $[NO_2]$ and $[NO]$. However, the reaction of hydrocarbons with OH radicals eventually leads to conversion of NO to NO_2 and subsequent accumulation of O_3. The reactions are as follows:

$$\text{RH(Hydrocarbon)} + \dot{\text{O}}\text{H} \rightarrow \dot{\text{R}} + \text{H}_2\text{O} \tag{1.5}$$

$$\dot{\text{R}} + \text{O}_2 \rightarrow \text{R}\dot{\text{O}}_2 \tag{1.6}$$

$$\text{R}\dot{\text{O}}_2 + \text{NO} \rightarrow \text{R}\dot{\text{O}} + \text{NO}_2 \tag{1.7}$$

$$\text{R}\dot{\text{O}} + \text{O}_2 \rightarrow \text{R'CHO} + \text{H}\dot{\text{O}}_2 \tag{1.8}$$

$$\text{H}\dot{\text{O}}_2 + \text{NO} \rightarrow \text{NO}_2 + \dot{\text{O}}\text{H} \tag{1.9}$$

where R represent a generic alkyl group. Thus, the reactions of hydrocarbons with OH radicals ultimately contribute to tropospheric O_3 formation. Therefore, accurate rate constants for reactions with the OH radicals are necessary to assess the ozone levels for any given area as well as the tropospheric lifetimes of hydrocarbons.

The reactions of many hydrocarbons with OH radicals have been studied extensively under simulated tropospheric conditions, and compilations of rate constants appear in Atkinson (1989, 1994). Air quality modelers have used these chemistry data along with meteorological data, emissions data and transport mechanisms to assess air pollution control strategies (Seinfeld 1988, Dodge 2000). However, these gas-phase chemistry data have not considered the effects of particulate matter on gas-phase reactions. Traditionally, tropospheric chemistry has been studied under two separate branches: reactions in the gas-phase and reactions forming aerosol components. Thus, information concerning the effects of aerosol particle concentration, composition or size on tropospheric gas-phase kinetics has not been clearly established.

Currently, there is growing concern over the role of aerosols in atmospheric chemistry (Kolb et al. 1997, Hemminger 1999, Seinfeld, 2000). It is well known that aerosols play a crucial role in the depletion of ozone in the stratosphere (Shen et al. 1995). Cloud and fog studies have indicated that droplets can significantly alter the course of gas-phase chemistry (Seinfeld et al. 1994). Also, the formation of secondary aerosols from the oxidation of organic compounds, and their detrimental effects on human health and atmospheric visibility are well known (Odum et al. 1997). However, few studies have been performed to elucidate the effects of aerosols on gas-phase chemistry pertinent to the troposphere.

Recently the catalytic activities of inorganic particles such as TiO_2, SiO_2, Fe_2O_3 and fly ash were investigated (Warneck et al. 1996; Guillard et al. 1993; Behnke et al. 1987, 1988). Photodegradation of naphthalene on TiO_2, Fe_2O_3 and fly ash surfaces were observed (Guillard et al. 1993). Studies of the effects of TiO_2 and SiO_2 aerosols on the OH radical/alkane gas-phase reactions indicated a significant impact of TiO_2 aerosols on the kinetics of the OH radical/alkane reactions. However, a significant impact was not observed with SiO_2 aerosols (Behnke et al. 1987, 1988). Recent studies also indicate that the heterogeneous production of HNO_2 from NO_2 on suspended soot particles proceeds 10^5 to 10^7 times faster than on other surfaces (Ammann et al. 1998). These results indicate that aerosols can affect gas-phase chemistry in the atomosphere, and the effects of aerosols on the reaction kinetics depend on aerosol composition and the properties of organic compounds. However, these studies have been performed using aerosols that are not major constituents of atmospheric aerosols. Thus, it is necessary to investigate the interactions of aerosols that are more prevalent in the atmosphere with gas-phase reactions of major organic compounds.

Particles are emitted to the atmosphere by both natural sources, such as wind-borne dust, sea spry, volcanic eruptions, and wildfire; and from anthropogenic activities, such as the combustion of fuels. In addition, the gas-phase oxidation of a number of compounds can lead to products that condense into the particulate phase. Particles in the atmosphere are removed by dry deposition (deposition at the earth's surface) and wet deposition (scavenging by droplets during precipitation). The residence times of particles in the troposphere vary only from a few days to a few weeks, while tropospheric trace gases have lifetimes ranging from less than a second to a century (Pandis et al. 1995). The short residence time of aerosols in the troposphere results in significant spatial variations in particle concentration, size, and composition.

The aerosols in the troposphere consist of a nuclei mode (particles below 0.1 μm in diameter) from recent gas-to-particle conversion; an accumulation mode ($0.1 < D_p < 1$ μm) from condensational growth and coagulation of the nuclei mode; and a coarse mode ($D_p > 1$ μm) from direct mechanical generation at the Earth's surface (Seinfeld & Pandis 1998). However, the boundaries dividing these sections are not precise.

Size distribution and concentration of atmospheric aerosols are generally expressed in three different ways based on properties such as number, surface area, and mass (volume). These three properties are important for different reasons. For example, the number concentration is the governing factor for condensation and coagulation processes (Hinds 1982). Mass concentration has been used to define air quality standards for particles. Particle surface area plays a key role in adsorption and catalytic activity

(Augustine 1996). Thus, surface area is a crucial factor to examine in studies of the effects of aerosols on OH radical reactions with organic compounds. Particles in the size range from 0.01 to 1 μm provide most of the atmospheric aerosol surface area (Willeke & Whitby 1975). Typical aerosol concentrations in different regions are listed in Table 1-1 and typical aerosol size distributions in an urban area are shown in Figure 1-1.

Table 1-1. Typical concentrations of tropospheric aerosols.

Region	Concentrations		
	Number (# cm^{-3})[a]	Surface Area (μm^2 cm^{-3})[b]	Mass (μg m^{-3})[a,c]
Remote continental	50 ~ 10,000	20 ~ 200	2 ~ 10
Rural	2,000 ~ 10,000	100 ~ 800	10 ~ 40
Urban (polluted)	$10^5 \sim 4\times10^6$	1,000 ~ 3,000	100 ~ 300

[a] From Seinfeld & Pandis 1998.
[b] From Willeke & Whitby 1975.
[c] Values are masses of particles less than 10 μm in diameter (PM_{10}).

The chemical composition of atmospheric aerosols varies with size range and sources. However, carbonaceous material, nitrate, sulfate, ammonium, sea salt and water are generally present in varying amounts. Ammonium, sulfate, nitrate, sodium, and chloride typically account for 25% to 50% of the nonwater atmospheric aerosol mass (Seinfeld et al. 1994). The typical compositions of tropospheric aerosols are listed in Table 1-2.

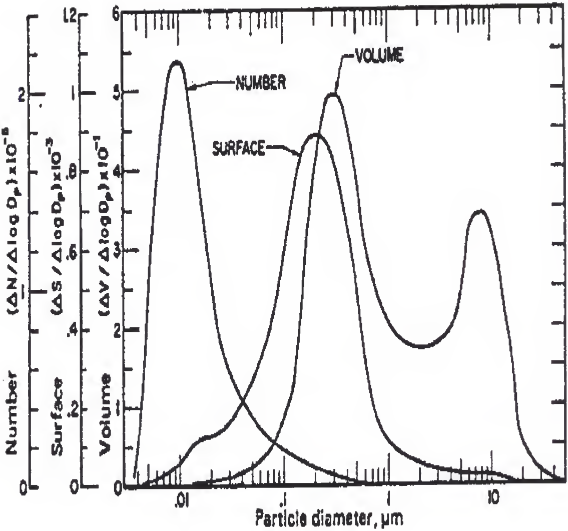

Figure 1-1. Typical aerosol size distributions in an urban area (adapted from National Research Council, 1979).

Table 1-2. Typical compositions of tropospheric aerosols[a].

Region	Weight Percentage, %					
	Elemental carbon	Organic carbon	NH_4^+	NO_3^-	SO_4^{2-}	N/D[b]
Remote (11 areas)	0.3	11	7	3	22	56
Nonurban contienental (14 areas)	5	24	11	4	37	19
Urban (19 areas)	9	31	8	6	28	18

[a] From Heintzenberg 1989.
[b] Undetermined.

The aim of this doctoral research was to determine the effects of atmospheric aerosols on the gas-phase reactions of OH radicals with organic compounds. In order to investigate the effects on different organic compounds, three different types of organics were tested. Alkanes, aromatics, and oxygenated compounds were tested due to their abundance in the troposphere (Lurmann et al. 1992). The mean concentrations of each species determined in the Southern California Air Quality Study are listed in Table 1-3. A series of aliphatic alcohols and alkanes with varying carbon numbers were tested to investigate effects on the size of organic compounds. Inorganic salts such as ammonium sulfate, ammonium nitrate and sodium chloride aerosols were used as test aerosols because of their abundance in the troposphere. In addition, sodium sulfate and ammonium chloride aerosols were tested to elucidate the effects of individual anionic and cationic constituents of the aerosols on the OH radical/organic reactions. The results of this doctoral research provide the necessary foundation to alter the kinetic rate constants used in existing air quality modeling programs. These results may dramatically change predictions made regarding the effectiveness of proposed air pollution control strategies.

Table 1-3. Mean concentrations and percents of species groups for overall summer and fall surface data from the Southern California Air Quality Study[a].

Species	Concentration, ppbC[b]		Percent of NMOC, %[b]	
	Summer	Fall	Summer	Fall
Alkanes	353 (229)	756 (568)	44.4 (6.9)	45.4 (6.1)
Alkenes	65 (46)	181 (160)	8.3 (2.4)	10.0 (2.6)
Aromatics	139 (104)	342 (272)	16.3 (4.8)	20.1 (3.7)
Oxygenated compounds	109 (63)	107 (50)	16.1 (9.2)	9.9 (6.8)
Unidentified compounds	115 (68)	225 (140)	14.9 (4.6)	15.2 (3.6)
NMOC[c]	783 (383)	1580 (1069)	-	-

[a] From Lurmann et al. 1992.
[b] Values in parentheses represent standard deviations.
[c] Nonmethane organic compounds.

CHAPTER 2
EXPERIMENTAL SYSTEM

System Description

A new experimental system was set up to investigate the effects of aerosols on the kinetics of OH radical/organic reactions. A schematic of the experimental system appears in Figure 2-1. One hundred liter, 2-mil Tedlar® bags (SKC Inc., 231-50, 76 cm × 91 cm) with irradiation provided by eight 40-W black lamps (Sylvania F40/350BL) were used as the reactors for the OH radical/organic reactions. The lamps provided UV radiation in the 300 to 400 nm region. Only light of wavelengths larger than 290 nm is available in the troposphere due to the presence of absorbing species such as atomic and molecular oxygen, nitrogen, and O_3 in the upper atmosphere (Finlaysion-Pitts & Pitts Jr. 2000). The spectral distribution of a black lamp is shown in Figure 2-2. The bag and the lamps were housed inside a custom built enclosure that was lined with a highly reflective coating to enhance light distribution. A fan was mounted in the enclosure to maintain an even temperature distribution around the bag.

The aerosol was generated by using a Collison atomizer to atomize an aqueous solution containing the aerosol base material (Peters et al. 1994, Li & Lundgren 1997). The atomization of solutions with compressed air is one of the simplest ways to generate a polydispersed aerosol (Hinds 1982). In an atomizer, compressed air at a pressure of 5 to 40 psig enters the atomizer through an orifice, expanding at high speed past the liquid inlet. The pressure drop from the air flow draws a filament of liquid into the air stream

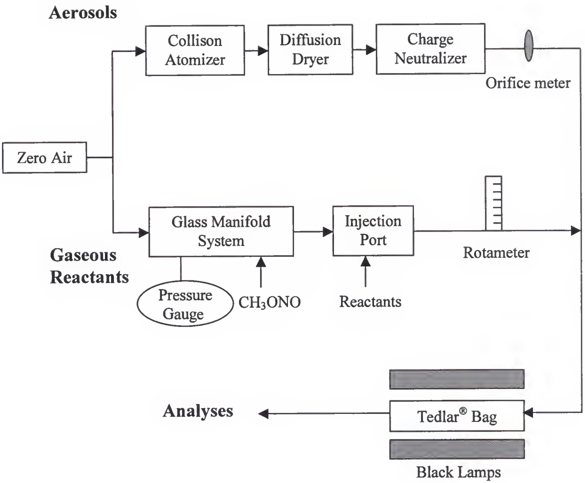

Figure 2-1. Schematic of the experimental apparatus.

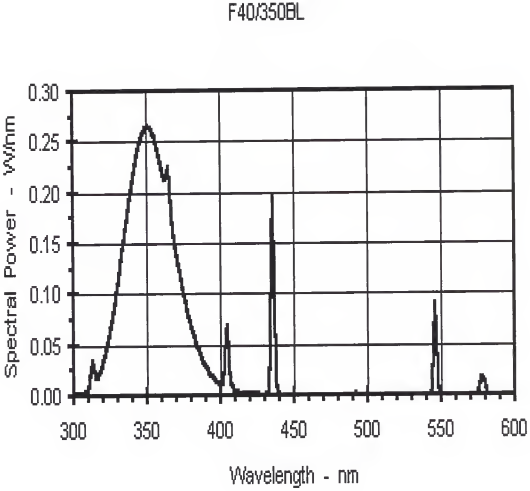

Figure 2-2. Spectral distribution of a typical black lamp.

which then breaks up into droplets. The smaller droplets follow the air stream and exit the atomizer, while the larger droplets are removed by impaction to the walls. A schematic of a Collison atomizer appears in Figure 2-3. A compressed air cylinder (Praxair Technology, Inc., Part No. Al 0.0Z) was used as the source of air. The aerosol generated was passed through a diffusional dryer (Hinds 1982, Wang et al. 1992) and a charge neutralizer before being admitted to the bag. A diffusional dryer with silica gel was used to minimize aerosol losses in the dryer. A ^{85}Kr charge neutralizer (TSI Inc., Model 3012) was used to neutralize highly charged particles that were generated using the Collison atomizer. In a charge neutralizer, the radioactive source (^{85}Kr) ionizes the neighboring atmosphere into positive and negative ions. Aerosols carrying a high charge level can discharge by capturing ions of opposite polarity. After a short time (less than 2 s), a charge equilibrium called Bolzmann equilibrium is reached where the aerosol carries a bipolar distribution (Hinds, 1982). Thus, particles admitted to the bag were carrying charges as shown in Table 2-1.

The aerosol concentration in the bag was controlled by changing the amount of aerosol flow into the bag. The aerosol flow rate was measured using a calibrated orifice meter. Flow rate measuring devices such as a rotameter and mass flow meter could not be used to monitor the aerosol flow because most of the aerosols would be lost by deposition onto the float in the rotameter or the heated surface in the mass flow meter. A calibration curve for the orifice meter can be found in Appendix A. The size distribution of the particles in the Tedlar® bag was determined using an electrical aerosol analyzer (EAA, Model 3030, TSI, Inc). The EAA provided measurement of particle number size distributions in the range of 0.01 to approximately 1 μm. These data were converted

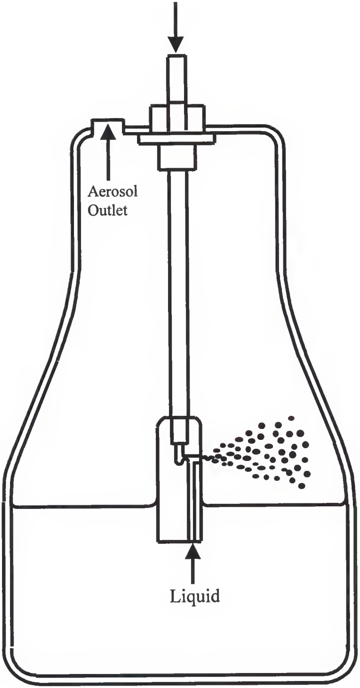

Figure 2-3. A schematic of a Collison atomizer (adapted from Li, 1999).

Table 2-1. Distribution of charge on aerosol particles at Boltzmann Equilibrium[a].

Particle Diameter (μm)	Percentage of Particles Carrying the Indicated Number of Charges								
	<-3	-3	-2	-1	0	+1	+2	+3	>+3
0.01				0.3	99.3	0.3			
0.05			0.6	19.3	60.2	19.3	0.6		
0.1		0.3	4.4	24.1	42.6	24.1	4.4	0.3	
0.5	4.6	6.8	12.1	17.0	19.0	17.0	12.1	6.8	4.6
1.0	11.8	8.1	10.7	12.7	13.5	12.7	10.7	8.1	11.8
5.0	29.8	5.4	5.8	6.0	6.0	6.0	5.8	5.4	29.8

[a] Adapted from Hinds 1982.

from number distribution to surface area and volume distributions assuming spherically shaped particles.

The gaseous reactants were introduced into the bag by two methods: direct syringe injection and via an evacuable glass manifold system. A 10 μL Hamilton syringe was used to inject the organic compounds into a stream of zero air flowing into the bag. The injection was made into a septum placed inside a Swagelock union tee that was connected to the inlet of the bag. A custom designed evacuable glass manifold system was used to admit known amounts of highly volatile reactants such as methyl nitrite and nitric oxide. The system contained a 1.87 L glass bulb and two MKS Baratron pressure gauges with a combined measuring range of 10^{-3} to 10^{3} Torr. The reactant was expanded into the evacuated glass bulb to give the desired pressure, and admitted into the bag by a stream of zero air. The flow rate of air into the bag was monitored using a calibrated rotameter, and the concentrations of gaseous reactants were determined from the total volume of air and the admitted volume of the reactants in the bag. A calibration curve for the rotameter can be found in Appendix A. Gas analyses were conducted using a Finnigan-MAT GCQ system (Model 9001 gas chromatograph coupled to a tandem mass spectral detector).

Aerosol Loss Studies

To adequately study heterogeneous kinetics, it is essential to control aerosol characteristics such as size distribution, concentration, composition and stability. A change in aerosol characteristics during an experiment can significantly affect the reaction kinetics. However, particles in a chamber interact with the walls as well as other particles to change their size distribution and concentration. Coagulation and deposition on the walls are the most dominant aerosol loss processes in a chamber (Corner & Pendlebury 1951). These processes are governed by several factors such as diffusion (thermal force), gravity, and electrical forces.

Coagulation is a process that involves particle collision due to the relative motion between particles and subsequent adhesion to form larger particles. The net result is a decrease in number concentration and an increase in particle size. Thus, coagulation of particles causes a decrease in number concentration and surface area. However, the mass concentration remains constant during the coagulation process. Coagulation is a spontaneous and ever-present phenomenon for aerosols due to the Brownian motion of particles. To estimate the optimal aerosol conditions at which the effects of coagulation were minimized, a simple calculation was conducted, assuming the existence of monodisperse particles. It is important to note that the particles generated from the Collison atomizer were polydispersed. However, the calculated results for the monodisperse particles provide a general guide. The coagulation rate of monodisperse particles undergoing Brownian motion depends on the number concentration, size, and diffusion coefficient of the particles. The rate is represented by the following equation (Hinds 1982):

$$\frac{dN}{dt} = -KN^2 \tag{2.1}$$

$$K = 4\pi D_p D \tag{2.2}$$

where N is the number concentration, K is the coagulation coefficient, D_p is the particle diameter, and D is the diffusion coefficient of the particle. The number concentration as a function of time can be obtained by integrating equation (2.1) assuming K to be constant:

$$N(t) = \frac{N_o}{1 + N_o K t} \tag{2.3}$$

where N_o is the original number concentration at time zero and $N(t)$ is the number concentration at time t. Also, the following relationship is applicable since the particulate mass concentration (C_m) remains constant during coagulation (assuming liquid particles):

$$C_m = N_o \frac{\pi}{6} \rho_p D_o^3 = N(t) \frac{\pi}{6} \rho_p \left(D_p(t)\right)^3 \tag{2.4}$$

---

where D_o is the initial particle size, $D_p(t)$ is the particle size at time t, and ρ_p is the density of the particle. Rearranging equation (2.4) and substituting equation (2.3) gives the following relationships for particle size changes during coagulation:

$$D(t) = D_o\left[\frac{N_o}{N(t)}\right]^{1/3} = D_o(1+N_oKt)^{1/3} \tag{2.5}$$

By analogy, the total surface area of aerosols can be represented by the following equations:

$$\frac{S(t)}{S_o} = \frac{N(t)\pi(D_p(t))^2}{N_o\pi D_o^2} = \frac{1}{(1+N_oKt)^{1/3}} \tag{2.6}$$

$$\text{or} \quad S(t) = \frac{S_o}{(1+N_oKt)^{1/3}} \tag{2.6a}$$

where S_o is the initial total surface area, and $S(t)$ is the total surface area of particles at time t. Using equations (2.3) and (2.6a), changes in the aerosol number concentration and total surface area were calculated for monodisperse particles with a diameter of 0.05 μm and at different initial concentrations ($N_o = 10^4, 10^5, 10^6, 10^7$ cm^{-3}). The particle diameter of 0.05 μm was chosen since the median number diameter of the aerosols tested in this doctoral research was 0.05 μm (see Table 4-1). A diffusion coefficient (D) of 2.37×10^{-5} cm^{2}s^{-1} was used (Hinds 1982). Plots of $N(t)/N_o$ and $S(t)/S_o$ over a 1 h period are shown in Figure 2-4. This figure clearly illustrates the profound effect that coagulation has on both number concentration and surface area over time as a function of initial concentration. For initial concentrations of 10^4, 10^5, 10^6, and10^7 cm^{-3}, the values

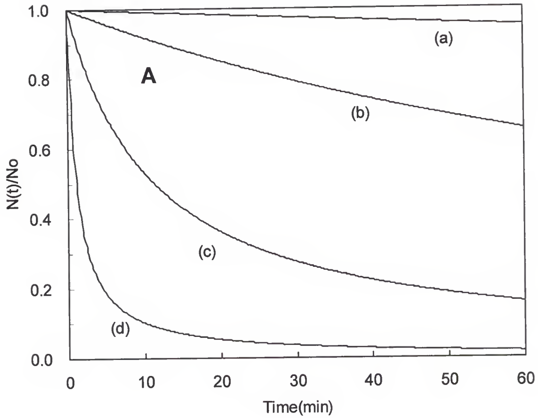

Figure 2-4. Normalized number concentrations of particles as a function of time due to coagulation for monodisperse particles with diameters of 0.05 µm at initial concentrations of (a) 10^4, (b) 10^5, (c) 10^6, and (d) 10^7 cm^{-3}. Plot (A) represents number concentration and plot (B) represents total surface area.

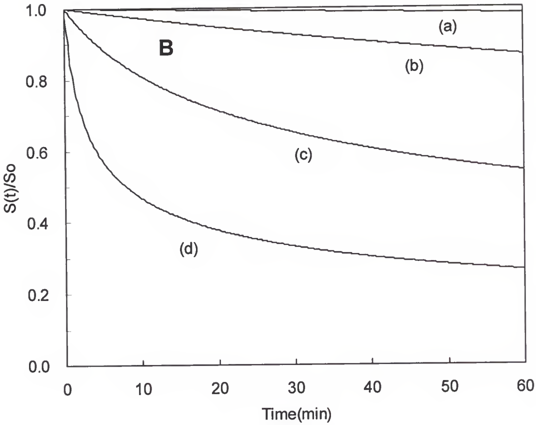

Figure 2-4--continued

of $N(t)/N_o$ after 1 h were 0.95, 0.65, 0.16, and 0.02, respectively. The corresponding values of $S(t)/S_o$ were 0.98, 0.87, 0.54, and 0.27. A decrease in the surface area of more than 46% of the initial value is realized after 1 h when the initial concentration is larger than 10^6 cm^{-3}. Thus, to minimize the effects of coagulation over short time periods, the initial aerosol number concentration should be less than 10^5 cm^{-3}.

The loss of particles by deposition on the walls is inevitable since particles adhere when they collide with a surface. Deposition is due to Brownian and turbulent diffusion, gravitational sedimentation, and electrostatic forces (McMurry & Rader 1985), and results in decreases in number, surface, and volume concentrations. To estimate the loss of particles by deposition in a Tedlar® bag, the loss rates of each process was calculated for monodisperse particles with diameters of 0.05 μm in a 100 liter cylindrically shaped bag (r = 19 cm, H=91 cm). The bag was assumed to be cylindrically shaped since the characteristic dimensions of the bag can be properly defined.

Diffusion is generally the dominant force for smaller particles (less than 0.1 μm). The cumulative number of particles deposited per unit area of surface by diffusion, *n(t)* in with units of number of particles per cm^2, is expressed by the following equation assuming a uniform concentration (N_o, with units of number of particles per cm^3) in the bulk phase (Hinds 1982):

$$n(t) = 2N_o\left(\frac{Dt}{\pi}\right)^{1/2} \tag{2.7}$$

where D is the diffusion coefficient, and t is the time. Assuming that deposition due to diffusion is the only loss process in the bag, the following balance equation holds:

$$N_o V = N(t)V + n(t)S \tag{2.8}$$

where *S* is the total surface area and *V* is the total volume of the container. Rearranging equation (2.8) gives the following relationship for the number concentration of aerosols as a function of time:

$$N(t) = N_o - n(t)\left(\frac{S}{V}\right) = N_o\left(1 - 2\left(\frac{Dt}{\pi}\right)^{1/2}\left(\frac{S}{V}\right)\right) \tag{2.9}$$

Equation (2.9) shows that deposition by diffusion depends on the shape of the container (*S/V*) as well as the diffusion coefficient of the particle (*D*).

The loss of particles by gravitational sedimentation depends on the terminal settling velocity of the particle (V_{TS}) and the height (*H*) of the container. The number concentration of aerosols as a function of time due to gravitational sedimentation is expressed by the following equation assuming a uniform particle concentration in the container (Hinds 1982):

$$N(t) = N_o \exp\left(\frac{-V_{TS}t}{H}\right) \tag{2.10}$$

The terminal settling velocity of particles (V_{TS}) with diameters less than 10 μm (Reynolds number $< 2\times10^{-3}$) is expressed by the Stokes- Cunningham law (Hinds 1982):

$$V_{TS} = \frac{\rho_p D_p^2 g C_c}{18\eta} \tag{2.11}$$

where g is the acceleration gravity, C_c is the Cunningham correction factor, and η is the viscosity of air. Gravity is generally the dominant force for particles larger than 1.0 μm.

Changes in number concentrations of aerosols due to deposition by diffusion and gravitational sedimentation for monodisperse particles with diameters of 0.05 μm in a 100 liter cylindrically shaped bag were calculated using equations (2.9) and (2.10). Estimated particle losses by gravitational sedimentation were negligible (less than 0.1% of the initial particle number concentration) if a 1 h time period was considered. Deposition by diffusion was the dominant deposition process under the conditions used. However, only 5% of the initial particle number was determined to deposit to the surface under a 1 hr period. Thus, particle losses by diffusion and gravitational sedimentation were not expected to change aerosol characteristics significantly in a Tedlar® bag over a 1 h period. The calculated $N(t)/N_o$ values are listed in Table 2-2.

The surfaces of Teflon® (polytetrafluoroethylene) films are quite electrostatic. Therefore, the electrical force is an important factor for aerosol dynamics in a Teflon® chamber (Finlayson-Pitts & Pitt Jr. 2000). McMurry & Radar (1985) showed that particles in the 0.05 to 1 μm size range were removed in a 250 liter Teflon® chamber primarily by electrostatic attraction to the Teflon® surfaces. A characteristic value of 45 volts/cm was found as the electric field intensity (McMurry & Radar, 1985). Since Tedlar® (polyvinylflouride) has a chemical structure similar to Teflon®, the surfaces of Tedlar® films are very likely electrostatic, and the aerosol dynamics in a Tedlar® bag are likely influenced by electrical forces. As described earlier in the experimental description section, aerosols in this doctoral research carried charges with Boltzmann distribution since the generated aerosols passed through a charge neutralizer before being admitted to the Tedlar® bag. As can be seen in Table 2-1, the charge distributions depend on the size of particle. Particles carry more charge as their sizes increase. When a charged particle is placed in an electric field, it experiences an electrical force that ultimately influences the particle's velocity, V_{TE}. Mathematically, the velocity of particles with diameters less than 10 μm is expressed as (Hinds 1982):

$$V_{TE} = \frac{neEC_c}{3\pi\eta D_p} \tag{2.12}$$

where *n* is the number charge acquired by a particle, *e* is the elementary unit of charge, and *E* is the electric field intensity. The number concentration of aerosols as a function of time as a result of deposition due to electrical forces in a cylindrically shaped container having an electric field in a horizontal direction is

$$N(t) = N_o \exp\left(\frac{-2V_{TE}t}{r}\right) \tag{2.13}$$

where r is the cross-sectional radius of the container. Changes in number concentrations of aerosols due to electrical deposition for monodisperse particles with diameters of 0.05 μm in a 100 liter cylindrically shaped bag were calculated using equation (2.13). An electric filed intensity of 45 volts/cm was assumed, and the $N(t)/N_o$ values obtained are listed in Table 2-2. Since most of the charged 0.05 μm sized particles are singly charged (see Table 2-1), the calculation was performed only for singly charge particles. Estimated losses due to electrical deposition were significant; 98% of the singly charged particles were estimated to deposit to the surface within a 15 min period. Since approximately 40% of 0.05 μm-sized particles are singly charged at the Boltzmann equilibrium condition, 39% of the initial particle number was determined to deposit due to electrical forces within a 15 min period. Neutral particles were assumed not to deposit as a result of electrical forces. Thus, particle loss by electrical deposition was expected to change aerosol characteristics significantly in a Tedlar® bag over a 1 h period.

Table 2-2. Normalized number concentrations of particles as a function of time ($N(t)/N_o$) due to deposition losses for monodisperse particles with diameters of 0.05 μm in a 100 liter cylindrically shaped bag. Losses are in parentheses.

Time (min)	$N(t)/N_o$			
	Diffusion	Gravitational Sedimentation	Electrical Force[a]	Total Losses[b]
15	0.978 (0.022)	1.000 (0.000)	0.609 (0.391)	0.588 (0.413)
30	0.970 (0.030)	0.999 (0.001)	0.602 (0.398)	0.571 (0.429)
45	0.963 (0.037)	0.999 (0.001)	0.602 (0.398)	0.564 (0.436)
60	0.957 (0.043)	0.999 (0.001)	0.602 (0.398)	0.558 (0.442)

[a] Values for particles carrying charges with Boltzmann equilibrium in an electric field of 45 volts/cm.

[b] Obtained by adding the losses due to each process using the following formula:

$$\left(\frac{N(t)}{N_o}\right)_{Total} = 1 - \sum\left(1 - \frac{N(t)}{N_o}\right)_{deposition\ process}.$$

The number concentration of aerosols as a function of time as a result of all deposition processes was obtained by adding the losses due to each process using the following equation.

$$\left(\frac{N(t)}{N_o}\right)_{Total} = 1 - \sum\left(1 - \frac{N(t)}{N_o}\right)_{deposition\ process} \tag{2.14}$$

The $N(t)/N_o$ values obtained are listed in Table 2-2, and plots of $N(t)/N_o$ are shown in Figure 2-5. The total losses by deposition for monodesperse particles with diameters of 0.05 μm in a 100 liter cylindrically shaped bag were significant in a 1 h period. The estimated $N(t)/N_o$ value was 0.558, indicating that approximately 44% of the initial particles were lost as a result of deposition over a 1 h period. Even though the calculation is based on monodispesre particles and a cylindrically shaped bag, the results indicate that aerosol characteristics in a Tedlar® bag are expected to change significantly in a 1 hr period, and electrical deposition is the dominant process causing the changes.

Laboratory experiments were performed to characterize the stability of aerosols in a Tedlar® bag. Aerosol size distributions were measured at different times after introducing aerosols. The initial number concentration was maintained below 10^5 cm^{-3} to minimize changes in aerosol characteristics as a result of coagulation. The initial aerosol number, surface area, and mass median diameters were approximately 0.05 μm, 0.15 μm, and 0.20 μm, respectively. Figure 2-6 shows the size distribution changes of aerosols in the Tedlar® bag over a 1 h period. As can be seen in Figure 2-6, loss of particles in the bag is apparent, and the volume decrease with time is significant. This indicates that deposition is the main loss process for aerosols in the Tedlar® bag. The number concentration and surface area of the aerosols decreased to 34% and 50% of the initial value in 30 min and 60 min, respectively (Table 2-3). The decreases in number concentrations were comparable to the values calculated in Table 2-1.

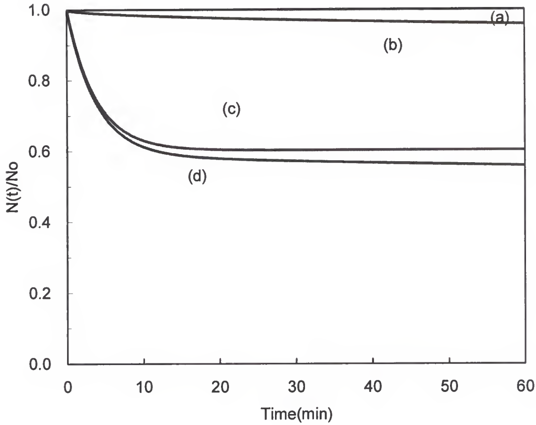

Figure 2-5. Normalized number concentrations of particles as a function of time ($N(t)/N_o$) by deposition for monodisperse particles with diameters of 0.05 μm due to (a) gravitational sedimentation, (b) diffusion, (c) electrical deposition, and (d) total processes.

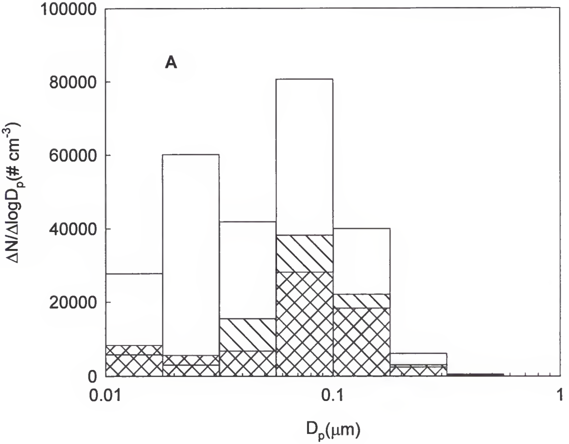

Figure 2-6. Size distributions of the aerosols in the bag at different times; initially (☐), after 30 min (▧), and after 60 min (▩). (A) Number (B) Surface Area (C) Volume

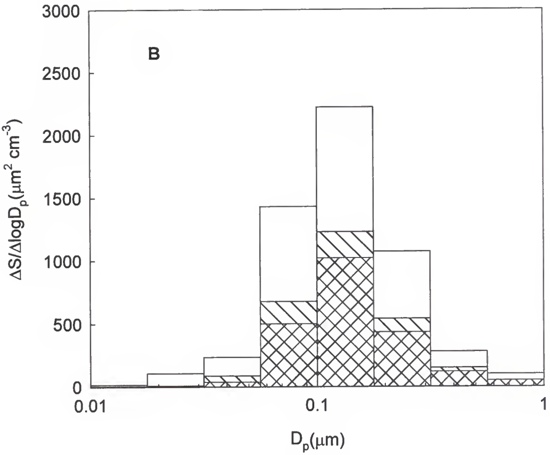

Figure 2-6--continued

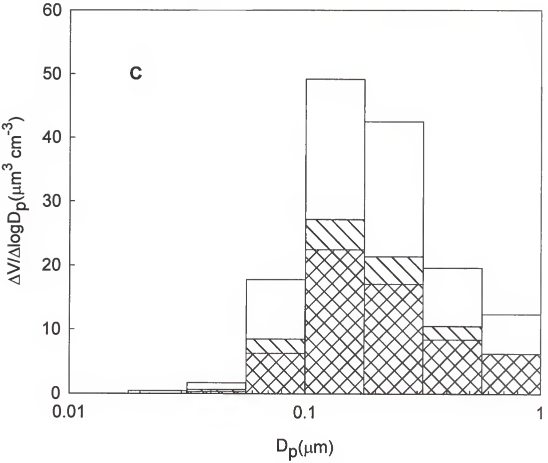

Figure 2-6—continued

Table 2-3. Aerosol concentrations in the Tedlar® bag as a function of time.

Times (min)	Concentrations[a]		
	Number (#/cm^3)	Surface Area (μm^2/cm^3)	Volume (μm^3/cm^3)
0	6.43×10^4	1370	35.9
30	2.20×10^4 (0.34)	685 (0.50)	18.6 (0.52)
60	1.75×10^4 (0.27)	543 (0.40)	15.2 (0.42)

[a] Values in parentheses represent values of $N(t)/N_o$, $S(t)/S_o$, $V(t)/V_o$ determined from the experiments.

These results lend credence to the hypothesis that the electrical force was the dominant loss process for particles in a Tedlar® bag. Therefore, short duration experiments were critical to obtaining kinetic constants representative of the original aerosol conditions. To minimize changes in aerosol properties during the heterogeneous studies, short reaction times (less than 10 min) were applied to each experiment. Decreases in aerosol surface area were less than 10% during these time scales.

Organic Reactant Loss Studies

To obtain accurate kinetic data, it was essential that the major loss process for organic reactants in the Tedlar® bag was reaction with the OH radicals. There were a variety of possible loss processes for the reactants that had to be accounted for in this doctoral research. In general, the loss processes involved either interaction with the walls of the bag, photolysis, or interaction with another species. In addition, uptake of the organics by the aerosols was a possible loss mechanism in the heterogeneous kinetic studies. These losses could lead to significant errors in the interpretation of the kinetic data. Thus, several experiments were conducted before performing the kinetic studies to ensure that the major loss process for the reactants was due to reaction with the OH radicals. First, to check for losses via interactions between the reactants and the walls, reactants were mixed thoroughly in the Tedlar® bag and concentration changes were monitored using the GCQ system. Second, to check for losses of the reactants via photolysis, the reactants were introduced to the bag and irradiated. The concentrations of the reactants before and after irradiation were measured. Finally, to address the issue of organic uptake by the aerosols, the reactants were admitted to the bag with aerosols, and the concentration changes of the reactants were monitored. Each of the above experiments was conducted on a time scale that was comparable to that used in the kinetic experiments in this doctoral research.

CHAPTER 3

EFFECTS OF AMMONIUM SULFATE AEROSOLS ON THE GAS-PHASE REACTIONS OF THE HYDROXYL RADICAL WITH ORGANIC COMPOUNDS

Background

The aim of this study was to determine the effects of atmospheric aerosols on the gas-phase reactions of OH radicals with different types of organic compounds. In order to investigate the effects on different organic compounds, three different types of organics were selected. N-hexane, p-xylene, and 1-propanol were chosen as representatives of alkanes, aromatics, and oxygenated compounds. N-hexane and p-xylene were chosen because they were identified in the Southern California Air Quality Study as being one of the twenty five most abundant species found in the atmosphere based on the fraction of non-methane carbon (Lurmann et al. 1992). 1-Propanol was chosen to represent oxygenated compounds because the reactivity of 1-propanol toward OH radicals was similar to the reactivity of n-hexane (Atkinson 1989). Ammonium sulfate was used as the test aerosol because sulfate and ammonium were the most abundant inorganic anionic and cationic species in the troposphere (Heintzenberg 1989).

Experimental Methods

The relative rate technique (Finlayson-Pitts & Pitts Jr. 1986) was used to investigate the effects of aerosols on the kinetics of the OH radical/organic reaction. This method relies on the comparison of the rates of disappearance of a “reference” (R) organic compound with a known OH radical reaction rate constant and a compound of interest, the “sample” (S), with an unknown OH radical reaction rate constant. The OH radicals react with the reference and sample, and the reactions are governed by individual rate constants k_s and k_r:

$$\dot{\mathrm{O}}\mathrm{H} + \mathrm{S} \xrightarrow{k_s} \mathrm{Products} \tag{3.1}$$

$$\dot{\mathrm{O}}\mathrm{H} + \mathrm{R} \xrightarrow{k_r} \mathrm{Products} \tag{3.2}$$

Provided that the sole loss process for the reference and reactant is reaction with OH radicals, the following relationship holds:

$$\ln\left[\frac{S_o}{S_t}\right] = \frac{k_s}{k_r}\ln\left[\frac{R_o}{R_t}\right] \tag{3.3}$$

The subscripts o and t denote time zero and t, respectively. Plots of experimental data for $\ln[S_o/S_t]$ vs. $\ln[R_o/R_t]$ should yield a straight line with a slope of k_s/k_r and an intercept of zero. Thus, knowing k_r, the value of k_s can be calculated using the slope. As mentioned in Chapter 1, compilations of rate constants for many organic compounds exist. Thus, the relative rate method is widely used to determine unknown rate constants (Atkinson, 1989, 1994). However, all published rate constant data for gas-phase reactions were determined under relatively pristine laboratory conditions. Thus, values for overall rate constants in the presence of aerosols do not exist. Hence, in this study, the relative rate (= k_s/k_r) was used as a measure of the effects of aerosols on the gas-phase reactions.

Experiments were carried out in 100-liter, 2-mil Tedlar® bags, with irradiation provided by eight 40-W black lamps. A detailed description of the system with a schematic diagram (Figure 2-1) appears in Chapter 2. All experiments were performed at room temperature, 298 ± 2K, and atmospheric pressure, ~ 760 Torr. Hydroxyl radicals were generated by the photolysis of methyl nitrite in air at wavelengths greater than 300 nm (Atkinson et al. 1981). The reactions leading to the formation of the OH radical are:

$$CH_3ONO + h\nu \rightarrow CH_3\dot{O} + NO \tag{3.4}$$

$$CH_3\dot{O} + O_2 \rightarrow CH_2O + H\dot{O}_2 \tag{3.5}$$

$$H\dot{O}_2 + NO \rightarrow \dot{O}H + NO_2 \tag{3.6}$$

According to published data (Atkinson 1989, 1994), the reactions of O_3 and NO_3 radicals with the organics studied are negligible. However, several experiments were conducted in the presence of excess NO to suppress O_3 and NO_3 radical formation, and to ensure that reaction with OH radicals was the primary loss process for the organics.

Methyl nitrite was synthesized by the dropwise addition of a 50% sulfuric acid solution into a methanol-saturated solution of sodium nitrite, according to the method of Taylor et al. (1980). The methyl nitrite produced was swept out of the reaction flask by a stream of high-purity nitrogen, passed through a saturated sodium hydroxide trap to remove traces of sulfuric acid, dried by passing through a calcium sulfate trap, and collected at 196K. The methyl nitrite was purified using a glass vacuum manifold system, and then subsequently stored in a stainless steel lecture bottle. The purity of the methyl nitrite was >99+ %, as verified by an FT-IR spectrometer.

Purely Gas-Phase Study

Experiments were carried out in the absence of aerosols to determine a baseline for the studies. An evacuable glass manifold system with two pressure gauges of a combined measuring range of 10^{-3} to 10^{3} Torr was used to admit methyl nitrite into the bag. Methyl nitrite was expanded into a 1.87 l evacuated glass bulb to give the desired pressure, and admitted into the bag by a stream of purified air. Three organic compounds, 1-propanol, n-hexane, and p-xylene were directly injected to the stream of purified air flowing into the bag during the methyl nitrite loading process. The bag was typically filled with 80 l of the air/reactant mixture. Initial concentrations for gaseous compounds were typically 30 to 50 ppm of methyl nitrite, 8 to 14 ppm of 1-propanol, 4 to 6 ppm of n-hexane, 1 to 4 ppm of p-xylene, and 20 to 30 ppm of NO. One experiment was carried out in the presence of NO, and four experiments in the absence of NO.

After admitting the gaseous reactants, initial concentration measurements were conducted. The reactant mixture was then photolyzed in 2 min increments for a total of 10 min of photolysis. Gas analyses were carried out initially and following each irradiation on a Finnigan-MAT GCQ system. The gas chromatograph (Model 9100) is equipped with a split/splitless injector, a six-port stainless steel injection valve, and a 30 m × 0.25 mm i.d. DB-WAX capillary column (J&W Scientific Co.). Split injections of 2 ml of sample were made with the six-port injection valve. Samples were drawn from the bag through a particle filter, then to a heated (150 °C) 2 ml stainless loop at about 1 l $\min^{-1}$ before being injected onto the column. The column temperature was programmed at 40 °C for 1 min, then increased at 40 °C $\min^{-1}$ to 100 °C, and held for 1.5 min at the final temperature. Helium flowed at a constant linear velocity of 45 cm s^{-1}.

Calibration curves for each compound and typical chromatograms for the mixtures can be found in Appendices B and C, respectively.

Separate experiments were conducted to ensure that the major loss process for the reactants was due to reaction with the OH radicals. In general, the loss processes involved either interaction with the walls of the bag, photolysis, or interaction with another species. First, to check for losses via interactions between the reactants and the walls, n-hexane, p-xylene, and 1-propanol were mixed thoroughly in the Tedlar® bag, sampled for GC analysis, left to stand for 30 min, and then sampled again. GC analyses of the mixture before and after standing were, within the experimental errors (approximately 3%), indistinguishable. Second, to check for losses of the reactants via photolysis, the three organics were introduced to the bag, sampled for GC analysis, irradiated for 10 min, and then subsequently sampled. No changes in GC analyses of samples taken before and after irradiation were observed. A potential complication following irradiation of the gas mixtures is the formation of products that interfere with the GC analysis of reactants. Separate experiments were therefore carried out in which mixtures of methyl nitrite and each reactant were irradiated and analyses performed to check for possible overlapping retention times in the GC analyses. No such interferences were observed for irradiation times typical of the present work (up to 10 min).

Study in the Presence of Aerosols

The effects of aerosols on the reaction kinetics were studied using ammonium sulfate aerosols. First, gaseous reactants consisting of methyl nitrite, n-hexane, p-xylene, and 1-propanol were introduced into the Tedlar® bag using the same method described earlier. The bag was typically filled with 65 l of the air/reactant mixture. After admitting the gaseous reactants to the bag, the aerosol was introduced. The aerosol was generated by atomizing an aqueous solution containing 1% ammonium sulfate by mass using a Collison atomizer (Peters et al. 1994, Li & Lundgren 1997). The purity of ammonium sulfate was >99.7%. The aerosol generated was passed through a diffusional dryer (Hinds 1982, Wang et al. 1992) and a ^{85}Kr charge neutralizer before being admitted to the bag. (Note: In addition to removing water, the drier is not expected to change the chemical composition of the particles since the drier only uses silica gel.) The bag was typically filled with 15 l of the air/aerosol mixture.

The size distribution of the particles was determined using an electrical aerosol analyzer (EAA, Model 3030, TSI, Inc). The EAA provided measurement of particle number size distributions in the range of 0.01 to approximately 1 μm. The EAA data were converted from number distribution to surface area and volume distributions assuming spherically shaped particles. The aerosol number median diameter and number concentration were approximately 0.05 μm and 6.5×10^4 cm^{-3}, respectively. These corresponded to a surface area median diameter, surface area, mass median diameter, and mass concentration of approximately 0.15 μm, 1,400 μm^2 cm^{-3}, 0.20 μm, and 62 μg m^{-3}, respectively. These values are in the range of atmospheric aerosols for polluted urban areas (Willeke & Whitby 1975, Hughes et al. 1998). The initial aerosol number, surface area, and volume distributions are shown in Figure 3-1.

Initial concentrations for gaseous compounds were the same as those used in the purely gas-phase studies. The bag was flushed twice with zero air between experiments. After flushing, the bag was filled with zero air, and the particle concentration was

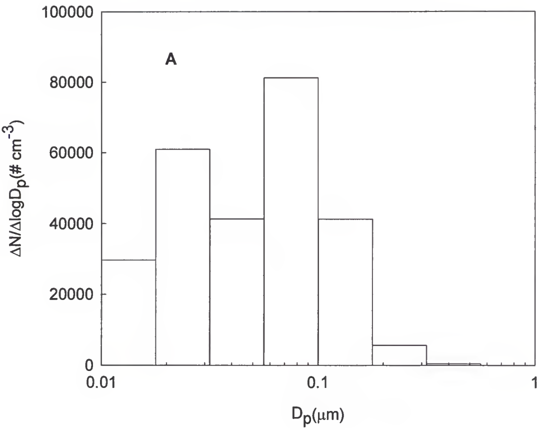

Figure 3-1. Size distributions of the aerosols in the bag. (A) Number (B) Surface area (C) Volume

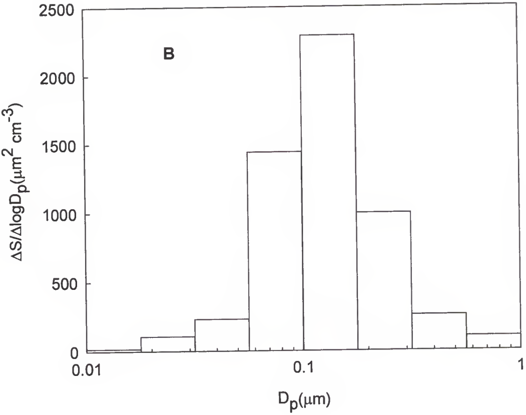

Figure 3-1--continued

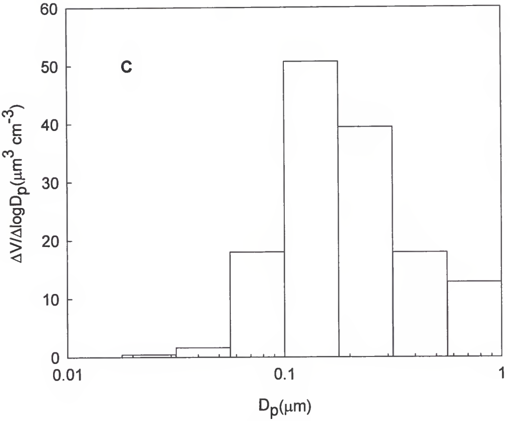

Figure 3-1--continued

measured by the EAA to check the amount (if any) of residual particle. In all cases, the amount of residual particle in the bag was negligible (<10 $\mu m^2\ cm^{-3}$).

As mentioned in Chapter 2, the size distribution and concentration of the aerosols in the bag could change because of coagulation, sedimentation and deposition to the walls (Crump & Seinfeld 1981). To avoid a change in aerosol characteristics during an experiment, each experiment consisted of only one irradiation time varying between 2 and 6 min. The change of aerosol surface area for this time scale was less than 10%. A total of 20 experiments were carried out, 7 in the presence of NO, and 13 in the absence of NO.

There are several possible loss processes for the gaseous reactants when aerosols are present in the bag. These losses could lead to significant errors in the interpretation of kinetic data. Based on the purely gas-phase studies, losses due to interactions between gaseous species, wall interactions, and photolysis of the reactants were negligible. Another possible loss mechanism for the organics in the bag was uptake by the aerosols or water vapor. Several additional experiments were carried out to study these possible interferences. First, to address the issue of organic uptake by the particles, 1-propanol, n-hexane, and p-xylene were admitted to the bag with aerosols and left to stand for 30 min. The concentration changes of the gas-phase reactants were monitored via GC, and were negligible (less than 5%). Second, to examine the effects of water vapor, humidified air was introduced into the reactants/air mixture. No significant changes in GC analyses were observed over a 30 min period. Finally, to check for possible interferences by irradiation, the above mentioned mixtures were irradiated for 6 minutes. GC analyses were conducted before and after irradiation. No observable concentration changes of the gaseous reactants were detected. These results indicated that the interactions with aerosols and water vapor were not significant. Thus, the reaction with the OH radical was the predominant loss process for the reactants in the bag.

Results and Discussion

Reactions in the Absence of Aerosols

The relative rates of the following competing reactions in the absence of aerosols were obtained by linear least-squares analyses of five different runs:

$$\dot{\mathrm{O}}\mathrm{H} + \text{n-hexane} \xrightarrow{k_h} \text{Products} \tag{3.7}$$

$$\dot{\mathrm{O}}\mathrm{H} + \text{p-xylene} \xrightarrow{k_x} \text{Products} \tag{3.8}$$

$$\dot{\mathrm{O}}\mathrm{H} + \text{1-propanol} \xrightarrow{k_p} \text{Products} \tag{3.9}$$

Three pairs of relative rates were obtained from the studies, including 1-propanol/n-hexane (k_p/k_h), n-hexane/p-xylene (k_h/k_x) and 1-propanol/p-xylene (k_p/k_x). Figure 3-2 shows plots of $\ln[(Reactant_1)_0/(Reactant_1)_t]$ vs. $\ln[(Reactant_2)_0/(Reactant_2)_t]$ for the three pairs of reactants. There was no significant difference between data obtained in the presence versus the absence of NO. Thus, the reactions with O_3 and NO_3 radicals were indeed negligible. Linear least-squares analyses of the data from the purely gas-phase studies in Figure 3-2 yield $k_p/k_h = 0.85 \pm 0.05$, $k_h/k_x = 0.53 \pm 0.02$, and $k_p/k_x = 0.45 \pm 0.03$. Error limits represent 95% confidence intervals.

A comparison between the gas-phase studies performed at the University of Florida and those performed elsewhere can be made by comparing the newly derived rate constant ratios to those obtained using data available in the literature. The recommended

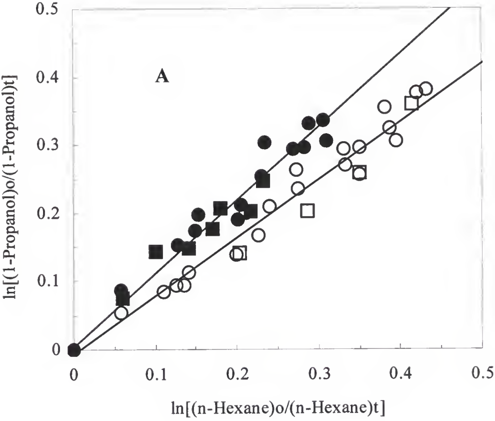

Figure 3-2. Plots of ln[*(Reactant$_1$)$_o$/(Reactant$_1$)$_t$*] vs. ln[*(Reactant$_2$)$_o$/(Reactant$_2$)$_t$*] in the absence of aerosols (○: in the absence of NO, □: in the presence of NO) and the presence of $(NH_4)_2SO_4$ aerosols (●: in the absence of NO, ■: in the presence of NO) using the following pairs: (A) 1-propanol/n-hexane; (B) n-hexane/p-xylene; (C) 1-propanol/p-xylene. The lines represent linear least squares fit to the data.

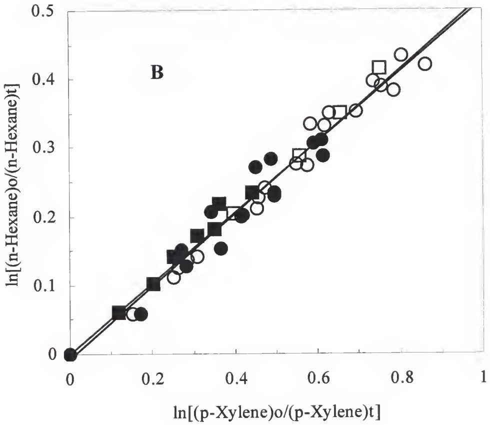

Figure 3-2--continued

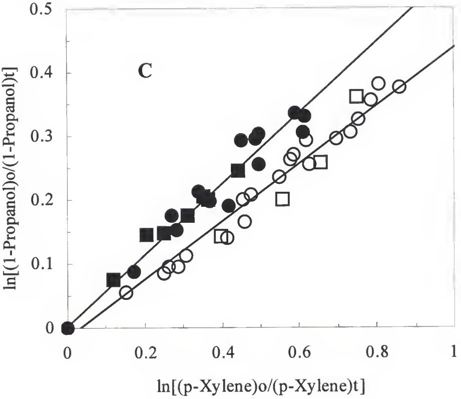

Figure 3-2--continued

rate constants for the OH radical reaction with n-hexane, p-xylene, and 1-propanol are 5.61×10^{-12} cm^3 molecule^{-1} s^{-1}, 14.3×10^{-12} cm^3 molecule^{-1} s^{-1}, and 5.53×10^{-12} cm^3 molecule^{-1} s^{-1}, respectively, with overall uncertainties of 25%, 40%, and 30%, respectively (Atkinson 1989, 1994). The relative rates calculated using the recommended rate constants are 0.99, 0.39, and 0.39 for 1-propanol/n-hexane, n-hexane/p-xylene, and 1-propanol/p-xylene, respectively. Considering the overall uncertainties of the recommended rate constants, the observed relative rates are in agreement with the literature values, thereby validating the technique used in this study.

Reactions in the Presence of Aerosols

The relative rates of the reactions of the OH radical with the three organic compounds in the presence of ammonium sulfate aerosols were obtained by linear least-squares analyses of the data. Plots of $\ln[(Reactant_1)_o/(Reactant_1)_t]$ vs. $\ln[(Reactant_2)_o/(Reactant_2)_t]$ are shown in Figure 3-2. There was no significant difference between data obtained in the presence versus the absence of NO. As shown in Figure3-2A, a change in the relative OH reaction rates of 1-propanol as compared to n-hexane in the presence of ammonium sulfate aerosols is apparent. The relative rate increased by approximately 26%, from 0.85 ± 0.05 in the absence of aerosols to 1.07 ± 0.05 in the presence of ammonium sulfate aerosols. Errors represent 95% confidence intervals. This indicates that ammonium sulfate aerosols promote the reaction of 1-propanol with OH radicals significantly as compared to n-hexane. However, no influence on the relative rate of n-hexane/p-xylene was observed, as can be seen in Figure 3-2B. The relative rates were 0.53 ± 0.02 in the absence of aerosols, and 0.51 ± 0.02 in the presence of ammonium sulfate aerosols. This indicates that ammonium sulfate aerosols have the same effect on the OH radical reaction kinetics of n-hexane and p-xylene. Based on these results, the change in the relative rate of the 1-propanol/p-xylene system should be the same as that observed in the 1-propanol/n-hexane system. This was confirmed by Figure 3-2C. The relative rate for 1-propanol/p-xylene increased by 23%, from 0.45 ± 0.03 to 0.56 ± 0.02 in the presence of aerosols.

Implications for Tropospheric Chemistry Modeling

Based on the relative rates obtained, the reaction rate of the 1-propanol/OH radical reaction is affected by aerosols. The rate constant of the 1-propanol/OH radical reaction may be increased from 5.53×10^{-12} cm^3 molecule^{-1} s^{-1} (which is the recommended rate constant) to 6.99×10^{-12} cm^3 molecule^{-1} s^{-1} (26% increase) under real atmospheric conditions. Using an average tropospheric concentration for OH radicals of 1.5×10^6 molecule cm^{-3}, the estimated tropospheric lifetime of 1-propanol decreases from 1.4 days to 1.1 days. Based on this information, the ozone forming potential of 1-propanol should also be modified. The formation of ozone from the gas-phase reactions of 1-propanol in the atmosphere can be expressed by the following simplified reactions using the recommended rate constants given by Atkinson (1989, 1994):

$$\text{1-Propanol} + \dot{\text{O}}\text{H} \rightarrow \dot{\text{R}} + \text{H}_2\text{O} \qquad k_{3.10} = 5.53\times10^{-12}\ \text{cm}^3\ \text{molecule}^{-1}\ \text{s}^{-1} \quad (3.10)$$

$$k'_{3.10} = 6.91\times10^{-12}\ \text{cm}^3\ \text{molecule}^{-1}\ \text{s}^{-1}$$

$$\dot{\text{R}} + \text{O}_2 \rightarrow \text{R}\dot{\text{O}}_2 \qquad k_{3.11} = 8.00\times10^{-12}\ \text{cm}^3\ \text{molecule}^{-1}\ \text{s}^{-1} \quad (3.11)$$

$$\dot{R}O_2 + NO \rightarrow \dot{R}O + NO_2 \qquad k_{3.12} = 8.90\times10^{-12}\ \mathrm{cm^3\ molecule^{-1}\ s^{-1}} \qquad (3.12)$$

$$NO_2 + h\nu \rightarrow NO + O \qquad k_{3.13} = 8.33\times10^{-3}\ \mathrm{s^{-1}} \qquad (3.13)$$

$$O + O_2 \xrightarrow{M} O_3 \qquad k_{3.14} = 1.50\times10^{-14}\ \mathrm{cm^3\ molecule^{-1}\ s^{-1}} \qquad (3.14)$$

where R is an alkyl group and M represents any third body. The above reactions were implemented in Acuchem (Braun et al. 1986) to obtain concentration versus time profiles for all reactants and products. The rate constant for reaction (3.10) was varied between the recommended value from purely gas-phase studies ($k_{3.10}$) and the value obtained using the results of this study ($k'_{3.10}$). It is important to note that there are limitations to the Acuchem modeling since no data exist concerning the effects of aerosols on the reactions of the R or RO radicals. A recent paper by Jacob (2000) indicated that these reactions may be unaffected by the presence of aerosols. Thus, the rate constants of reaction involving these species were not altered. Average tropospheric concentrations for the OH radical, NO, and O_2 of 1.50×10^{6}, 9.84×10^{11}, and 5.17×10^{18} molecule cm^{-3}, respectively, were used. The initial concentration for 1-propanol was 2.46×10^{8} molecule cm^{-3}, and a 12 h reaction time period was used. As shown in Figure 3-3, the ozone concentration is increased by up to 25% when the new rate constant is used. Clearly this result has profound implications for the use of air quality models for the assessment of air pollution control strategies.

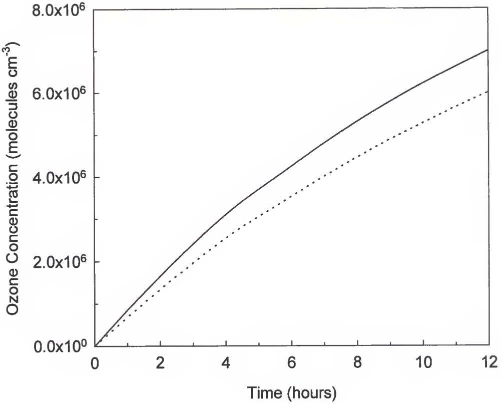

Figure 3-3. Estimated ozone concentrations obtained from the atmospheric reactions of 1-propanol using the recommended rate constant (······) and the new rate constant (——) of the 1-propanol/OH radical reaction.

CHAPTER 4

EFFECTS OF AMMONIUM SULFATE AEROSOLS ON THE GAS-PHASE REACTIONS OF THE HYDROXYL RADICAL WITH C_1-C_6 ALIPHATIC ALCOHOLS

Background

As in the previous study (Chapter 3), promotion of the reactions of OH radicals with 1-propanol as compared to the reactions with n-hexane or p-xylene were observed in the presence of ammonium sulfate aerosols. Considering that ammonium and sulfate are major constituents of atmospheric aerosols (Heintzenberg 1989), the results suggested that the kinetics of OH radical reactions of selected VOCs could be affected by atmospheric aerosols. Therefore, it is important to investigate the effects of atmospheric aerosols on the reactions of a series of organic compounds with varying carbon number.

Over seventy alcohols are present in the atmosphere as a result of both biogenic and anthropogenic emissions (Graedel et al. 1986). Among these, the C_1 to C_5 alcohols are widely used in industrial applications, and are also emitted from biological processes. Methanol and ethanol have also been used as gasoline additives to reduce the reactivity of evaporative and tailpipe emissions from vehicles (Seinfeld et al. 1994). Ethanol has been used as a fuel in Brazil for over 20 years (Grosjean et al. 1998). Thus, the tropospheric chemistry of alcohols is important. The most prominent loss mechanism for the alcohols in the daytime is reaction with OH radicals (Atkinson 2000), and reaction sequences for the simpler aliphatic alcohols are known (Atkinson 2000, Azad & Andino 1999). Kinetic studies of OH radical reactions with alcohols have been performed in purely gas-phase environments (Atkinson 1989, 1994). In general, the gas-phase kinetic rate constants of OH radical reactions with VOCs increase with increasing carbon chain length. A structure-activity relationship has been developed to estimate unknown kinetic constants for OH radical reactions (Kwok & Atkinson 1995, Neeb 2000). However, few studies have been performed to investigate the effects of aerosols on these kinetic constants.

The work presented in this chapter examines the effects of ammonium sulfate aerosols on the kinetics of the OH radical reactions with C_1-C_6 aliphatic alcohols. Small aliphatic alcohols such as methanol, ethanol, 1-butanol, 1-pentanol and 1-hexanol were selected because of their importance in tropospheric chemistry. The results from these straight chain alcohol studies could provide insight to the relationship between the promoting effects of aerosols and chain number, if present. Two different aerosol concentrations typical of polluted urban conditions were tested.

Experimental Methods

The apparatus and experimental procedures were described in Chapters 2 and 3. Thus, only a brief summary is given here. The relative rate ($= k_s/k_r$) was used as a measure of the effects of aerosols on the kinetics of the OH radical/alcohol reaction. The relative rates of the alcohols and the reference compound in the absence and presence of aerosols were determined, and changes in the relative rates were used as an indication of the effects of aerosols on the reactions.

Experiments were carried out in 100-liter, 2-mil Tedlar® bags, with irradiation provided by eight 40-watt black lamps. All experiments were performed at room temperature, 298 ± 2K, and atmospheric pressure, ~ 760 Torr. Hydroxyl radicals were generated by the photolysis of methyl nitrite in air at wavelengths greater than 300 nm. Methyl nitrite was synthesized by the dropwise addition of a 50% sulfuric acid solution into a methanol-saturated solution of sodium nitrite, according to the method of Taylor et al. (1980).

The gaseous reactants were introduced into the bag by either direct syringe injection or via an evacuable glass manifold system. Methyl nitrite was expanded into a 1.87 l evacuated glass bulb to give the desired pressure, and admitted into the bag by a stream of purified air. The alcohols and the reference compounds were directly injected to the stream of purified air flowing into the bag during the methyl nitrite loading process. After admitting the gaseous reactants to the bag, the aerosol was introduced. The aerosol was generated by atomizing an aqueous solution containing 1 wt % of ammonium sulfate using a Collison atomizer. The purity of the ammonium sulfate was >99.7%. The aerosol generated was passed through a diffusional dryer and a ^{85}Kr charge neutralizer (TSI, Inc.) before being admitted to the bag. The aerosol concentration in the bag was controlled by changing the air flows of both the gaseous reactants and the aerosol. The bag was typically filled with 80 l of the air/reactant/aerosol mixture.

Gas analyses were carried out with a Finnigan-MAT GCQ system. The gas chromatograph (Model 9100) was equipped with a split/splitless injector and a 30 m x 0.25 mm i.d. DB-WAX capillary column (J&W Scientific Co.). Split injections of 1 mL of sample were made with a gas tight syringe (Hamilton Co.). Samples were drawn from the bag through a particle filter to prevent any interferences in GC analyses from the aerosols. Particle size distributions were determined using an electrical aerosol analyzer (EAA, Model 3030, TSI, Inc).

Ethanol, 1-Butanol, 1-Pentanol and 1-Hexanol Study

The relative rates of OH radical reactions with ethanol, 1-butanol, 1-pentanol, and 1-hexanol in the absence and presence of ammonium sulfate aerosols were determined using p-xylene as a reference compound. P-xylene was chosen as the reference since its behavior in the presence of ammonium sulfate aerosols had been characterized previously (see Chapter 3). In order to minimize interferences between reactants and products, the following combinations of alcohols and reference compound were employed: 1-butanol / 1-pentanol / p-xylene, 1-hexanol / p-xylene, and ethanol / p-xylene. First, experiments were carried out in the absence of aerosols to determine baselines for the studies. Irradiations were carried out for 2 to 10 min (1-butanol / 1-pentanol), 1 to 5 min (1-hexanol), or 1 to 8 min (ethanol). Concentration measurements were conducted initially and after each irradiation using the GCQ system. The GC column temperature was programmed at 40°C for thirty seconds, then increased at a rate of 10°C min^{-1} to 90°C, and at a rate of 40°C min^{-1} to a final temperature of 180°C for the 1-butanol, 1-pentanol, and 1-hexanol studies. For the ethanol study, the column was held at 40°C for thirty seconds and then temperature programmed to 55°C at a rate of 5°C min^{-1} and 140°C at a rate of 40 °C min^{-1}. All mass spectral analyses were performed in the positive electron ionization mode. Initial concentrations for gaseous compounds were typically 30 ppm of methyl nitrite, 5.0 ppm of 1-butanol, 2.8 ppm of 1-pentanol, 3.7 ppm of 1-hexanol, 21 ppm of ethanol, and 1.2 ppm of p-xylene.

To verify the gas-phase rate constants obtained for the alcohol/OH reactions, additional relative rate experiments were conducted using cyclohexane as the reference compound. Also, the rate constant of the p-xylene/OH radical reaction was determined using cyclohexane and n-octane as reference compounds because literature values for the gas-phase rate constants of the p-xylene/OH radical reaction exhibited a significant degree of scatter (Atkinson 1989). The rate constant of the p-xylene/OH radical reaction obtained in this study was subsequently used to derive the rate constants of the alcohol/OH radical reactions. The alcohol/OH rate constants obtained using p-xylene and cyclohexane as reference compounds were compared to literature values to validate the relative rate technique used in this study. Initial concentrations of cyclohexane, n-octane, and p-xylene were 2.8 ppm, 1.9 ppm, and 1.2 ppm respectively. Initial concentrations of the alcohols were the same as those reported previously.

The effects of ammonium sulfate aerosols on the kinetics of the OH radical/alcohol reactions were studied in the presence of two different aerosol concentrations. Total surface areas were 1400 μm^2 cm^{-3} (Condition I) and 3400 μm^2 cm^{-3} (Condition II) ; these values are typical of total atmospheric aerosol surface areas found in polluted urban areas (Willeke & Whitby 1975, Hughes et al. 1998). Initial characteristics of aerosols admitted to the chamber are listed in Table 4-1, and the surface area distributions of the aerosols are shown in Figure 4-1. To avoid a change in aerosol characteristics during an experiment, only one irradiation time varying between 1 and 10 minutes was applied for each experiment. The change in aerosol surface area for these time scales was less than 10%. Initial concentrations of the gaseous compounds and the GC column conditions were the same as those used in the purely gas-phase studies.

Table 4-1. Initial aerosol characteristics in the bag for aerosol conditions I and II.

	I	II
Number		
Median Diameter (μm)	0.05	0.07
Concentration (# cm^{-3})	6.5×10^4	9.9×10^4
Surface Area		
Median Diameter (μm)	0.15	0.15
Concentration (μm^2 cm^{-3})	1400	3400
Mass		
Median Diameter (μm)	0.20	0.20
Concentration (μg m^{-3})	62	180

Methanol Study

The relative rate technique relies on choosing a reference compound with a rate constant similar to the rate constant of the sample compound. A large difference in rate constants between the reference compound and the sample compound results in large differences in concentration changes between the two compounds, thereby increasing the errors in the relative rate. Based on literature data (Atkinson 1994), the rate constant of the p-xylene/OH radical reaction (14.3×10^{-12} cm^3 $molecule^{-1}$ s^{-1}) is more than 10 times larger than the rate constant of the methanol/OH radical reaction (9.44×10^{-13} cm^3 $molecule^{-1}$ s^{-1}).

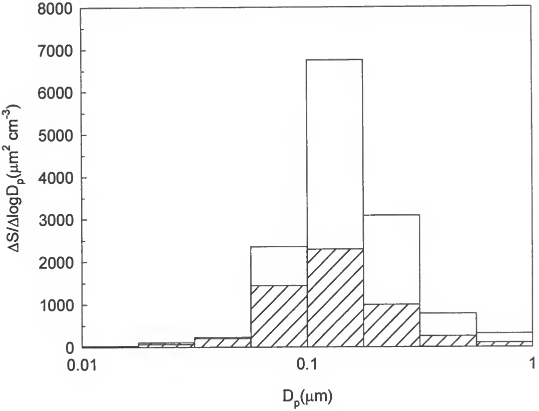

Figure 4-1. Surface area distributions of the aerosols in the bag (▨: Aerosol Condition I, □: Aerosol Condition II).

Thus, p-xylene could not be used as a reference compound for the methanol study. Ethanol, with an OH radical reaction rate constant of 3.27×10^{-12} cm^3 molecule^{-1} s^{-1} was used as a reference compound for the methanol study. The published ethanol/OH radical rate constant is within the range of the published rate constant for the methanol/OH radical reaction (Atkinson 1994). To confirm the gas-phase methanol rate constant, and therefore verify our experimental technique, the rate constant of the methanol/OH radical reaction in the absence of aerosols was also determined using cyclohexane as a reference compound. Initial concentrations of methanol, ethanol, and methyl nitrite were typically 30 ppm, 10 ppm, and 60 ppm, respectively. The GC column was programmed at 40°C for thirty seconds, then increased at a rate of 5°C min^{-1} to 60°C. Irradiations were carried out for 1 to 7 min in the absence of ammonium sulfate aerosols, and the experimental conditions in the presence of ammonium sulfate aerosols were identical to those used in the other alcohol studies mentioned previously.

Separate loss studies analogous to those described in Chapter 2 were conducted for all of the alcohols in the absence and presence of aerosols. The reaction with OH radicals was found to be the dominant loss process for all compounds studied. Other losses (wall interactions, gas-aerosol interactions, and photolysis) were negligible (<5%, total) over time scales identical to those used in the studies.

Results and Discussion

Reactions in the Absence of Aerosols

The relative rates of the OH radical reactions with the alcohols in the absence of aerosols were obtained by linear least-squares analyses of two different runs (with a total of 10-12 points) for each alcohol/reference compound combination. The data are plotted in accordance with equation (3.3), and the plots are shown in Figures 4-2 through 4-5. All plots generate good straight lines, and the relative rates (k_s/k_r) obtained as well as the reference compounds used are reported in Table 4-2. Errors represent 95% confidence intervals.

Gas-phase "sample" rate constants (k_s) were obtained by using the rate constants (k_r) of OH radical reaction with the reference compounds, p-xylene and ethanol. The OH rate constants for p-xylene and ethanol that were determined in this study were used to calculate the “sample” rate constants. The rate constant of the p-xylene/OH radical reaction was determined using cyclohexane and n-octane as reference compounds. Plots of ln[$(p\text{-}Xylene)_0/(p\text{-}Xylene)_t$] versus ln[$(Cyclohexane)_0/(Cyclohexane)_t$] and ln[$(n\text{-}Octane)_0/(n\text{-}Octane)_t$] are shown in Figure 4-6. The calculated rate constants for the p-xylene/OH radical reaction are in excellent agreement with each other (Table 4-3), giving an average rate constant of 12.9×10^{-12} cm^3 molecule^{-1} s^{-1} at 298 ± 2K. This value is within the recommended value of Atkinson (1989). The rate constant of the ethanol/OH radical reaction was determined using cyclohexane and p-xylene as reference compounds. The average rate constant of 2.7×10^{-12} cm^3 molecule^{-1} s^{-1} for the ethanol/OH reaction at 298 ± 2K is within the recommended value (Atkinson et al. 1999). The resulting rate constants of the OH reaction with the alcohols (using all references, including cyclohexane) are listed in Table 4-3. The recommend rate constant (Atkinson et al. 1999) of 7.21×10^{-12} cm^3 molecule^{-1} s^{-1} at 298 K was used for the cyclohexane/OH radical reaction. As can be seen in Table 4-3, there is excellent agreement between the

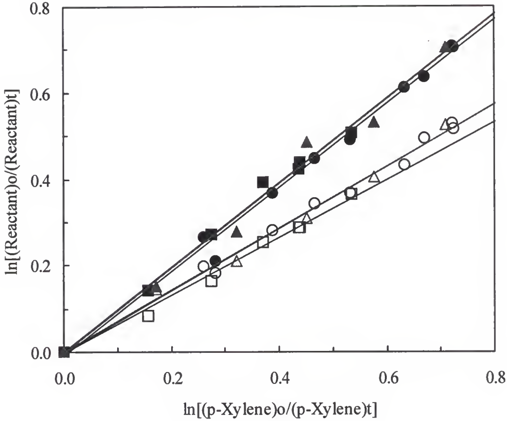

Figure 4-2. Plots of ln[*(Reactant)$_o$/(Reactant)$_t$*] vs. ln[*(p-Xylene)$_o$/(p-Xylene)$_t$*] in the absence of aerosols (○: 1-butanol, ●: 1-pentanol) and the presence of $(NH_4)_2SO_4$ aerosols (□: Aerosol Condition I, △: Aerosol Condition II for 1-butanol and ■: Aerosol Condition I, ▲: Aerosol Condition II for 1-pentanol). The lines represent linear least squares fit to the data.

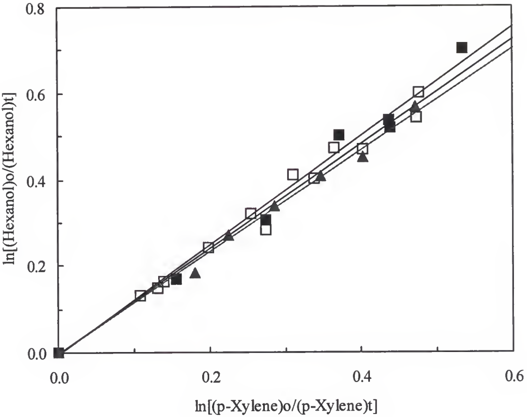

Figure 4-3. Plots of ln[*(1-Hexanol)$_o$/(1-Hexanol)$_t$*] vs. ln[*(p-Xylene)$_o$/(p-Xylene)$_t$*] in the absence of aerosols (□) and the presence of $(NH_4)_2SO_4$ aerosols (■:Aerosol Condition I, ▲: Aerosol Condition II). The lines represent linear least squares fit to the data.

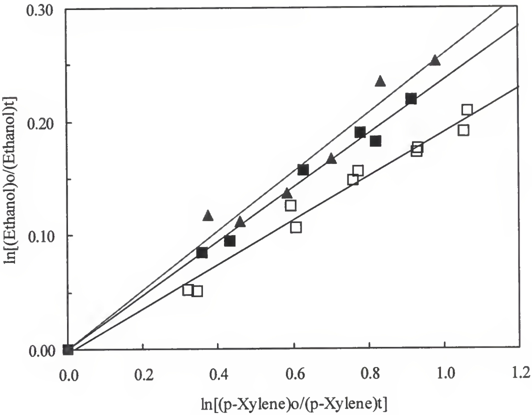

Figure 4-4. Plots of ln[*(Ethanol)$_o$/(Ethanol)$_t$*] vs. ln[*(p-Xylene)$_o$/(p-Xylene)$_t$*] in the absence of aerosols (□) and the presence of $(NH_4)_2SO_4$ aerosols (■:Aerosol Condition I, ▲: Aerosol Condition II). The lines represent linear least squares fit to the data.

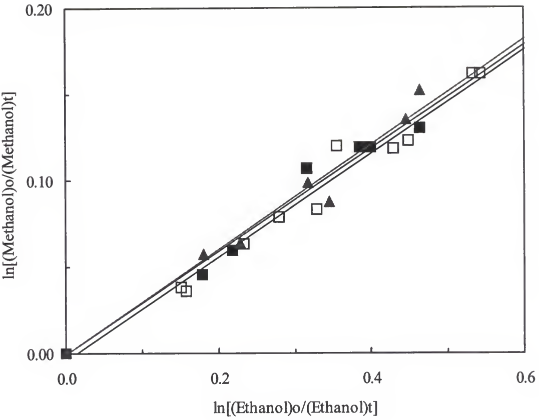

Figure 4-5. Plots of ln[*(Methanol)$_o$/(Methanol)$_t$*] vs. ln[*(Ethanol)$_o$/(Ethanol)$_t$*] in the absence of aerosols (□) and the presence of $(NH_4)_2SO_4$ aerosols (■:Aerosol Condition I, ▲: Aerosol Condition II). The lines represent linear least squares fit to the data.

Table 4-2. Relative rates (k_s/k_r) for the reactions of OH radical with aliphatic alcohols in the absence and presence of aerosols at 298 K.

Sample Compound	Reference Compound	Relative rates (k_s/k_r)[a]		
		In the absence of aerosols	In the presence of ammonium sulfate aerosols	
			I	II
methanol	ethanol	0.30 ± 0.03	0.30 ± 0.02	0.30 ± 0.02
Ethanol	p-xylene	0.19 ± 0.01	0.24 ± 0.01	0.26 ± 0.02
1-propanol	p-xylene	0.45 ± 0.03[b]	0.56 ± 0.02[b]	0.55 ± 0.03
1-butanol	p-xylene	0.72 ± 0.03	0.67 ± 0.03	0.72 ± 0.03
1-pentanol	p-xylene	0.98 ± 0.05	0.98 ± 0.03	0.98 ± 0.06
1-hexanol	p-xylene	1.23 ± 0.08	1.26 ± 0.07	1.17 ± 0.04

[a] Errors represent 95% confidence intervals.

[b] Determined in Chapter 3.

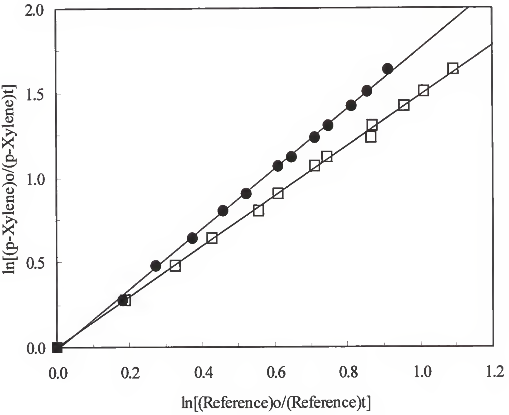

Figure 4-6. Plots of ln[*(Reference)$_o$/(Reference)$_t$*] vs. ln[*(p-Xylene)$_o$/(p-Xylene)$_t$*] in the absence of aerosols using n-octane as a reference compound (☐) and cyclohexane as a reference compound (●).

Table 4-3. Gas-phase relative rates (k_s/k_r) and rate constant (k_s) for the reactions of OH radical with aliphatic alcohols and p-xylene at room temperature.

Sample compound	Reference compound	Relative rates (k_s/k_r)[a]	Rate constants (10^{-12} cm^3 $molecule^{-1}$ s^{-1})	
			This work[a]	Recommended[b]
methanol	ethanol	0.30 ± 0.03	0.81 ± 0.08[c]	0.93 ± 0.23 (± 25 %)[d]
	cyclohexane	0.12 ± 0.01	0.84 ± 0.05[e]	0.89[f]
ethanol	p-xylene	0.19 ± 0.01	2.5 ± 0.2[g]	3.2 ± 0.8 (± 25 %)[d]
	cyclohexane	0.40 ± 0.04	2.9 ± 0.3[e]	3.2[f]
1-propanol	p-xylene	0.45 ± 0.03	5.8 ± 0.4[g]	5.5 ± 1.7 (± 30 %)[d]
	cyclohexane	0.77 ± 0.05	5.5 ± 0.4[e]	
1-butanol	p-xylene	0.72 ± 0.03	9.3 ± 0.4[g]	8.1 ± 2.4 (± 30 %)[d]
	cyclohexane	1.26 ± 0.04	9.1 ± 0.3[e]	
1-pentanol	p-xylene	0.98 ± 0.05	12.6 ± 0.7[g]	11.1 ± 3.9 (± 35 %)[h]
	cyclohexane	1.66 ± 0.08	12.0 ± 0.6[e]	
1-hexanol	p-xylene	1.23 ± 0.08	15.9 ± 1.0[g]	12.5 ± 4.4 (± 35 %)[h]
	cyclohexane	1.98 ± 0.10	14.3 ± 0.7[e]	
p-xylene	cyclohexane	1.77 ± 0.03	12.8 ± 0.2[e]	14.3 ± 5.7 (± 40 %)[i]
	n-octane	1.49 ± 0.03	12.9 ± 0.2[j]	

[a] Errors represent 95% confidence intervals.

[b] Values in parentheses represent overall uncertainties in percent form.

[c] Obtained by using k_r(ethanol) = 2.7×10^{-12} cm^3 $molecule^{-1}$ s^{-1} determined in this study.

[d] From Atkinson et al. 1999.

[e] Obtained by using k_r(cyclohexane) = 7.21×10^{-12} cm^3 $molecule^{-1}$ s^{-1} (Atkinson 1997).

[f] From DeMore et al. 1997.

[g] Obtained by using k_r(p-xylene) = 12.9×10^{-12} cm^3 $molecule^{-1}$ s^{-1} determined in this study.

[h] From Atkinson 1994.

[i] From Atkinson 1989.

[j] Obtained by using k_r(n-octane) = 8.71×10^{-12} cm^3 $molecule^{-1}$ s^{-1} (Atkinson 1997).

calculated rate constants using different references for each alcohol/OH reaction. These data illustrate that our system shows internal consistency.

Many kinetic studies of OH radical reactions with alcohols have been performed, and recommended values for rate constants appear in Atkinson (1994, 1999). However, only a few studies have been conducted for 1-butanol, 1-pentanol and 1-hexanol (Wallington et al. 1987, 1988, Nelson et al. 1990). Thus, the recommended values were based on these limited data. Considering overall uncertainties in the recommended rate constants, the observed gas-phase rate constants using p-xylene as a reference compound are generally in very good agreement with the recommended values. The observed rate constant of the methanol/OH radical reaction is 14% lower than the recommended values, and within the overall uncertainties reported in the literature (±25%). For ethanol and 1-propanol, the observed rate constants are 22% lower and 6% higher, respectively, than the recommended values. However, both are within the overall uncertainties reported in the literature of ±25% and ±30%, respectively. The observed rate constants for 1-butanol and 1-pentanol are 15% and 14% higher than the recommended values, and are within the reported overall uncertainties of ±35%. The observed rate constant for the 1-hexanol/OH radical reaction is $(15.9 \pm 1.0) \times 10^{-12}$ cm^3 $molecule^{-1}$ s^{-1}, and is 27% higher than the previously recommended value of Atkinson (1994), but within the reported overall uncertainty of ±35%. In addition, this value is in excellent agreement with the recently reported rate constant of $(15.8 \pm 3.5) \times 10^{-12}$ cm^3 $molecule^{-1}$ s^{-1} of Aschmann and Atkinson (1998). Thus, our data fall within the acceptable ranges of published rate constants, thereby validating the relative rate technique used in this study.

Reactions in the Presence of Aerosols

The relative rates of the reactions of the OH radical with C_1- C_6 aliphatic alcohols in the presence of ammonium sulfate aerosols were determined at two aerosol concentrations. The total surface area of aerosols were 1400 $\mu m^2\ cm^{-3}$ and 3400 $\mu m^2\ cm^{-3}$ for aerosol conditions I and II, respectively. Plots of $\ln[(Sample)_o/(Sample)_t]$ vs. $\ln[(Reference)_o/(Reference)_t]$ for the purely gas-phase conditions as well as for aerosol conditions I and II are shown in Figure 4-2 through Figure 4-5. The experimentally determined relative rates are listed in Table 4-2. No significant effects on the kinetics of OH radical reactions with 1-butanol, 1-pentanol or 1-hexanol were observed for either aerosol concentration. The relative rates of the 1-butanol/OH radical reaction, 1-pentanol /OH radical reaction and 1-hexanol/OH radical reaction versus the p-xylene/OH radical reaction in the absence and presence of aerosols were identical, within the error limits. However, as shown in Figure 4-4, the relative rate of the ethanol/OH radical reaction versus the p-xylene/OH radical reaction increased by 26% (from 0.19 ± 0.01 to 0.24 ± 0.01) for aerosol condition I and 37% (from 0.19 ± 0.01 to 0.26 ± 0.02) for aerosol condition II. Errors represent 95% confidence intervals. This indicates that ammonium sulfate aerosols promote the reaction of ethanol with OH radicals significantly as compared to p-xylene. This promotion effect is similar to the effect determined in the previous study (see Chapter 3) with the 1-propanol/OH radical reaction. However no significant additional increase in the promotion effects on the 1-propanol/OH radical reaction and ethanol/OH radical reaction were observed in studies using higher aerosol concentrations.

The effects of aerosols on the methanol/OH radical reaction were compared to the ethanol/OH radical reaction. No changes in the relative rates of the methanol/OH radical reaction versus the ethanol/OH radical reaction in the absence and presence of ammonium sulfate aerosols were observed for either aerosol concentrations. The relative rates of the methanol/OH radical reaction versus the ethanol/OH radical reaction were 0.30 ± 0.03, 0.30 ± 0.02, and 0.30 ± 0.02 for the purely gas-phase condition, aerosol condition I, and aerosol condition II, respectively. This indicates that the effects of ammonium sulfate aerosols on the kinetics of the methanol/OH radical reaction and the ethanol/OH radical reaction are the same. Therefore, ammonium sulfate aerosols promote the methanol/OH radical reaction as much as the ethanol/OH radical reaction. The average increases in the relative rates of the OH radical reactions of methanol, ethanol, and 1-propanol versus p-xylene in the presence of ammonium sulfate aerosols are 32%, 32%, and 23%, respectively.

Discussion

The results of this study show that ammonium sulfate aerosols promote the reactions of OH radicals with aliphatic alcohols containing fewer than four carbons as compared to the reaction of OH radicals with p-xylene. However, no effects were observed for the reactions of OH radicals with aliphatic alcohols containing more than three carbons.

Henry's law solubility is believed to play an important role in the uptake of gaseous compounds by liquid aerosols (Kolb et al. 1997). Henry's constants in units of M atm^{-1} for methanol, ethanol, 1-propanol, 1-butanol, 1-hexanol, and p-xylene are 2.2×10^{2},

1.9×10^2, 1.3×10^2, 1.3×10^2, 5.4×10^1, and 1.3×10^{-1}, respectively (Snider & Dawson 1985, Yaws & Yang 1992, Staudinger & Roberts 1996). Differences in the Henry's constant of the alcohols are relatively small. Thus, if one only considers the Henry's law constants, one might expect the OH initiated reactions of the alcohols to be promoted in identical fashions in the presence of aerosols. However, this is not the case. Thus, Henry's law constants are not the primary factor affecting the enhancement noticed in the OH radical reaction with the smaller ($<C_4$) alcohols.

Steric effects may explain the observed variations in the relative rate constants in the presence of aerosols. Because of their relatively small size, more molecules of the $<C_4$ alcohols should be able to interact with the surfaces of the aerosols as compared to the alcohols containing more than three carbon atoms. If more alcohols can interact with the surface, and the reactions are influenced by the presence of the surfaces, then the rate constants will be enhanced.

The data presented in Table 4-2 indicate that, within errors, there is essentially no difference in the relative rates under the two aerosol conditions. If the differences observed between the purely gas-phase studies and the studies conducted using aerosol condition I are due to surface effects, one might expect to see an increase in the relative rates using the higher aerosol concentrations of study II. However, the number of active sites available for interaction must be considered. It is likely that the active aerosol surface sites are already saturated at aerosol condition I. Thus, significant additional promoting effects on the OH radical reactions with methanol, ethanol, and 1-propanol were not observed as the aerosol surface area was increased. Data on the adsorption capacities of ammonium sulfate particles for alcohols are not available. However, indirect comparisons using the adsorption capacities of water may be instructive. Donaldson & Anderson (1999) calculated the saturation coverage of selected alcohols and acids at the air-water interface at room temperature based on surface tension measurements. The saturation coverage of methanol was estimated at 9.2×10^{13} molecules cm^{-2} at the air-water interface. The total aerosol surface area and the number of methanol molecules in the bag for condition I were 1.12 cm^2 and 5.90×10^{19} molecules, respectively. These values indicate a total coverage of 5.27×10^{19} molecules cm^{-2}, exceeding the saturation coverage estimate by approximately 10^6 times. Therefore, all the active sites on the ammonium sulfate aerosols were likely saturated by the organic reactants under the conditions used in this work. Due to limitations with our analytical equipment, concentrations of the alcohols could not be reduced to produce coverage values less than the estimated saturation coverage.

Based on the data obtained in this study, the reaction rates of OH radicals with methanol, ethanol, and 1-propanol are affected by aerosols. The recommended rate constants of OH radical reaction with methanol, ethanol, and 1-propanol (in units of 10^{-12} cm^3 $molecule^{-1}$ s^{-1}) may be increased from 0.944, 3.27, and 5.53 to 1.25, 4.32, and 6.80 (32%, 32%, and 23% increases), respectively, under real atmospheric conditions. Using an average tropospheric concentration for OH radicals of 1.5×10^6 molecule cm^{-3} (Seinfeld et al. 1995), the estimated tropospheric lifetimes of methanol, ethanol, and 1-propanol decrease from 8.2, 2.4, and 1.4 days to 6.2, 1.8, and 1.1 days, respectively. It is important to note that these results may impact ozone formation potential calculations such as the maximum incremental reactivity (MIR) calculation used in the new California Low Emission Vehicle and Clean Fuel Regulations (Carter 1994). MIR quantifies ozone formation potentials of VOCs using air quality modeling in which the OH radical reaction rate constants for VOCs are used.

CHAPTER 5
EFFECTS OF AEROSOL COMPOSITION ON THE ·OH RATE CONSTANT OF A SELECTED ALCOHOL

Background

In the studies reported in Chapters 3 and 4, promotion of the reactions of OH radicals with 1-propanol as compared to the reactions with p-xylene were observed in the presence of ammonium sulfate aerosols. Thus, it is important to investigate the effects of other aerosol compositions prevalent in the troposphere on the OH radical reactions. As discussed in Chapter 1, the chemical composition of aerosols in the troposphere varies with size range and sources. However, carbonaceous material, nitrate, sulfate, ammonium, sea salt and water are generally present in varying amounts (Heintzenberg 1989). Ammonium, sulfate, nitrate, sodium, and chloride typically account for 25% to 50% of the nonwater atmospheric aerosol mass (Seinfeld et al. 1994). Thus, inorganic salts such as ammonium sulfate, ammonium nitrate and sodium chloride aerosols were used as the test aerosols in this study, and the effects of aerosol compositions on the kinetics of the OH radical reactions with 1-propanol were investigated. In addition, sodium sulfate and ammonium chloride aerosols were tested to elucidate the effects of individual anionic and cationic constituents of the aerosols on the 1-propanol/·OH reaction.

Experimental Methods

The experimental methods and apparatus were described in Chapters 2 and 3, thus only a brief summary is given here. The relative rate technique was used to investigate the effects of aerosols on the kinetics of the 1-propnaol/$^{\cdot}$OH reaction. P-xylene was used as a reference compound since its behavior in the presence of ammonium sulfate aerosols had been characterized (see Chapter 3). The relative rates of the 1-propanol/$^{\cdot}$OH reaction versus the p-xylene/$^{\cdot}$OH reaction in the absence and presence of aerosols were determined, and changes in the relative rates were used as an indication of the effects of aerosols on the reactions.

Experiments were carried out in 100-liter, 2-mil Tedlar® bags (SKC Inc.), with irradiation provided by eight 40-watt black lamps (Sylvania F40/350BL). All experiments were performed at room temperature, 298 ± 2K, and atmospheric pressure, ~ 760 Torr. Hydroxyl radicals were generated by the photolysis of methyl nitrite in the Tedlar® bag at wavelengths greater than 300 nm (Atkinson et al. 1981). The aerosol was generated by atomizing an aqueous solution containing 1 wt % of the inorganic salt using a Collison atomizer. Ammonium sulfate, ammonium nitrate, sodium chloride, ammonium chloride, and sodium sulfate were used as the aerosol base materials. Ammonium chloride and sodium sulfate aerosols were used to specifically investigate the influences of the cations and anions on the $^{\cdot}$OH initiated reactions. The aerosol generated was passed through a diffusional dryer and a ^{85}Kr charge neutralizer (TSI, Inc.) before being admitted to the bag. The bag was typically filled with 80 l of the air/reactant/aerosol mixture. Two different aerosol concentrations typical of polluted urban conditions were tested.

Gas analyses were carried out with a Finnigan-MAT GCQ system equipped with a 30 m x 0.25 mm i.d. DB-WAX capillary column (J&W Scientific Co.), and particle size distributions were determined using an electrical aerosol analyzer (EAA, Model 3030, TSI, Inc). The GC column conditions were identical to the conditions described in Chapter 3. Initial concentrations for gaseous compounds were typically 30 to 50 ppm of methyl nitrite, 8 to 14 ppm of 1-propanol and 1 to 4 ppm of p-xylene. Total aerosol surface areas were 1400 μm^2 cm^{-3} (Condition I) and 3400 μm^2 cm^{-3} (Condition II). Initial characteristics of the aerosols admitted to the chamber can be found in Chapter 4 (Table 4-1). No significant differences in aerosol characteristics were observed between different aerosol base materials. To avoid a change in aerosol characteristics during an experiment, only one irradiation time varying between 1 and 10 minutes was applied for each experiment. In addition, separate gas-phase experiments were conducted in the presence of $NH_3(g)$ to investigate the mechanism by which aerosols promoted the 1-propanol/$^{\cdot}$OH reaction. The concentration of NH_3 was 30 to 40 ppm, and the other gaseous compound concentrations were identical to those described above.

Results and Discussion

Reactions in the Presence of Aerosols

The relative rates of the 1-propanol/$^{\cdot}$OH reaction versus the p-xylene/$^{\cdot}$OH reaction in the presence of aerosols were determined at two aerosol concentrations by linear least-squares analyses of the data. Plots of $\ln[(1\text{-}Propanol)_o/(1\text{-}Propanol)_t]$ vs. $\ln[(p\text{-}Xylene)_o/(p\text{-}Xylene)_t]$ for the purely gas-phase condition as well as for aerosol conditions I and II are shown in Figure 5-1, and the calculated relative rates are listed in Table 5-1. Errors represent 95% confidence intervals. Promotion of the 1-propanol/·OH reaction as compared to the p-xylene/·OH reaction in the presence of $(NH_4)_2SO_4$ aerosols was observed under both aerosol conditions. The relative rates of the 1-propanol/·OH reaction versus the p-xylene/·OH reaction increased from 0.45 ± 0.03 in the absence of aerosols to 0.56 ± 0.02 and 0.55 ± 0.03 for aerosol conditions I and II, respectively. Additional increases in the aerosol promoting effects on the 1-propanol/OH radical reaction were not observed in studies using higher aerosol concentrations (aerosol condition II). As discussed in Chapter 4, it is likely that the active aerosol surface sites were already saturated at aerosol condition I for $(NH_4)_2SO_4$. Thus, an additional promoting effect was not observed as the initial aerosol surface area was increased. Significant changes in the relative rates were not observed in the presence of NaCl aerosols at either aerosol condition. The relative rates were 0.44 ± 0.02 and 0.48 ± 0.03 for aerosol conditions I and II, respectively. For NH_4NO_3 aerosols, an increase in the relative rate was only observed at the higher aerosol concentration (aerosol condition II), while the relative rate at aerosol condition I was within the error limits of the relative rate determined in the absence of added aerosol. The relative rates obtained in the presence of NH_4NO_3 aerosols were 0.41 ± 0.03 and 0.53 ± 0.02 for aerosol conditions I and II, respectively. These results clearly show that the influences of aerosols on the kinetics of 1-propanol/·OH reaction depend on both composition and concentration of aerosols.

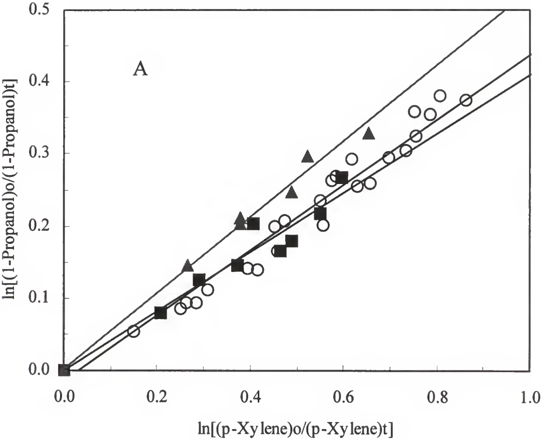

Figure 5-1. Plots of ln[*(1-Propanol)$_o$/(1-Propanol)$_t$*] vs. ln[*(p-Xylene)$_o$/(p-Xylene)$_t$*] in the absence of aerosols (○) and the presence aerosols (■:Aerosol Condition I, ▲: Aerosol Condition II) of the following aerosol compositions: (A) NH_4NO_3; (B) NaCl; (C) NH_4Cl; (D) Na_2SO_4. The lines represent linear least squares fit to the data.

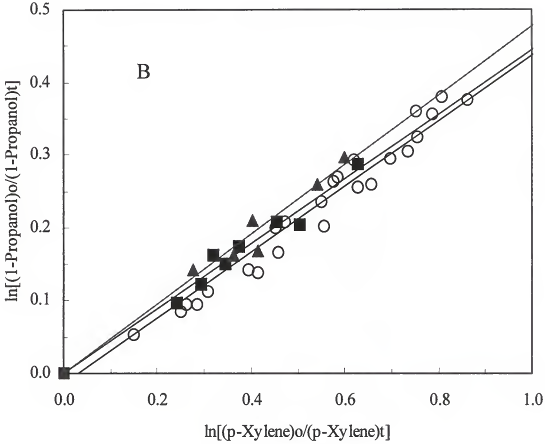

Figure 5-1--continued

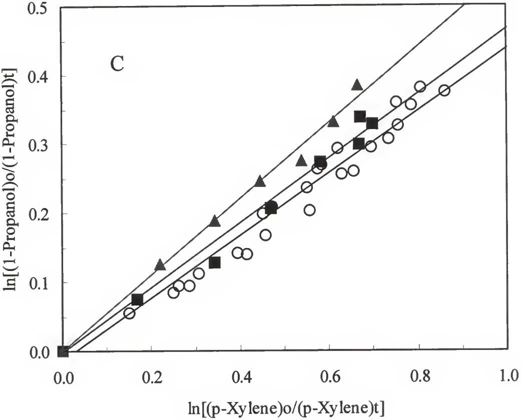

Figure 5-1--continued

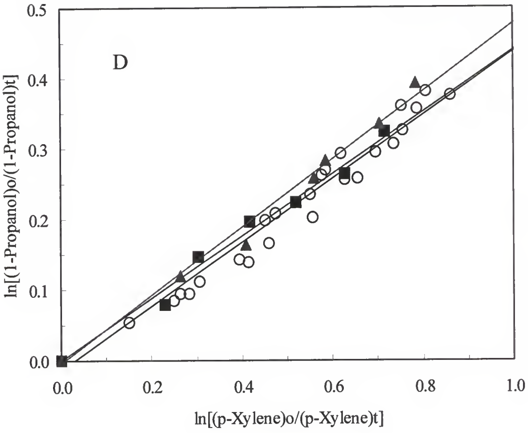

Figure 5-1--continued

Table 5-1. Relative rates of the 1-propanol/·OH reaction versus the p-xylene/·OH reaction in the absence and presence of aerosols for aerosol conditions I and II.

Aerosol composition		Relative rates[a]	
	In the absence of aerosols	0.45 ± 0.03[b]	
	In the presence of aerosols	I	II
$(NH_4)_2SO_4$		0.56 ± 0.02[b]	0.55 ± 0.03[b]
NH_4NO_3		0.41 ± 0.03	0.53 ± 0.02
NaCl		0.44 ± 0.02	0.48 ± 0.03
Na_2SO_4		0.44 ± 0.02	0.48 ± 0.02
NH_4Cl		0.47 ± 0.02	0.55 ± 0.02

[a] Errors represent 95% confidence intervals.
[b] Determined from experiments that are discussed in Chapters 3 and 4.

Currently, there is evidence that reactions occur at the surface of NaCl aerosols between gas-phase OH radicals and Cl^- in the aerosols. These reactions lead to the formation of gaseous Cl_2 (Knipping et al. 2000). The reaction sequence is as follows and a schematic of the reactions at the surface of NaCl aerosols is shown in Figure 5-2:

$$OH_{(g)} + Cl^-_{(surface)} \rightarrow \left(OH....Cl^-\right)_{(surface)} \tag{5.1}$$

$$\left(OH....Cl^-\right)_{(surface)} + \left(OH....Cl^-\right)_{(surface)} \rightarrow Cl_{2(g)} + 2OH^-_{(aq)} \tag{5.2}$$

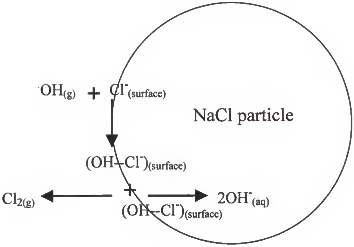

Figure 5-2. Schematic of the reactions at the surface of NaCl aerosols (Knipping et al. 2000).

In the presence of light, the Cl_2(g) will photolyze to give Cl(g).

$$Cl_{2(g)} + h\nu \rightarrow 2Cl_{(g)} \qquad (5.3)$$

If this is the case in the experiments described in this chapter, then Cl(g) will react with the gas-phase organic compounds. Thus, 1-propanol and p-xylene in the system will react with OH radicals and Cl simultaneously by the following reactions:

$$\mathrm{R} + \dot{\mathrm{O}}\mathrm{H} \xrightarrow{k_{OH}} \text{Products} \qquad (5.4)$$

$$\mathrm{R} + \mathrm{Cl} \xrightarrow{k_{Cl}} \text{Products} \qquad (5.5)$$

where R represents organic compounds. The rates of disappearance of organics due to each reaction are expressed by the following equations:

$$-\left(\frac{d[R]}{dt}\right)_{OH} = k_{OH}[OH][R] \tag{5.6}$$

$$-\left(\frac{d[R]}{dt}\right)_{Cl} = k_{Cl}[Cl][R] \tag{5.7}$$

$$-\left(\frac{d[R]}{dt}\right)_{Total} = k_{OH}[OH][R] + k_{Cl}[Cl][R] \tag{5.8}$$

Thus, the observed relative rates of the 1-propanol/p-xylene will be determined by the disappearance rates of the organics due to reaction with both OH radicals and Cl. The reactions of 1-propanol and p-xylene with Cl are much faster than the reactions with OH radicals, indicating that reactions with Cl can affect the relative rates obtained in the presence of NaCl aerosols. The literature rate constants of these reactions (Atkinson 1994, Finlayson-Pitts and Pitts Jr. 2000) are listed in Table 5-2. However, concentrations of OH radical and Cl in the system must be considered. Since the rate constants of reactions (5.1) and (5.2) are not known, an accurate estimate of Cl concentration in the system is not feasible. Thus, upper limits to the concentrations of OH radicals and Cl in the system were determined, and the rates of disappearance of the reactants were calculated using equations (5.6) and (5.7). An OH radical concentration of 7.4×10^{14} molecules cm^{-3} in the system was used, assuming all methyl nitrite (for 30 ppm of initial methyl nitrite concentration) photolyzes and generates OH radicals. A chlorine atom concentration of 1.9×10^{12} molecules cm^{-3} in the system was used, assuming all Cl^- in the NaCl aerosols generates Cl (for aerosol condition II). The calculated disappearance rates of the organics with Cl and OH radicals in the system are listed in Table 5-2.

Table 5-2. Rate constants and disappearance rates of the organics in the system for the organics/·OH reactions and the organics/Cl reaction.

Compounds	Rate constants (cm^3 molecue^{-1} s^{-1})		Disappearance rates in the system (molecue^{-1} s^{-1})	
	OH radical[a]	Cl[b]	OH radical[c]	Cl[d]
1-propanol[e]	6.44×10^{-12}	1.5×10^{-10}	1.2×10^{18}	7.0×10^{16}
p-xylene[f]	14.3×10^{-12}	1.5×10^{-10}	5.2×10^{17}	1.4×10^{16}

[a] Atkinson 1984

[b] Finlaysion-Pitts and Pitts Jr. 2000.

[c] Calculated using OH radical concentration of 7.4×10^{14} molecules cm^{-3}.

[d] Calculated using Cl concentration of 1.9×10^{12} molecules cm^{-3}.

[e] Calculated using 1-propanol concentration of 2.5×10^{14} molecules cm^{-3}.

[f] Calculated using p-xylene concentration of 5×10^{13} molecules cm^{-3}.

As shown in Table 5-2, the reactions of organics with Cl are minor pathways, and the reactions with OH radicals are the predominant reactions in the system. Thus, the relative rates obtained in this study are determined by the reactions with OH radicals. As a result, significant changes in the relative rates of the 1-propanol/·OH reaction versus the p-xylene/·OH reaction in the presence of NaCl aerosols were not observed in this study. In addition, separate loss studies were conducted to check for possible interferences by NaCl aerosols. First, 1-propanol and p-xylene were admitted to the bag with NaCl aerosols and left to stand for 30 min. The concentration changes of the organics were monitored via GC, and were negligible (less than 5%). Second, the above mentioned mixtures were irradiated for 10 min, and GC analyses were conducted before and after irradiation. No observable concentration changes of the organics were detected. These results provide further evidence to support the conclusion that the reactions of organics with Cl are insignificant in the system.

In our system, the possible species promoting the kinetics of the 1-propanol/$^{\cdot}OH$ reaction are NH_4^+, SO_4^{2-}, and NO_3^-, since increases in the relative rates were observed in the presence of $(NH_4)_2SO_4$ and NH_4NO_3 aerosols. To determine the species involved in the promoting effects, several experiments were performed in the presence of either Na_2SO_4 or NH_4Cl aerosols. An increase in the relative rate was not observed in the presence of Na_2SO_4 at either aerosol condition I or II. However, the relative rate increased in the presence of $(NH_4)_2SO_4$ under aerosol conditions I and II. Although the number of SO_4^{2-} sites available for reaction in the Na_2SO_4 and $(NH_4)_2SO_4$ aerosol studies were similar, the effects on the 1-propanol/p-xylene relative rates were different. Thus, the results indicate that SO_4^{2-} is not the dominant species affecting the rates of reaction. As shown in Table 5-1, the relative rates obtained in the presence of NH_4Cl aerosols were 0.47 ± 0.02 and 0.55 ± 0.02 for aerosol conditions I and II, respectively. The relative rate only increased in studies using NH_4Cl aerosols at aerosol condition II. In addition, the effects on the kinetics of the 1-propanol/$^{\cdot}OH$ reaction are identical for studies using NH_4Cl and NH_4NO_3 aerosols. These results indicate that either NH_4^+ promotes the reaction, or NO_3^- and Cl^- have the same promoting effects on the reaction. However, effects on the kinetics of the reaction were not observed in studies using NaCl aerosols at either aerosol condition. Thus, Cl^- and NO_3^- are not the aerosol constituents that promote the 1-propanol/$^{\cdot}OH$ reaction. Consequently, NH_4^+ is the species promoting the 1-propanol/$^{\cdot}OH$ reaction. Thus, increases in the relative rates were only observed when NH_4^+ was present in the aerosol. In addition, the total number of NH_4^+ sites using condition I for $(NH_4)_2SO_4$ aerosols and condition II for NH_4NO_3 and NH_4Cl aerosols are comparable when considering total aerosol surface area. The results for these three aerosol composition/condition scenarios indicate that the promoting effects on the 1-propanol/·OH reaction were identical, thus supporting our idea that the cation, NH_4^+, is the dominant species affecting the relative rates.

There are two hypotheses that may explain the mechanism by which NH_4^+ influences the ·OH-initiated photooxidation of 1-propanol:

1. NH_4^+ leads to the generation of $NH_3(g)$, which may then react with 1-propanol.
2. NH_4^+ lowers the activation energy of the 1-propanol/·OH reaction.

Each of these proposed mechanism is evaluated below.

As clearly shown in the following aerosol-gas equilibrium relations (Kim et al. 1993), NH_4^+ in the aerosol phase is in equilibrium with $NH_3(g)$.

$$(NH_4)_2SO_4(s) \leftrightarrows 2NH_4^+(aq)+SO_4^{2-}(aq) \tag{5.9}$$

$$H_2O(aq) \leftrightarrows H^+(aq)+OH^-(aq) \tag{5.10}$$

$$NH_4^+(aq)+OH^-(aq) \leftrightarrows NH_3(aq)+H_2O(aq) \tag{5.11}$$

$$NH_3(aq) \leftrightarrows NH_3(g) \tag{5.12}$$

$$NH_4NO_3(s) \leftrightarrows NH_3(g)+HNO_3(g) \tag{5.13}$$

$$NH_4Cl(s) \leftrightarrows NH_3(g)+HCl(g) \tag{5.14}$$

Thus, $NH_3(g)$ was present in the system for the studies conducted in the presence of NH_4^+ containing aerosols. The $NH_3(g)$ can subsequently react with either OH radicals, 1-propanol, or p-xylene. However, reaction of $NH_3(g)$ with only OH radicals will not change the relative rate of the 1-propanol/·OH reaction versus the p-xylene/·OH reaction. Equation (3-3) for the 1-propanol/·OH reaction versus the p-xylene/·OH reaction will still hold since OH radicals will still be available to both organics. However, reactions of $NH_3(g)$ with 1-propanol and p-xylene can change the relative rates obtained if the reactions are significant in the system. Then, the relative rates obtained are determined by not only the rate constants of the organic/·OH reactions but also the rate constants of the organic/$NH_3(g)$ reactions. Comparisons of the disappearance rates of the organics due to the reactions with $NH_3(g)$ and OH radicals are needed to determine whether the $NH_3(g)$ reaction affected the relative rates obtained. However, the disappearance rates of the organics due to reaction with $NH_3(g)$ can not be estimated since kinetic data for the $NH_3(g)$ reaction with 1-propanol and p-xylene are not available. Thus, an additional experiment was conducted to examine whether $NH_3(g)$ is indeed the species involved in promoting the 1-propanol/·OH reaction in the presence of aerosols containing NH_4^+. The relative rate of the 1-propanol/·OH reaction versus p-xylene/·OH reaction was determined for the 1-propanol / p-xylene / CH3ONO / $NH_3(g)$ system. If $NH_3(g)$ is the species involved in the promoting effects, an increase in the relative rate will be observed compared to the relative rate obtained for the 1-propanol / p-xylene / CH3ONO studies. However, a significant increase in the relative rate was not observed. The relative rate obtained for the 1-propanol / p-xylene / CH3ONO / $NH_3(g)$ system was 0.48 ± 0.02, and, within the error limits, is identical to the relative rate determined in the 1-propanol / p-xylene / CH3ONO studies (0.45 ± 0.02). A plot of $\ln[(1\text{-}Propanol)_o\ (1\text{-}Propanol)_t]$ vs. $\ln[(p\text{-}Xylene)_o/(p\text{-}Xylene)_t]$ is shown in Figure 5-3. The result clearly indicate that

$NH_3(g)$ plays an insignificant role in promoting the 1-propanol/·OH reaction in the presence of aerosols containing NH_4^+.

Another hypotheses that may explain the influence of NH_4^+ on the 1-propanol /·OH reaction is the formation of an intermediate species which can lower the activation energy of the 1-propanol/·OH reaction. A strong interaction between NH_4^+ and 1-propanol is feasible. Inoue et al. (1998) calculated the interaction energy between NH_4^+ and an aromatic system, and suggested that this interaction could play as important a role as hydrogen bonding does. They also suggested that the NH_4^+-aromatic interaction is solely influenced by the electrostatic property of the aromatic ring. Considering the electrostatic properties of p-xylene and 1-propanol (Atkins 1986), the interaction between NH_4^+ and 1-propanol is likely stronger than the interaction between NH_4^+ and p-xylene. Thus, it is very probable that 1-propanol and NH_4^+ easily form an intermediate species which can lower the activation energy of the initial ·OH attack. The average increase in the relative rates of the 1-propanol/·OH versus the p-xylene/·OH reactions was 22% in the presence of NH_4^+-containing aerosols. The required decrease in activation energy corresponding to a 22% increase in the rate constant was calculated using the Arrhenius equation; the calculated value was 118 cal/mol at room temperature. However, a literature value for the activation energy of the 1-propanol/·OH reaction is not available. Thus, only an indirect comparison is possible. Considering that the activation energies of the ethanol/·OH and methanol/·OH reactions are 467 and 1,192 cal/mol, respectively (DeMore et al. 1997), it is very probable that the activation energy of the 1-propanol/·OH reaction is lowered by the formation of an intermediate species between NH_4^+ and 1-propanol.

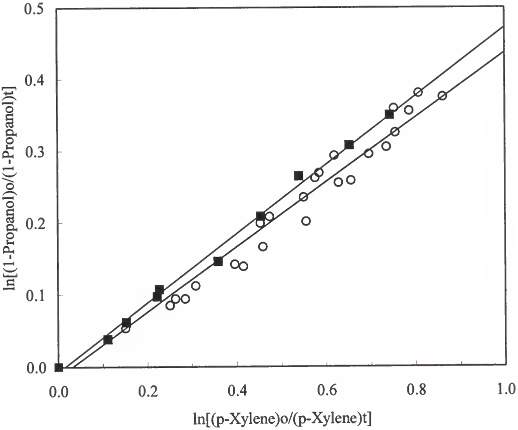

Figure 5-3. Plots of ln[*(1-Propanol)$_o$/(1-Propanol)$_t$*] vs. ln[*(p-Xylene)$_o$/(p-Xylene)$_t$*] for the 1-propanol / p-xylene / CH_3ONO system (○) and 1-propanol / p-xylene / CH_3ONO / NH_3 system(■). The lines represent linear least squares fit to the data.

Implications for Tropospheric Chemistry

The results of this study show that aerosols containing NH_4^+ increase the rate constant of the 1-propanol/$^{\cdot}$OH reactions. As seen in Table 1-2, NH_4^+ is a constituent of approximately 10% of the tropospheric aerosols (by mass). The results of this study strongly suggest that air quality models that utilize the 1-propanol/$^{\cdot}$OH reaction (and its associated rate constant) should be modified to include the effects of particles. Incorporating heterogeneous chemistry data including the effects of aerosol compositions and concentrations on the gas-phase chemistry are necessary to improve air quality models.

Currently, there is evidence for surface enrichment of the large polaizable Cl^- as compared to the small, nonpolarizable Na^+ in aqueous NaCl solutions. Consequently, the reactions between the more readily available Cl^- and gas-phase molecules are believed to be the predominant surface reaction on an aqueous NaCl aerosol (Knipping et al. 2000). Thus, the relative humidity of air is an important factor needed to determine the extent of the NaCl aerosol surface reactions, since the phase of NaCl aerosols is determined by the relative humidity of air (Martin 2000). However, the results of this study show that NH_4^+ influences the 1-propanol/$^{\cdot}$OH reaction, and indicate that the cation (rather than anion) in the aerosols plays an important role in the surface reactions. The differences between the results reported in this work and those of Knipping et al. (2000) may be due to the phase of aerosols studied. The phases of the NH_4^+-containing aerosols used in this study were likely solid, since the relative humidity of air in the system was approximately 18 to 38 %, values that are below the efflorescence (recrystallization) relative humidities of the aerosols studied. The efflorescence relative humidity of $(NH_4)_2SO_4$ is 40% (Seinfeld &

Pandis 1998). Accurate values of efflorescence relative humidities of NH_4NO_3 and NH_4Cl are not available. The estimated efflorescence relative humidities of NH_4NO_3 and NH_4Cl are 43 ~50 % and 56 ~ 64 %, respectively (Finlaysion-Pitts & Pitt Jr. 2000). Thus, reactions that have been shown to occur at the surface of aqueous aerosols might not be possible at the surface of solid aerosols, and cations could play an important role at the surface of solid aerosols. Thus, additional studies on the surface properties of inorganic aerosols that contain NH_4^+, NO_3^-, and SO_4^{2-} ions at different aerosol phases are needed to understand the surface reactions of tropsopheric aerosols.

CHAPTER 6

EFFECTS OF INORGAINIC AEROSOLS ON THE GAS-PHASE REACTIONS OF THE HYDROXYL RADICAL WITH SELECTED ALIPHATIC ALKANES

Background

More than 130 alkanes have been detected in ambient air (Graedel et al. 1986). Alkanes are emitted from any process involving the combustion of fossil fuels or other organic material. Alkanes were the most abundant nonmethane organic species in the Southern California Air Quality Study (see Table 1-3), thus the tropospheric chemistry of alkanes is important. Alkanes do not photolyze in the troposphere, and the reaction with O_3 is negligible. The OH radical reaction is generally the dominant daytime loss process of alkanes in the troposphere (Atkinson 2000). The OH radical reactions of alkanes proceed by H-atom abstraction from the C-H bonds, and reaction sequences for alkanes are known (Atkinson 2000). Kinetic studies of OH radical reactions with alkanes have been performed in purely gas-phase environments (Atkinson 1997). However, few studies have been performed to investigate the effects of aerosols on these kinetic constants.

Recent studies of the interaction of TiO_2 aerosols with the OH radical gas-phase reaction with alkanes indicated a significant impact of aerosols on the kinetics of the OH radical/alkane reactions. Also, the impacts of aerosols were more profound with higher carbon alkanes ($>C_8$). However, a significant impact was not observed with SiO_2 aerosols (Behnke et al. 1987, 1988). Also, as indicated in Chapter 3, a significant impact was not observed for the OH rate constant of n-hexane compared to p-xylene in the presence of ammonium sulfate aerosols. Therefore, studies including large alkanes with various aerosol compositions were needed to determine the effects of aerosols on alkane/·OH reactions. Specific alkanes to study include n-butane, n-pentane, n-octane, and n-decane. Butane and pentane were identified in the Southern California Air Quality Study as being one of the twenty five most abundant species found in the atmosphere based on the fraction of non-methane carbon (Lurmann et al. 1992). The remaining alkanes are also important constituents of air in urban areas.

The purpose of this study was to examine the effects of aerosol compositions and concentrations on the kinetics of the OH radical reactions with alkanes. Inorganic salts such as ammonium sulfate, ammonium nitrate and sodium chloride aerosols were selected, and two different aerosol concentrations typical of polluted urban conditions were tested.

Experimental Methods

The experimental methods and apparatus used in this study are described in Chapters 2 and 3. The relative rate technique (Atkinson et al. 1981) was used to investigate the effects of aerosols on the kinetics of the alkane/·OH reaction. The relative rates of the alkanes and the reference compound in the absence and presence of aerosols were determined, and changes in the relative rates were used as an indication of the effects of aerosols on the reactions.

Experiments were carried out in 100-liter, 2-mil Tedlar® bags (SKC Inc.), with irradiation provided by eight 40-watt black lamps (Sylvania F40/350BL). All experiments were performed at room temperature, 298 ± 2K, and atmospheric pressure, ~ 760 Torr. Hydroxyl radicals were generated by the photolysis of methyl nitrite in the Tedlar® bag at wavelengths greater than 300 nm (Atkinson et al. 1981). The aerosol was generated by atomizing an aqueous solution containing 1 wt % of the inorganic salt using a Collison atomizer. Ammonium sulfate, ammonium nitrate, and sodium chloride were used as the aerosol base materials for all studies. The aerosol generated was passed through a diffusional dryer and a ^{85}Kr charge neutralizer (TSI, Inc.) before being admitted to the bag. The bag was typically filled with 80 l of the air/reactant/aerosol mixture. Two different aerosol concentrations typical of polluted urban condition were tested. In order to minimize interferences between reactants and products, the following combinations of alkanes and reference compound were employed: n-octane / n-decane / p-xylene, n-hexane / p-xylene, and n-butane / n-pentane / p-xylene. P-xylene was used as a reference compound since its behavior compared to n-hexane in the presence of ammonium sulfate aerosols had been characterized previously (see Chapter 3).

Gas analyses were carried out with a Finnigan-MAT GCQ system. A 30 m x 0.25 mm i.d. DB-5ms capillary column (J&W Scientific Co.) was used for the gas chromatograph, and split injections of 2 ml of sample were made with a six-port injection valve. The GC column temperature was programmed at 40°C for ninety seconds, then increased at a rate of 30°C min^{-1} to a final temperature of 150°C. All mass spectral analyses were performed in the positive electron ionization mode. Initial concentrations for gaseous compounds were typically 30 to 60 ppm of methyl nitrite, 12 to 20 ppm of n-butane, 8 to 10 ppm of n-pentane, 1 to 2 ppm of n-octane, 1 to 2 ppm of n-decane, and 1 to 2 ppm of p-xylene, respectively. For the n-hexane / p-xylene study, the conditions applied for the n-hexane / 1-propanol / p-xylene study in Chapter 3 were used. A 30 m × 0.25 mm i.d. DB-WAX capillary column (J&W Scientific Co.) was used for the gas chromatograph. Detailed conditions are described in Chapter 3.

Particle size distributions were determined using an electrical aerosol analyzer (EAA, Model 3030, TSI, Inc). Total aerosol surface areas were 1400 $\mu m^2\ cm^{-3}$ (Condition I) and 3400 $\mu m^2\ cm^{-3}$ (Condition II), and detailed initial characteristics of aerosols admitted to the chamber can be found in Chapter 4 (Table 4-1 and Figure 4-1).

Results and Discussions

Reactions in the Absence of Aerosols

The relative rates of the OH radical reactions with the alkanes in the absence of aerosols were obtained by linear least-squares analyses of two different runs for the following combinations of alkanes and reference compound: n-butane / n-pentane / p-xylene, and n-octane / n-decane / p-xylene. The data are plotted in accordance with equation (3.3), and plots are shown in Figures 6-1 and 6-2. All plots are good straight lines, and the relative rates (k_s/k_r) are reported in Table 6-1. Errors represent 95% confidence intervals. The relative rate of the n-hexane/$^{\cdot}$OH reaction versus p-xylene/$^{\cdot}$OH reaction in the absence of aerosols was determined in a previous study (Chapter 2) and the plots of $\ln[(n\text{-}Hexane)_0/(n\text{-}Hexane)_t]$ vs. $\ln[(p\text{-}Xylene)_0/(p\text{-}Xylene)_t]$ are shown in Figure 6-3.

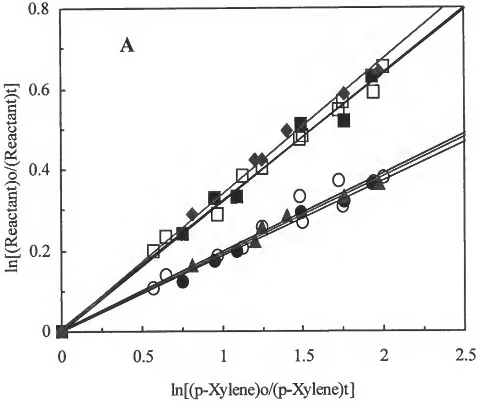

Figure 6-1. Plots of ln[*(Reactant)$_o$/(Reactant)$_t$*] vs. ln[*(p-Xylene)$_o$/(p-Xylene)$_t$*] in the absence of aerosols (○: n-butane, □: n-pentane) and the presence of aerosols (●: Aerosol Condition I, ▲: Aerosol Condition II for n-butane and ■: Aerosol Condition I, ◆: Aerosol Condition II for n-pentane). The lines represent linear least squares fit to the data.
Plot A represents data in the presence of $(NH_4)_2SO_4$ aerosols.
Plot B represents data in the presence of NH_4NO_3 aerosols.
Plot C represents data in the presence of NaCl aerosols.

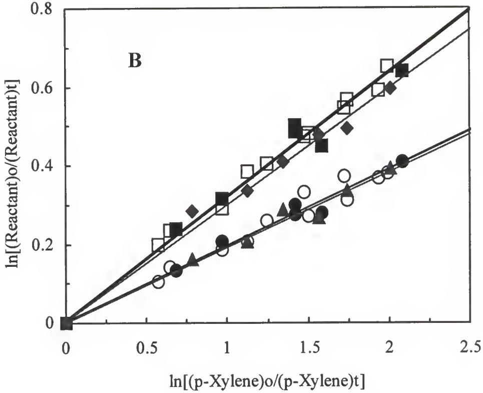

Figure 6-1--continued

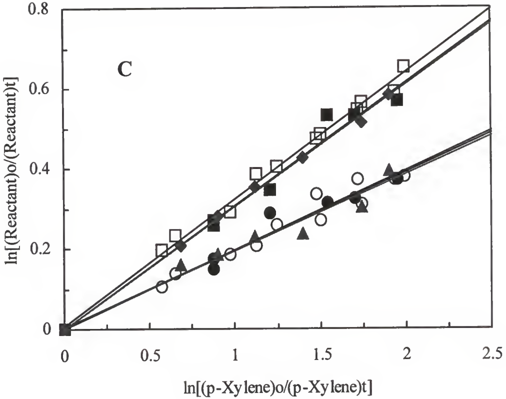

Figure 6-1--continued

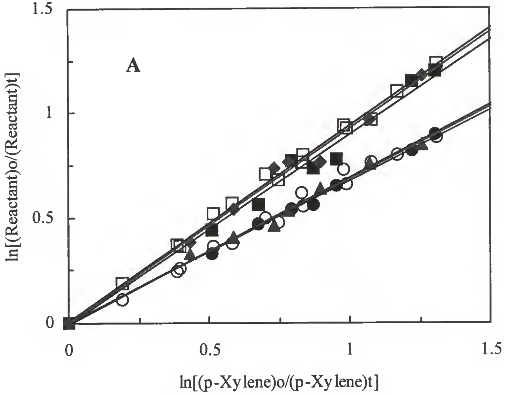

Figure 6-2. Plots of ln[*(Reactant)$_o$/(Reactant)$_t$*] vs. ln[*(p-Xylene)$_o$/(p-Xylene)$_t$*] in the absence of aerosols (○: n-octane, □: n-decane) and the presence of aerosols (●: Aerosol Condition I, ▲: Aerosol Condition II for n-octane and ■: Aerosol Condition I, ◆: Aerosol Condition II for n-decane). The lines represent linear least squares fit to the data.
Plot A represents data in the presence of $(NH_4)_2SO_4$ aerosols.
Plot B represents data in the presence of NH_4NO_3 aerosols.
Plot C represents data in the presence of NaCl aerosols.

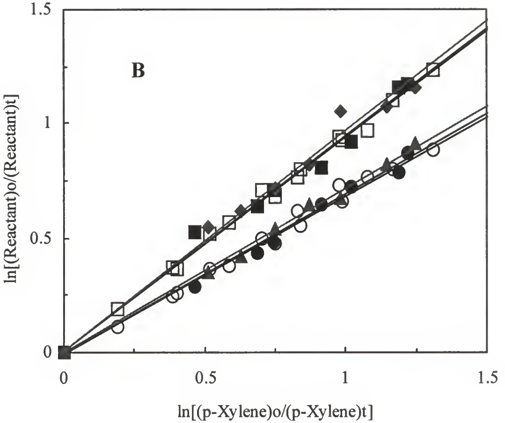

Figure 6-2--continued

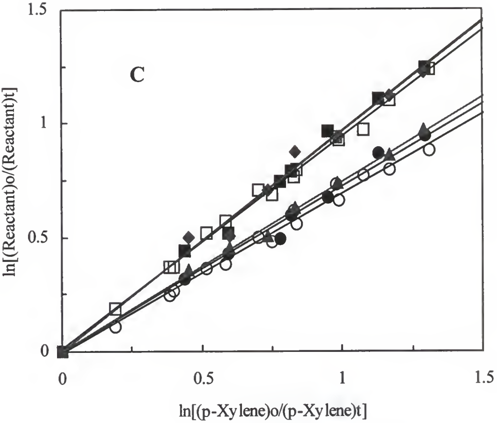

Figure 6-2--continued

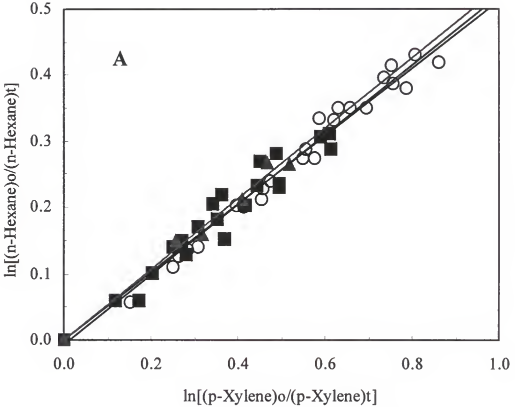

Figure 6-3. Plots of ln[*(n-Hexane)$_o$/(n-Hexane)$_t$*] vs. ln[*(p-Xylene)$_o$/(p-Xylene)$_t$*] in the absence of aerosols (○) and the presence of aerosols (■: Aerosol Condition I, ▲: Aerosol Condition II) of the following aerosol compositions: (A) $(NH_4)_2SO_4$; (B) NH_4NO_3; (C) NaCl. The lines represent linear least squares fit to the data.

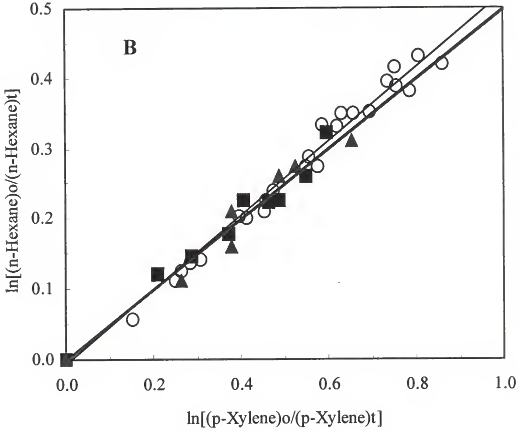

Figure 6-3--continued

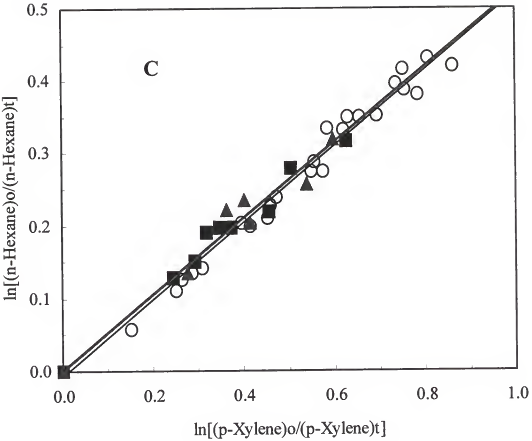

Figure 6-3--continued

Gas-phase "sample" rate constants (k_s) were placed on an absolute basis by using the rate constants (k_r) of OH radical reaction with p-xylene. The rate constant of the p-xylene/·OH reaction (12.9×10^{-12} cm^3 molecule^{-1} s^{-1} at 298 ± 2K) determined in Chapter 4 was used because the literature rate constants of the p-xylene/·OH reaction exhibited a significant degree of scatter (Atkinson, 1989). The resulting rate constants of the alkanes and the recommended values by Atkinson (1997) are listed in Table 6-1.

Table 6-1. Gas-phase relative rates (k_s/k_r) and rate constant (k_s) for the reactions of OH radical with the alkanes using p-xylene as a reference compound at room temperature.

Compound	Relative rates (k_s/k_r)[a]	Rate constants (10^{-12} cm^3 molecule^{-1} s^{-1})	
		This work[a, b]	Recommended[c]
n-butane	0.19 ± 0.02	2.5 ± 0.3	2.44 ± 0.49
n-pentane	0.31 ± 0.02	4.0 ± 0.3	4.00 ± 0.80
n-hexane	0.53 ± 0.02[d]	6.8 ± 0.3	5.45 ± 1.36
n-octane	0.70 ± 0.03	9.0 ± 0.4	8.71 ± 1.74
n-decane	0.93 ± 0.03	12.0 ± 0.4	11.2 ± 2.80

[a] Errors represent 95% confidence intervals.
[b] Obtained by using k_r(p-xylene) = 12.9×10^{-12} cm^3 molecule^{-1} s^{-1} determined in Chapter 4.
[c] From Atkinson et al. 1997.
[d] Determined in Chapter 3.

Considering overall uncertainties in the recommended rate constants, the observed gas-phase rate constants of the alkanes using p-xylene as a reference compound are generally in good agreement with the recommended values. As shown in Table 5-1, the observed rate constants of the n-butane/·OH reaction and n-pentane/·OH reaction are in excellent agreement with the recommended values. The observed and recommended rate constants of the n-butane/·OH reaction are 2.5×10^{-12} cm^3 molecule^{-1} s^{-1} and 2.44×10^{-12} cm^3 molecule^{-1} s^{-1}, respectively. The observed and recommended rate constant of the n-pentane/·OH reaction are identical at 4.0×10^{-12} cm^3 molecule^{-1} s^{-1}. For n-hexane, the observed rate constant is 25% higher than the recommended value, but within the overall uncertainty reported in the literature. The observed rate constants for n-octane and n-decane are 3% and 7% higher than the recommended values, and are within the reported overall uncertainties. Thus, our data fall within the acceptable ranges of published rate constants, thereby validating the relative rate technique used in this study.

Reactions in the Presence of Aerosols

The relative rates of the reactions of the OH radical with the alkanes in the presence of inorganic aerosols were determined at two aerosol concentrations. Ammonium sulfate, ammonium nitrate, and sodium chloride were tested. The total surface area of aerosols were 1400 μm^2 cm^{-3} and 3400 μm^2 cm^{-3} for aerosol conditions I and II, respectively. Plots of $\ln[(Alkane)_0/(Alkane)_t]$ vs. $\ln[(p\text{-}Xylene)_0/(p\text{-}Xylene)_t]$ for the purely gas-phase condition as well as for aerosol conditions I and II are shown in Figures 6-1 through 6-3. The experimentally determined relative rates are listed in Table 6-2.

Table 6-2. Relative rates of the alkane/·OH reactions versus the p-xylene/·OH reaction in the absence and presence of aerosols for aerosol conditions I and II.

	Relative rates[a]				
Compound	n-butane	n-pentane	n-hexane	n-octane	n-decane
In the absence of aerosols	0.19 ± 0.02	0.31 ± 0.02	0.53 ± 0.02[b]	0.70 ± 0.03	0.93 ± 0.03
In the presence of aerosols					
$(NH_4)_2SO_4$					
I	0.19 ± 0.01	0.32 ± 0.02	0.51 ± 0.02[b]	0.68 ± 0.01	0.90 ± 0.04
II	0.19 ± 0.01	0.34 ± 0.01	0.53 ± 0.03	0.69 ± 0.02	0.92 ± 0.04
NH_4NO_3					
I	0.19 ± 0.01	0.32 ± 0.02	0.50 ± 0.03	0.69 ± 0.02	0.94 ± 0.04
II	0.19 ± 0.01	0.30 ± 0.01	0.50 ± 0.04	0.72 ± 0.02	0.96 ± 0.04
NaCl					
I	0.20 ± 0.01	0.31 ± 0.02	0.52 ± 0.02	0.73 ± 0.03	0.97 ± 0.02
II	0.19 ± 0.02	0.30 ± 0.01	0.51 ± 0.04	0.74 ± 0.02	0.96 ± 0.04

[a] Errors represent 95% confidence intervals.
[b] Determined in Chapter 3.

As indicated in Chapter 3, significant changes in the relative rates of the n-hexane/·OH reaction versus the p-xylene/·OH reaction were not observed in the presence of aerosols for the aerosol compositions and concentrations considered. As shown in Table 6-2, no significant effects on the kinetics of OH radical reactions with n-butane, n-pentane, n-octane or n-decane were observed for the aerosol compositions and concentrations considered. The relative rates of the n-butane/·OH reaction, n-pentane

/·OH reaction, n-octane/·OH reaction and n-decane/·OH reaction versus the p-xylene/·OH reaction in the absence and presence of aerosols were identical, within the error limits. The results indicate that $(NH_4)_2SO_4$, NH_4NO_3, and NaCl aerosols do not promote the alkane/·OH reactions as compared to the p-xylene/·OH reaction for n-butane, n-pentane, n-hexane, n-octane, and n-decane. These results are quite different from those determined by Behnke et al. (1987, 1988). Behnke et al. (1987, 1988) used TiO_2 particles, which, when exposed to UV generate OH radicals because of the semiconducting nature of TiO_2. Since $(NH_4)_2SO_4$, NH_4NO_3, and NaCl aerosols do not have semiconducting properties, it is likely that additional OH radicals were not generated at the particles' surfaces. Benke et al. (1987) also did not observed an enhancement of the alkane (n-butane, n-pentane, n-hexane, n-octane, and n-nonane) /·OH reaction in the presence of SiO_2. Silicon dioxide particles are not capable of generating surface OH radicals. These results support the idea that the semicoducting property of the aerosol is the factor that determines the promoting effects on the alkane/·OH reactions.

In Chapter 5, interactions between cations in aerosol particles and the organic compounds were considered as the process influencing the promotion of the 1-propanol /·OH reaction in the presence of aerosols. To address this issue, possible interactions between aerosols and alkanes are considered. Since the interaction between cations in aerosol particles and the organic compounds is electrostatic (Inoue et al. 1998), the interaction strength depends on the polarity of the gas-phase organic compound. Thus, the polarity of the gas-phase organic compounds should be considered. Aliphatic alkanes are non-polar compounds and the dipole moments of the alkanes are zero (Dean 1992). Thus, there are no permanent partial negative charges in the molecules to interact with cations in aerosol particles. Consequently, promotion of the alkane/$^{\cdot}$OH reaction due to an interaction between aerosol ions and gas-phase compounds is not feasible for the alkanes studied. Thus, no significant changes in the relative rates of the alkane/$^{\cdot}$OH reactions versus the p-xylene/.OH reaction were observed in the presence of non-semicoducting aerosols. The results suggest that the polarities of the gas-phase compounds were also important factors to consider when examining the organic/$^{\cdot}$OH reaction in the presence of aerosols. Furthermore, the results indicate that the alkane/$^{\cdot}$OH reactions (for >C3 alkanes) in the troposphere will not be affected by inorganic aerosols which are major constituents of the tropospheric aerosols (i.e. non-semiconduting aerosols containing NH_4^+, SO_4^{2-}, NO_3^-, Na^+, and Cl^-).

CHAPTER 7
CONCLUSIONS AND RECOMMENDATIONS

Laboratory experiments were performed to investigate the effects of inorganic aerosols on the kinetics of the hydroxyl radical reactions with organic compounds. Experiments were conducted in 100-liter Tedlar® bags using the relative rate technique. $(NH_4)_2SO_4$, NH_4NO_3, NaCl, NH_4Cl, and Na_2SO_4 aerosols at two different aerosol concentration that are typical of polluted urban conditions were tested. Total surface areas were 1400 $\mu m^2\ cm^{-3}$ (Condition I) and 3400 $\mu m^2\ cm^{-3}$ (Condition II). The following results were obtained from this doctoral research.

1. To investigate the effects on different organic types, relative rate studies of the OH radical initiated reactions of n-hexane, p-xylene, and 1-propanol were conducted in the presence of ammonium sulfate aerosols. Results showed that ammonium sulfate aerosols promoted the reaction of 1-propanol with OH radicals as compared to the reactions of n-hexane with OH radicals and p-xylene with OH radicals. The relative rate of the 1-propanol/·OH reaction versus the n-hexane/·OH reaction increased from 0.85 ± 0.05 in the absence of $(NH_4)_2SO_4$ aerosols to 1.07 ± 0.05 in the presence of aerosols. Also, the relative rate of the 1-propanol/·OH reaction versus the p-xylene /·OH reaction increased from 0.45 ± 0.03 in the absence of $(NH_4)_2SO_4$ aerosols to 0.56 ± 0.02 in the presence of aerosols.
2. A series of aliphatic alcohols with varying carbon numbers were tested to investigate the effects of aerosols as a function of the size of organic compounds. The effects of

ammonium sulfate aerosols on the kinetics of the hydroxyl radical reactions with C_1 - C_6 aliphatic alcohols were investigated. P-xylene was used as a reference compound for the C_2 - C_6 aliphatic alcohols study, and ethanol was used as a reference compound for the methanol study. Results indicated that ammonium sulfate aerosols promoted the ethanol/OH radical and 1-propanol/OH radical reactions as compared to the p-xylene/OH radical reaction. The relative rate of the ethanol/·OH reaction versus the p-xylene/·OH reaction increased from 0.19 ± 0.01 in the absence of aerosols to 0.24 ± 0.01 and 0.26 ± 0.02 under aerosol conditions I and II, respectively. The relative rate of the 1-propanol/·OH reaction versus the p-xylene/·OH reaction increased from 0.45 ± 0.03 in the absence of aerosols to 0.56 ± 0.02 and 0.55 ± 0.03 under aerosol conditions I and II, respectively. However, significant changes in the relative rates of the 1-butanol/·OH, 1-pentanol/·OH, and 1-hexanol/·OH reactions versus the p-xylene/·OH reaction were not observed for either aerosol concentration. The relative rates of the methanol/·OH reaction versus the ethanol/·OH reaction were identical in the absence and presence of aerosols. These results indicated that ammonium sulfate aerosols promoted the methanol/·OH reaction as much as the ethanol/·OH reaction (as compared to the p-xylene/·OH reaction). The results suggest that the size of the alcohol molecule determines the extent of the promoting effects.

3. The effects of aerosol composition on the rate constant of 1-propanol were investigated using $(NH_4)_2SO_4$, NH_4NO_3, NaCl, NH_4Cl, and Na_2SO_4 aerosols. P-xylene was used as a reference compound. Results indicated that the aerosols promoted the 1-propanol/·OH reaction versus the p-xylene/·OH reaction, and the extent of the promoting effects depended on the aerosol composition and

concentration. Increases in the relative rates of the 1-propanol/$^{\cdot}$OH reaction versus the p-xylene/$^{\cdot}$OH reaction were only observed for $(NH_4)_2SO_4$ aerosol conditions I and II, and NH_4NO_3 aerosol condition II. Additional studies conducted with Na_2SO_4 and NH_4Cl aerosols showed an increase in the relative rates of the 1-propanol/$^{\cdot}$OH reaction versus the p-xylene/$^{\cdot}$OH reaction for NH_4NO_3 aerosol condition II. These results indicated that NH_4^+ was the species promoting the 1-propanol/$^{\cdot}$OH reaction. This suggested the possibility of a strong interaction between NH_4^+ and 1-propanol that could change the transition state energy of the initial $^{\cdot}$OH attack.

4. The effects of aerosols on the $^{\cdot}$OH rate constant of several alkanes were investigated using $(NH_4)_2SO_4$, NH_4NO_3, and NaCl aerosols. N-butane, n-pentane, n-hexane, n-octane, and n-decane were studied using p-xylene as a reference compound. Significant changes in the relative rates of the n-butane/·OH, n-pentane/·OH, n-octane /·OH, and n-decane/·OH reactions versus the p-xylene/·OH reaction were not observed for aerosol concentrations I and II. These results suggested that the polarities of the gas-phase compounds were also important factors to consider when examining the organic/$^{\cdot}$OH reaction in the presence of aerosols.

Based on the results of this doctoral research, the following recommendations are made to aid in improving regional air quality models.

1. Air quality models should incorporate heterogeneous kinetics to improve their accuracy. Rate constants currently used in the air quality models should be validated in the presence of various atmospheric aerosols that are relevant to the troposphere.

2. A new method to determine absolute rate constants of the organic/·OH reactions in the presence of aerosols should be developed. Since the relative rate technique was used in this doctoral research, the relative rates of the reactant/·OH reactions versus the reference/·OH reaction were determined, and changes in the rate constants of the reactant/·OH reactions were estimated assuming no aerosol effects on the reference/·OH reaction. Thus, determining the absolute values of the rate constants of the reference/·OH reaction in the presence of aerosols is essential. The current absolute rate techniques use an excess concentration of organic compounds and measure the OH radical concentration changes with time using fluorescence spectroscopy (Finlayson-Pitts and Pitts, Jr., 2000). Since particles will likely interfere with the fluorescence signals, the conventional technique needs to be modified to apply to the heterogeneous kinetic studies.

   A method that involves measuring the changes in organic concentration over time in the presence OH radicals is another possible candidate. However, a fast detection system is essential, since the time scales of the OH radical reactions of organics are on the order of milliseconds. An analytical instrument such as a gas chromatograph (used in this doctoral research) is not ideal for a new method, since a single analysis requires more than a minute.

3. Several hypotheses were suggested to explain the mechanism by which aerosols promote organic/·OH reactions. Aerosol surface studies are needed to fully explain/justify the proposed mechanisms. The possible reactions between aerosol-phase compounds and gas-phase compounds and the reactions between gas-phase compounds at the surface should be considered.

4. One of difficulties in this doctoral research was maintaining constant aerosol characteristics over the course of an experiment. Since the aerosol losses in the bag were significant over a one hour period, only one irradiation time of less than 10 minutes was applied for each experiment. Thus, experiments using a larger bag will help to maintain constant aerosol characteristics for several hours, thus allowing for enough time to obtain several data point in one batch. Benke et al. (1988) used a 2.4 m^3 glass chamber and obtained a 20 hr residence time for 0.5 μm particles. McMurry & Grosjean (1985) used a 60 m^3 Teflon® bag for a heterogeneous study for over 3 hr period.
5. Since organic aerosols are major constituents of tropospheric aerosols, studies with organic aerosols are required. Currently, techniques for generating and controlling inorganic aerosols are well established. However, techniques to generate and control organic aerosols are needed.

APPENDIX A
CALIBRATIONS

Calibrations of Gas Flow Rate Measuring Devices

A calibrated rotameter was used to monitor the flow rate of the reactants admitted into the Tedlar® bags. The rotameter was calibrated using an electronic bubble flow meter (Gilibrator, Gilian). Ambient air was drawn through the rotameter and the Gilbrator via a vacuum pump. The Gilibrator reading and the corresponding rotameter scale reading were recorded at different flow rates. The readings were corrected for standard temperature and pressure. The calibration curve is shown in Figure A-1. The line represents a linear least squares fit to the data, and the corresponding slope and correlation coefficient are shown on the plot.

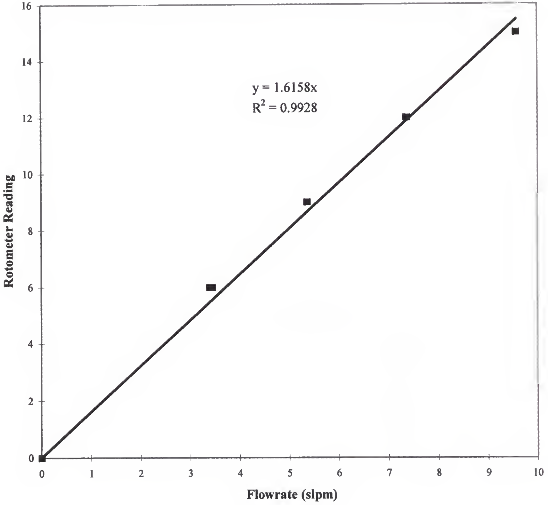

Figure A-1. Calibration curve of the rotameter used to monitor the flow rate of reactants admitted into a Tedlar® bag (Adapted from Azad, 1999).

For the aerosol flow rate measurement, an orifice meter was used. The orifice meter was calibrated using a calibrated wet test meter (Precision Scientific, Model No. 63126). Ambient air was drawn through the orifice meter and the wet test meter. The pressure drops across the orifice and the corresponding readings of the wet test meter were recorded at different flow rates. The pressure drops across the orifice were measured using a manometer. The volumes obtained using the wet test meter were corrected for standard temperature and pressure. The calibration curve is shown in Figure A-2.

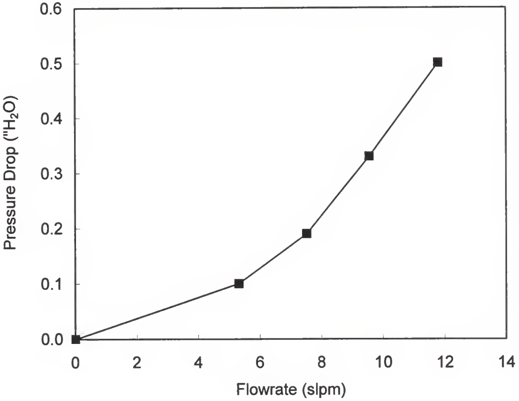

Figure A-2. Calibration curve of the orifice meter used to monitor the aerosol flow rate into a Tedlar® bag.

GC-MS Calibrations

One of the advantages of using the relative rate technique is that measuring absolute concentrations of reactants is not necessary. As shown in equation (3.3), only the relative concentrations of compounds are required to determine the relative rate. Thus, the signals from an instrument can be directly used to obtain a relative concentration if the responses are linear over the concentration range used. To determine whether the responses were linear over the concentration ranges used in this research, the GC-MS was calibrated. Known amounts of the compounds were injected to the air stream flowing into a 100 liter Tedlar® bag, and samples were taken from the Tedlar® bag in the same manner as the experimental samples. The samples were injected into the GC-MS, and the corresponding peak areas of the specific ion fragment (m/z, mass-to-charge ratio) were obtained. Signals at the following different ion fragments were monitored for the specified compounds: methanol (m/z = 31), ethanol(m/z = 45), 1-propanol(m/z = 41 + 59), 1-butanol(m/z = 39 + 41 +55), 1-petanol(m/z = 39 + 41 + 55), 1-hexanol(m/z = 39 + 41 + 55), n-butane(m/z = 41), n-pentane(m/z = 41), n-hexane(m/z = 41), n-octane(m/z = 41 + 57), n-decane(m/z = 41 + 57), p-xylene(m/z = 91 + 106), and cyclohexane(m/z = 39 + 41 + 56). This was repeated for various concentrations, and plots of the peak areas versus concentrations were generated. The calibration curves of the compounds are shown in Figures A-3 to A-15. The lines represent linear least squares fit to the data, and the corresponding slope and correlation coefficient values are shown on the plots. Two samples were taken for every concentration to check for internal consistency.

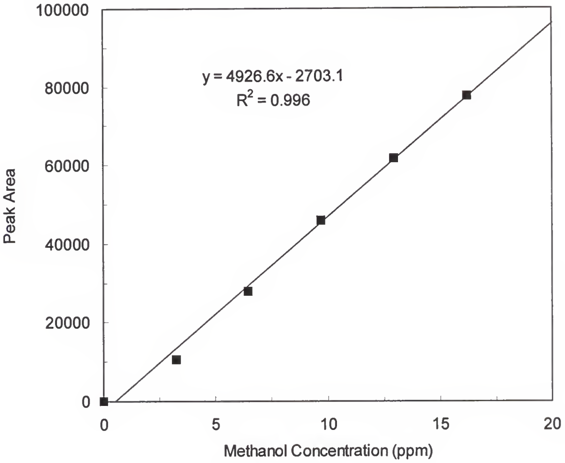

Figure A-3. GC-MS calibration curve for methanol using a 30 m × 0.25 mm i.d. (0.25 μm film thickness) DB-WAX capillary column.

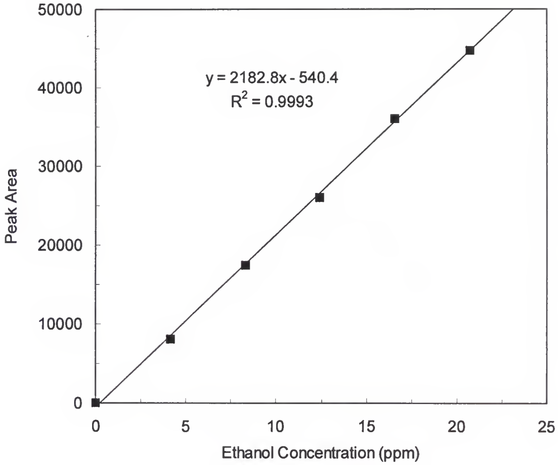

Figure A-4. GC-MS calibration curve for ethanol using a 30 m × 0.25 mm i.d. (0.25 μm film thickness) DB-WAX capillary column.

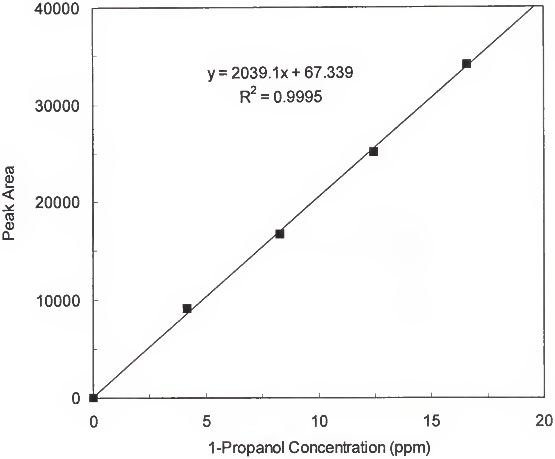

Figure A-5. GC-MS calibration curve for 1-propanol using a 30 m × 0.25 mm i.d. (0.25 μm film thickness) DB-WAX capillary column.

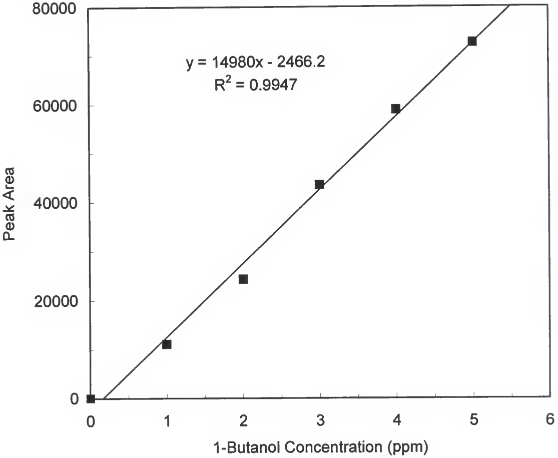

Figure A-6. GC-MS calibration curve for 1-butanol using a 30 m × 0.25 mm i.d. (0.25 μm film thickness) DB-WAX capillary column.

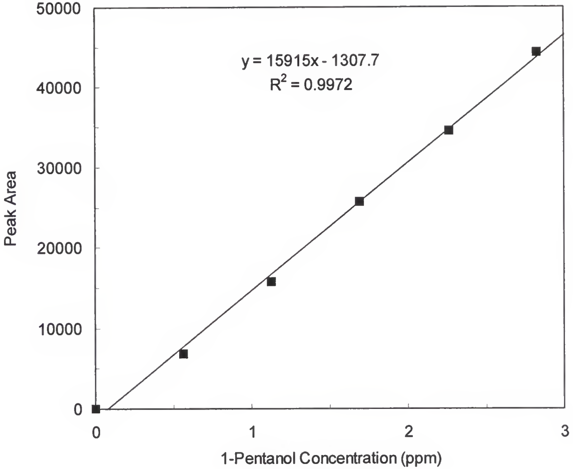

Figure A-7. GC-MS calibration curve for 1-pentanol using a 30 m × 0.25 mm i.d. (0.25 μm film thickness) DB-WAX capillary column.

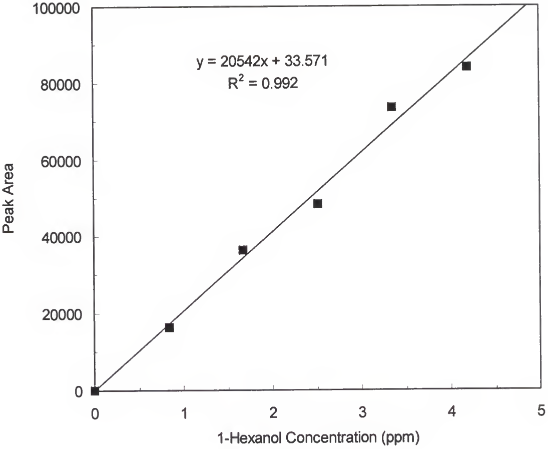

Figure A-8. GC-MS calibration curve for 1-hexanol using a 30 m × 0.25 mm i.d. (0.25 μm film thickness) DB-WAX capillary column.

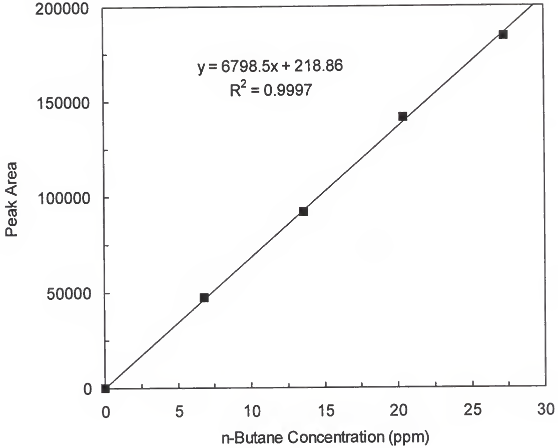

Figure A-9. GC-MS calibration curve for n-butane using a 30 m x 0.25 mm i.d. (0.25 μm film thickness) DB-5ms capillary column.

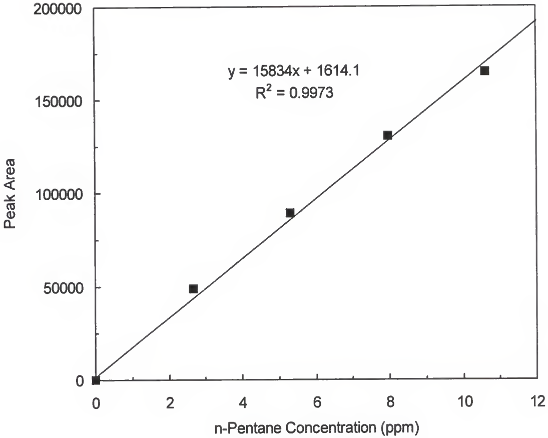

Figure A-10. GC-MS calibration curve for n-pentane using a 30 m x 0.25 mm i.d. (0.25 µm film thickness) DB-5ms capillary column.

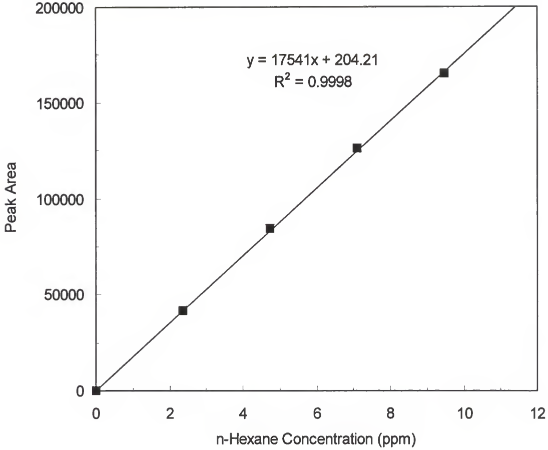

Figure A-11. GC-MS calibration curve for n-hexane using a 30 m × 0.25 mm i.d. (0.25 µm film thickness) DB-WAX capillary column.

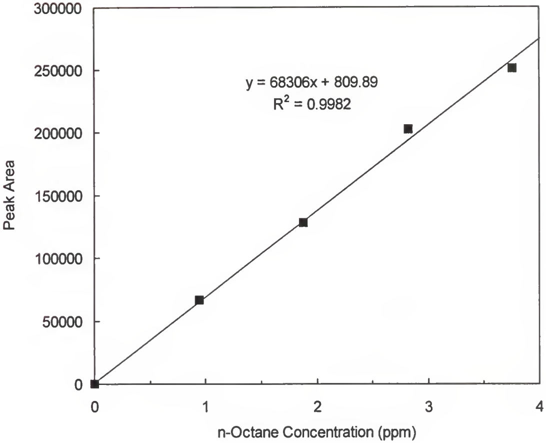

Figure A-12. GC-MS calibration curve for n-octane using a 30 m x 0.25 mm i.d. (0.25 µm film thickness) DB-5ms capillary column.

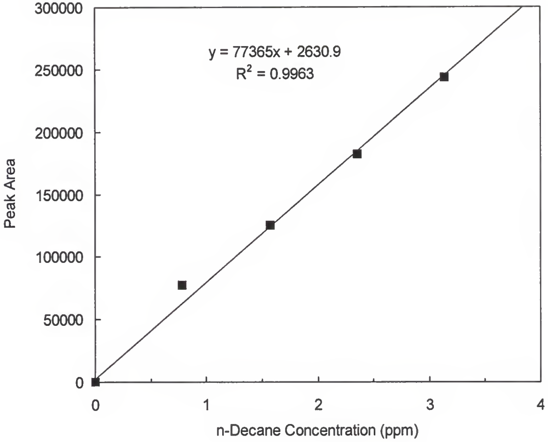

Figure A-13. GC-MS calibration curve for n-decane using a 30 m x 0.25 mm i.d. (0.25 μm film thickness) DB-5ms capillary column.

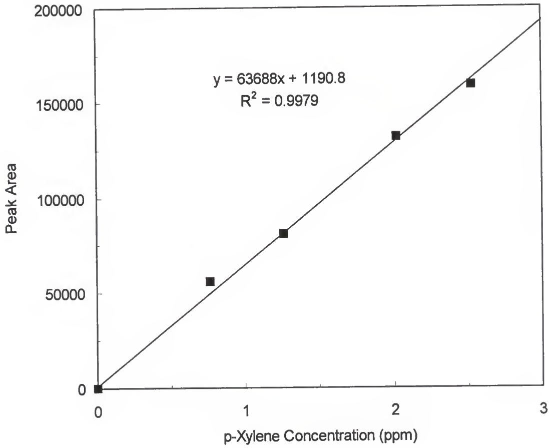

Figure A-14. GC-MS calibration curve for p-xylene using a 30 m × 0.25 mm i.d. (0.25 μm film thickness) DB-WAX capillary column.

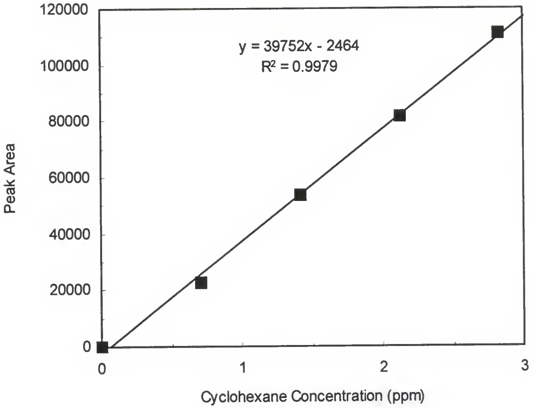

Figure A-15. GC-MS calibration curve for cyclohexane using a 30 m × 0.25 mm i.d. (0.25 μm film thickness) DB-WAX capillary column.

APPENDIX B
CHROMATOGRAMS

Typical chromatograms of the mixtures of the reactant and reference compounds employed in this doctoral research are shown in Figures B-1 to B-7. In the figures, the term TOT (Total Ion Count) and numbers in the individual frames refer to the fragment ions that were scanned in that frame. Names of the reactants corresponding to each peak are shown on the chromatograms. In addition, chromatograms after photolysis in the presence of aerosols are shown in each figure to show the peak separations between products and reactants. No significant difference in chromatograms in the absence and presence of aerosols was observed. Since product studies were not conducted in this doctoral research, the term "Product" was used to indicate the product peaks in the chromatograms.

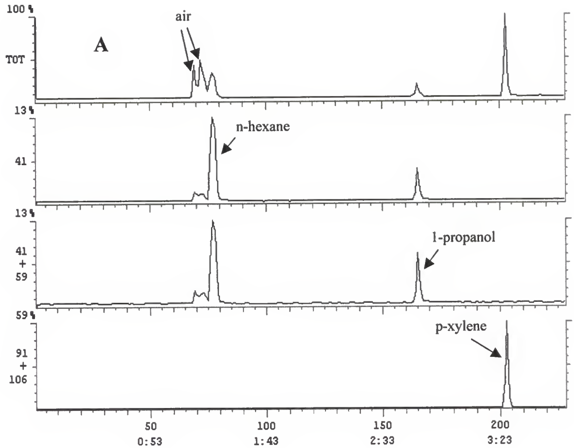

Figure B-1. Typical chromatograms of samples from a bag containing a mixture of 1-propanol / n-hexane / p-xylene / methyl nitrite: (A) before photolysis and (B) after photolysis.

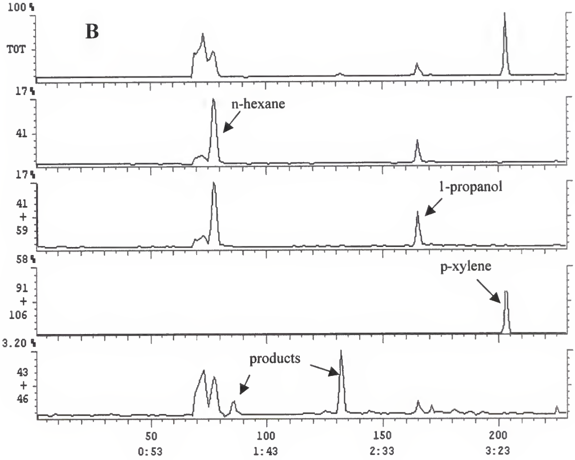

Figure B-1--continued

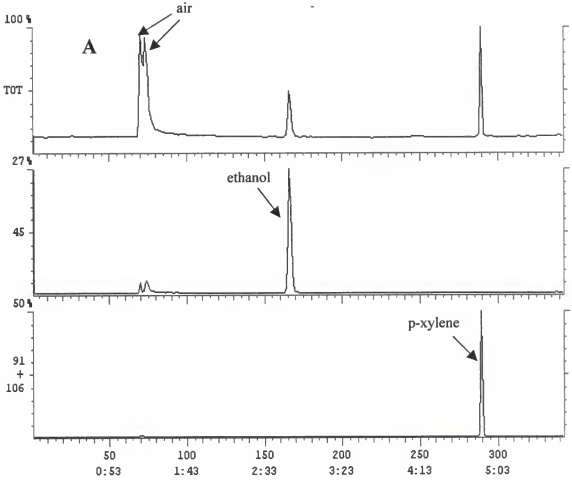

Figure B-2. Typical chromatograms of samples from a bag containing a mixture of ethanol / p-xylene / methyl nitrite: (A) before photolysis and (B) after photolysis.

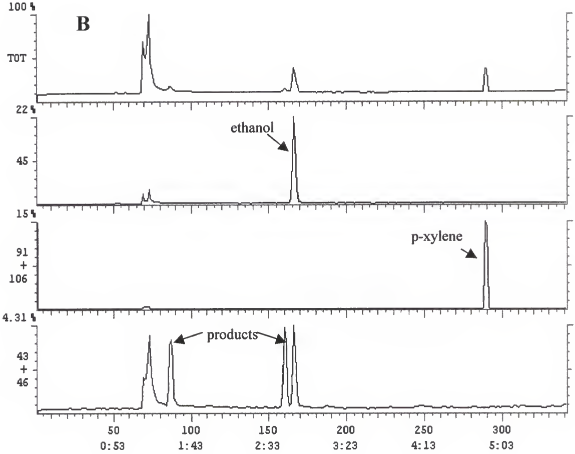

Figure B-2--continued

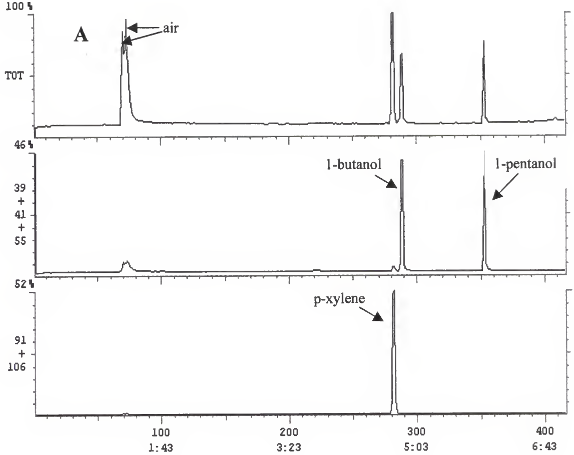

Figure B-3. Typical chromatograms of samples from a bag containing a mixture of 1-butanol / 1-pentanol / p-xylene / methyl nitrite: (A) before photolysis and (B) after photolysis.

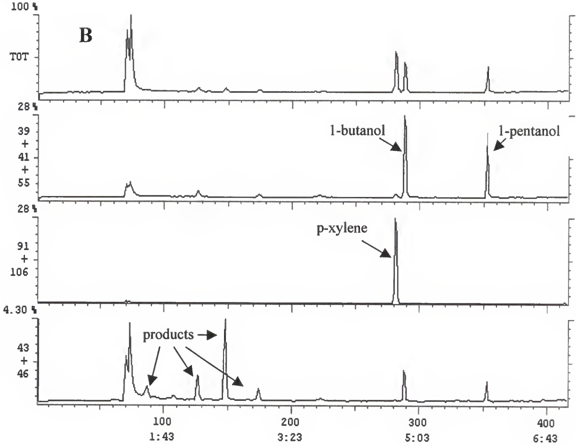

Figure B-3--continued

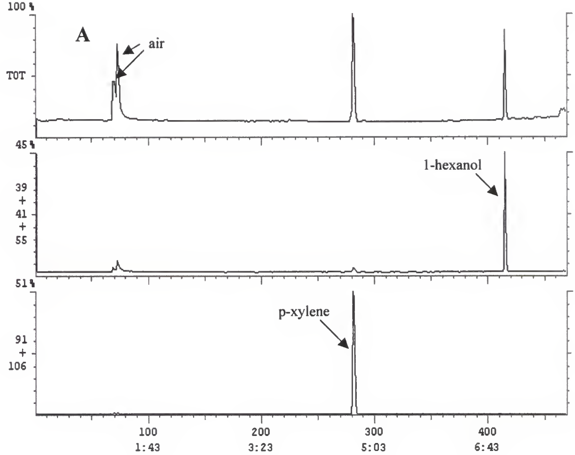

Figure B-4. Typical chromatograms of samples from a bag containing a mixture of 1-hexanol / p-xylene / methyl nitrite: (A) before photolysis and (B) after photolysis.

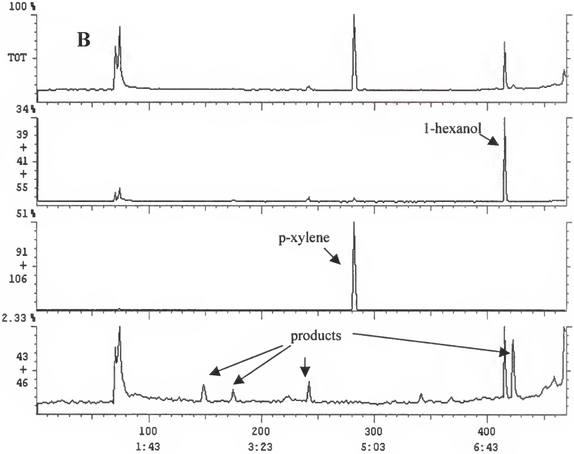

Figure B-4--continued

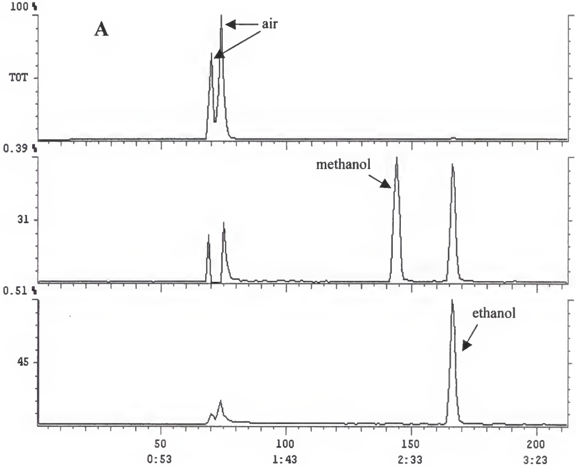

Figure B-5. Typical chromatograms of samples from a bag containing a mixture of methanol / ethanol / methyl nitrite: (A) before photolysis and (B) after photolysis.

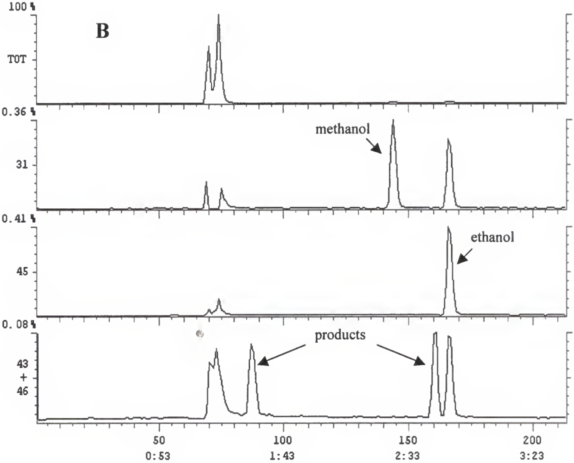

Figure B-5--continued

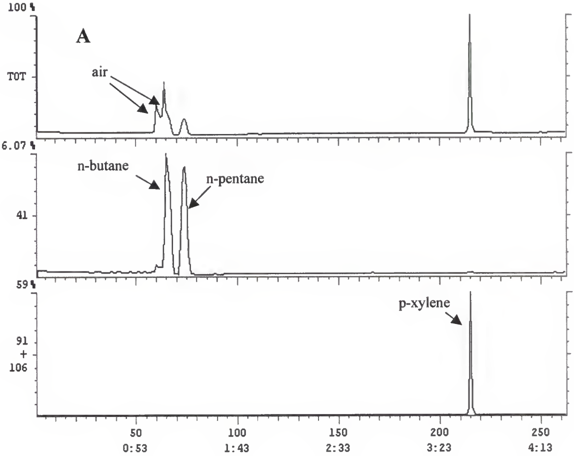

Figure B-6. Typical chromatograms of samples from a bag containing a mixture of n-butane / n-pentane / p-xylene / methyl nitrite: (A) before photolysis and (B) after photolysis.

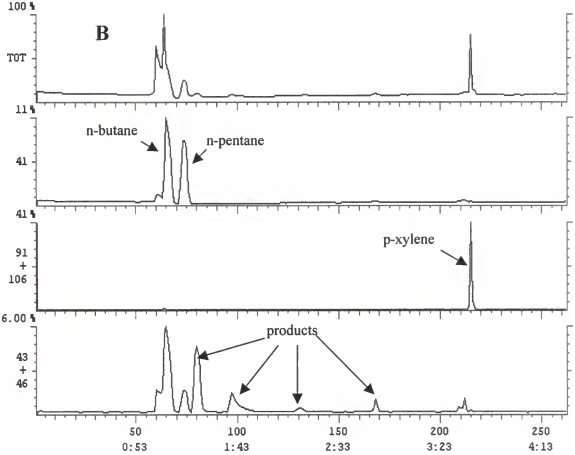

Figure B-6--continued

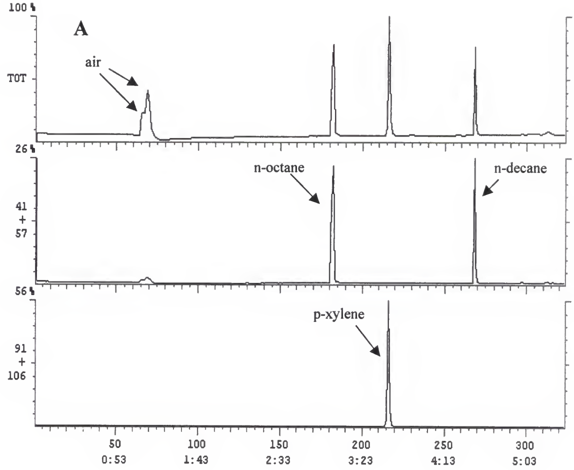

Figure B-7. Typical chromatograms of samples from a bag containing a mixture of n-octane / n-decane / p-xylene / methyl nitrite: (A) before photolysis and (B) after photolysis.

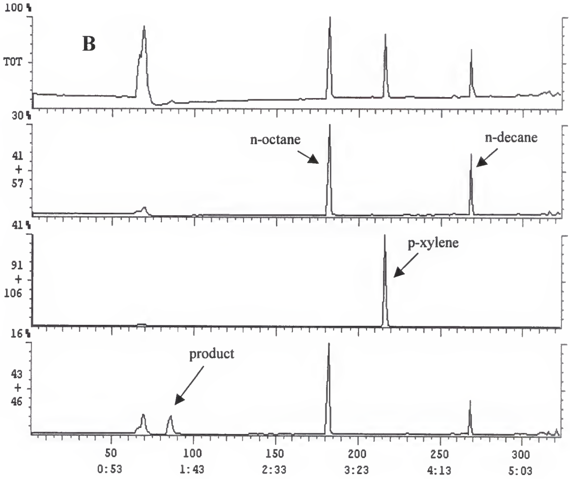

Figure B-7--continued

APPENDIX C
EXPERIMENTAL PROCEDURES

Methyl Nitrite Synthesis

Methyl nitrite was synthesized according to the method of Taylor et al. (1980) and used as a precursor of OH radicals in this doctoral research. The detailed synthesis procedure is as follows:

List of reactants

30 g of ACS grade sodium nitrite
25 mL concentrated (>95%) sulfuric acid
55 mL of de-ionized water
30 mL of ACS grade methanol
25 sodium hydroxide pellets

List of equipment

Drierite
dry ice
methanol
3-neck 250 mL Florence flask
2-neck 500 mL Florence flask
2 funnels (125 mL) with stopcocks
3 (20/40) glass adapters with celcon caps, viton o-rings
#15 o-ring / 20/40 glass adapter
2 #15 o-ring / ¼" O. D. glass adapter
1/4" – 1/4" stainless steel Swagelok union
3/8" –1/4" stainless steel Swagelok reducing union
glass impinger with stopcock and custom-made stopcock exit elbow
1/4" O.D. TFE Teflon® tubing
nitrogen (ultra high purity)
stainless steel lecture bottle with 90° elbow valve

cork stopper
Teflon®-coated magnetic stir bar
magnetic stirrer
2 beaker (250 mL)
2 glass stirs

Procedure

1. Assemble the apparatus as shown in Figure C-1. Before attaching the 125 mL funnel to the 2-neck flask, close the stopcock and fill the funnel with Drierite. Open the stopcock and allow the smaller Drierite particles and dust to fall out. Afterwards, attach the funnel to the 2-neck flask.

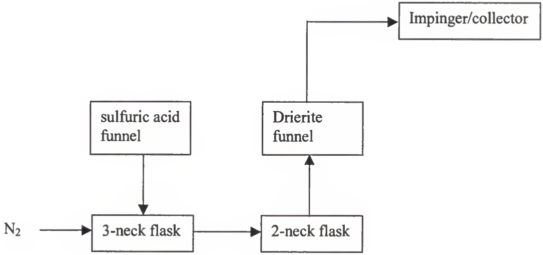

Figure C-1. Schematic of the apparatus used to synthesize methyl nitrite.

2. After making sure all valves and stopcocks in the system are open, open the nitrogen cylinder and run nitrogen through the system for at least an hour. Mix the reactants during this time.

3. Place 25 mL of de-ionized water in a beaker. Slowly add 25 mL of the concentrated sulfuric acid to obtain a 50/50 solution. Mix the solution in an ice bath to cool the contents.

4. Place 30 mL of de-ionized water in a beaker and slowly add 25 pellets of sodium hydroxide. Use a glass stirrer to mix the solution while it sits in the ice bath.

5. While leaving the nitrogen purge on, place sodium nitrite into the 3-neck flask along with a Teflon® stir bar. Add methanol and stir briskly with a magnetic stirrer so that the mixture is saturated with sodium nitrite. Reattach the 3-neck flask to the system after mixing.

6. With the stopcock closed, pour the sulfuric acid solution into the funnel above the 3-neck flask. Place the cork stopper in the funnel.

7. Pour the sodium hydroxide solution into the 2-neck flask.

8. With the nitrogen flowing, make sure the system is leak free. This is done by placing a beaker of water at the exit of the impinger/collector and ensuring that for every bubble produced in the 3-neck flask solution, there is a bubble produced in the beaker of water.

9. After the system has been purged for a few minutes, place the impinger/collector in a dewar containing a slurry of dry ice and methanol.

10. Turn off the lights and slowly open the stopcock of the sulfuric acid funnel so that a drop of sulfuric acid solution falls into the 3-neck flask every 5 seconds. Adjust the nitrogen flow accordingly so that there are not too many bubbles in the 3-neck flask. The entire reaction should take approximately 45 minutes.

11. After the sulfuric acid is gone, allow a few minutes for the last of the methyl nitrite to be captured in the impinger. Methyl nitrite should appear as a clear yellow liquid in the impinger.

12. Turn off the nitrogen flow. Close the impinger's exit and entrance stopcocks.

13. Take a stainless lecture bottle, after evacuating its contents using a pump for approximately 3 hours, and place it in a dry ice/methanol bath to allow it to cool for approximately 10 minutes.

14. Attach a Teflon® line with a glass o-ring adapter to the lecture bottle adapter using a clamp.

15. Take the impinger out of its dry ice/methanol bath and allow it to warm. Open the impinger entrance stopcock and then the lecture valve allowing the methyl nitrite to transfer into the lecture bottle.

16. Once the majority of the methyl nitrite has been transferred, close the lecture bottle valve.

Kinetic Study

The detailed procedure for the kinetic study is as follows:

1. Check the status of the GCQ system including the vacuum pressure and the air/water spectrum. The fore pressure and ion gauge pressure should be around 30 ~ 40 mTorr and 3 ~ 8×10^{-5} Torr, respectively. In the air/water spectrum, the peaks should be narrow and well resolved. Also, the heights of the peaks at m/z 18 (H_2O^+), m/z 28 (N_2^+), and m/z 32 (O_2^+) should be at least 20% of the height of the peak at m/z 19 (H_3O^+). Set up an analytical method for the GCQ system and download the method to the system.

2. Assemble the apparatus as shown in Figure 2-1.

3. Admit gaseous reactants to a Tedlar® bag by using the following procedure.

    (1) Attach the stainless steel lecture bottle containing methyl nitrite to the glass manifold system. A detailed diagram of the manifold system is shown in Figure C-2.

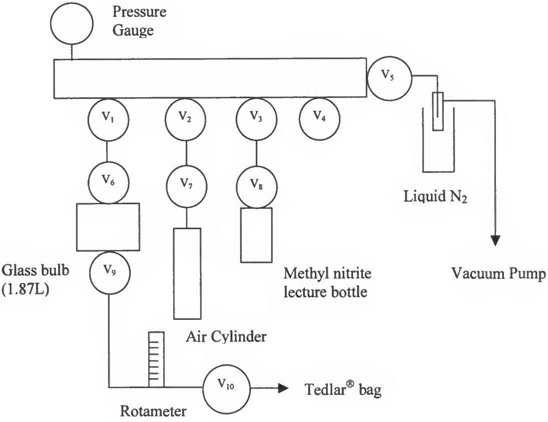

Figure C-2. Schematic diagram of the glass manifold system used to admit methyl nitrite into a Tedlar® bag. Valves are indicated by a "V" followed by a number.

(2) Evacuate the glass bulb and the transfer line of the stainless lecture bottle by using the following sequence:

- Assemble the liquid N_2 trap.
- Close valves 9, 7, 2, 8, and 4, and open valves 1, 6, and 5.
- Turn on the vacuum pump.

(3) Wait until the pressure of the system goes down as low as possible (to ~ 30 mTorr), then close valve 5. The pressure of the manifold should remain constant. An increase in the pressure is indicative of leaks in the manifold.

(4) Transfer the desired amount of methyl nitrite from the lecture bottle to the glass bulb by using the following sequence:

- Turn off the lights in the room to prevent unwanted photolysis of the methyl nitrite.
- Open valve 8 until the desired pressure is achieved. After that, close valves 8 and 6. Now the methyl nitrite is trapped in the glass bulb.
- Evacuating the manifold to remove residual methyl nitrite in the manifold by opening valve 5 until the pressure goes down to ~ 30 mTorr (or as low as possible).

(5) Transfer the methyl nitrite from the glass bulb to the bag by using the following sequence:

- Close valve 5, and open valves 7 and 2. Air will flow into the manifold. Wait until the pressure of the manifold is higher than the pressure in the glass bulb.
- Open valve 6 until the pressure of the manifold is slightly higher than atmospheric pressure (>760 Torr). Then quickly open valves 9 and 10. Now the air containing methyl nitrite will flow into the bag.
- Control valve 7 and monitor the total air volume flowing into the bag using a stopwatch and the calibrated roatmeter (see Figure A-1)
- The total air volume was 65L and 50 L for aerosol conditions I and II, respectively.
- Close valves 7 and 10, and open valve 5.

(6) During the methyl nitrite loading process, inject reactants to the stream of air flowing into the bag using a syringe.

(7) Repeat step (1) - (5) for admitting NO to the bag.

(8) Open valve 6 to pressurize the manifold. After the pressure of the manifold reaches atmospheric pressure, turn off the vacuum pump.

4. Admit aerosols to the bag by using following procedure:

(1) Control the air cylinder's regulator (30 ~ 40 psig) connected to the Collison atomizer to obtain 10 lpm of aerosol flow from the atomizer. The flow rate is measured using the calibrated orifice meter (see Figure A-2).

(2) Connect the aerosol flow outlet to the bag and admit the desired amount of aerosol to the bag (15 L of aerosol flow for aerosol condition I and 30 L of aerosol flow for aerosol condition II).

(3) Disconnect the aerosol flow to the bag, and close the air cylinder's valve.

(4) Determine aerosol size distributions in the bag using an EAA. The measuring procedure is as follows:

- Connect the sampling line to the EAA.

- Turn on the vacuum pump connected to the EAA.

- Check the following parameters:
  Aerosol flow rate: 4 lpm.
  Total flow rate: 50 lpm.
  Sheath air flow rate: 46 lpm.
  The ratio of ionizer current to ionizer voltage: 1.1 ± 0.16.

- Press the CONT. RUN button on the control box, then the EAA starts to measure particle numbers in the range of 0.001 to 1 μm.

- Record readings for each size interval.

In this doctoral research, only several representative bags were analyzed using the EAA. Proceed to step 5 without aerosol measurement for the general kinetic study.

5. Place the bag inside the wooden enclosure, and connect the sampling line to the GCQ system. Make sure a particle filter is installed in the line.

6. Measure the initial concentrations of the reactants using the GCQ via the 2 mL sampling loop by using the following procedure:

(1) Set up a GCQ sequence and start the rum from the computer.

(2) Switch the sampling valve on the gas chromatography to the CCW position. Open the toggle valve and turn on the diaphragm pump (Magnetek, Inc.) connected to the sampling loop for about 2 minutes to load the loop. The diaphragm pump will draw the sample to the loop at a flow rate of 1 lpm.

(3) Switch the sampling valve to the CW position and press the run button on the GC to start the analysis. Turn off the pump and close the toggle valve.

(4) After ending the GC run, repeat steps (1) and (3) for duplicate analyses.

(5) For a gas tight syringe injection, the injection procedure is as follows:

- Install a union tee with a septum between the particle filter and the diaphragm pump.

- Turn on the pump and wait approximately 30 seconds.

- Draw a sample using a gas-tight syringe through the septum, then turn off the pump.

- Inject the sample to the GC via the injection port.

7. After starting the second run for GC analyses, turn on the lamps to start the reactions (The reaction times for the experiments in this doctoral research varied from 1 to 10 minutes.). Turn off the lamps.

8. Repeat step 6 to measure the final concentrations of the reactants.

9. Evacuate the bag using a vacuum pump. Flush the bag at least twice by filling and evacuating the bag with zero air generated from the zero-air generator (Perma Pure Inc.).

LIST OF REFERENCES

Ammann, M., Kalberer, M., Jost, D. T., Tobler, L., Rossler, E., Piguet, D., Gaggeler, H. W., Baltensperger, U., 1998. Heterogeneous production of nitrous acid on soot in polluted air masses. *Nature* 395, 157-160.

Aschmann, S. M., Atkinson, R., 1998. Kinetics of the gas-phase reactions of the OH radical with selected glycol ethers, glycols, and alcohols. *International Journal of Chemical Kinetics* 30, 533-540.

Atkins, P. W., 1986. *Physical Chemistry*. pp 829, W. H. Freeman and Company, New York.

Atkinson, R., 1989. Kinetics and mechanisms of the gas-phase reactions of the hydroxyl radical with organic compounds. *Journal of Physical and Chemical Reference Data Monograph 1*, 1-246.

Atkinson, R., 1994. Gas-phase tropospheric chemistry of organic compounds. *Journal of Physical and Chemical Reference Data Monograph 2*, 1-216.

Atkinson, R., 1997. Gas-phase tropospheric chemistry of organic compounds: 1.Alkanes and alkenes. *Journal of Physical and Chemical Reference Data* 26, 215-290.

Atkinson, R., 2000. Atmospheric chemistry of VOCs and NOx. *Atmospheric Environment* 34, 2063-2101.

Atkinson, R., Baulch, D. L., Cox, R. A., Hampson, R. F. Jr., Kerr, J. A., Rossi, M. J., Troe, J., 1999. Evaluated kinetic and photochemical data for atmospheric chemistry, organic species: supplement VII. *Journal of Physical and Chemical Reference Data* 28, 191-393.

Atkinson, R., Carter, W. P. L., Winer, A. M., Pitts, J. N., Jr., 1981. An experimental protocol for the determination of OH radical rate constants with organics using methyl nitrite photolysis as an OH radical source. *Journal of the Air Pollution Control Association* 31, 1090-1092.

Augustine, R. L., 1996. *Heterogeneous Catalysis for the Synthetic Chemist*. Marcel Dekker, New York, NY.

Azad, K., 1999. Products of the gas-phase photooxidation reactions of 3,3-dimethylbutyraldehyde and 1-propanol with hydroxyl radicals. *Master Thesis*, University of Florida, Gainesville, FL.

Azad, K., Andino, J. M., 1999. Products of the gas-phase photooxidation reactions of 1-propanol with OH radicals. *International Journal of Chemical Kinetics* 31, 810-818.

Braun, W., Herron, J. T., Kahaner, D., 1986. *Documentation and Sample Run File for ACUCHEM/ACUPLOT a Computer Program for Modeling Complex Reaction.* National Bureau of Standards, Gaithersburg, MD.

Behnke, W., Hollander, W., Koch, W., Nolting, F., Zetzsch, C., 1988. A smog chamber for studies of the photochemical degradation of chemicals in the presence of aerosols. *Atmospheric Environment* 22, 1113-1120.

Behnke, W., Nolting, F., Zetzsch, C., 1987. A smog chamber study on the impact of aerosols on the photodegradation of chemicals in the troposphere. *Journal of Aerosol Science* 18, 65-71.

Carter, W. P. L., 1994. Development of ozone reactivity scales for volatile organic compounds. *Journal of the Air & Waste Management Association* 44, 881-899.

Corner, J., Pendlebury, E. D., 1951. The coagulation and deposition of a stirred aerosol. *Proceedings of the Physical Society of London Section B* 64, 645-654.

Crump, J. G., Seinfeld, J. H., 1981. Turbulent deposition and gravitational sedimentation of an aerosol in a vessel of arbitrary shape. *Journal of Aerosol Science* 12, 405-415.

Dean, J. A., 1992. *Lange's Handbook of Chemistry.* 14th Edition, McGraw-Hill, New York, NY.

DeMore, W. B., Sander, S. P., Golden, D. M., Hampson, R. F., Kurylo, M. J., Howard, C. J., Ravishankara, A. R., Kolb, C. E., Molina, M. J. 1997. *Chemical Kinetics and Photochemical Data for Use in Stratospheric Modeling*. JPL Publication 97-4, Jet Repulsion Laboratory, Pasadena, California.

Dodge, M. C., 2000. Chemical oxidant mechanism for air quality modeling: critical review, *Atmospheric Environment* 34, 2103-2130.

Donaldson, D. J., Anderson, D., 1999. Adsorption of atmospheric gases at the air-water interface. 2. C1-C4 alcohols, acids, and acetone. *Journal of Physical Chemistry A* 103, 871-876.

Finlayson-Pitts, B. J., Pitts, J. N. Jr., 1986. *Atmospheric Chemistry: Fundamentals and Experimental Techniques*. John Wiley & Sons, New York, NY.

Finlayson-Pitts, B. J., Pitts, Jr., J. N., 2000. *Chemistry of the Upper and Lower Atmosphere: Theory, Experiments and Applications*, pp179-248, Academic Press, San Diego.

Graedel, T. E., Hawkins, D. T., Claxton, L. D., 1986. *Atmospheric Chemical Compounds*. Academic Press, Orlando, FL.

Grosjean, E., Grosjean D., Gunawardena, R., Rasmussen, R. A., 1998. Ambient concentrations of ethanol and methyl tert-butyl ether in Porto Alegre, Brazil, March 1996-April 1997. *Environmental Science and Technology* 32, 736-742.

Guillard, C., Delprat, H., Hoang-Van, C., Pichat, P., 1993. Laboratory study of the rates and products of the phototransformations of naphthalene adsorbed on samples of titanium dioxide, ferric oxide, muscovite, and fly ash. *Journal of Atmospheric Chemistry* 16, 47-59.

Heintzenberg, J., Fine particles in the global troposphere: a review. *Tellus* 41B, 149-160, 1989.

Hemminger, J. C., 1999. Heterogeneous chemistry in the troposphere: a modern surface chemistry approach to the study of fundamental processes. *International Reviews in Physical Chemistry* 18, 387-417.

Hinds, W. C., 1982. *Aerosol Technology: Properties, Behavior, and Measurement of Airborne Particles*. John Wiley & Sons: New York.

Hughes, L. S., Cass, G. R., Gone, J., Ames, M., Olmez, I., 1998. Physical and chemical characterization of atmospheric ultrafine particles in the Los Angeles Area. *Environmental Science and Technology* 27, 1153-1161.

Inoue, Y., Sugio, S., Andzelm, J., Nakamura, N., 1998. A density functional study of the receptor-ligand interaction: stabilization energy in ammonium salt - aromatic interactions, *Journal of Physical Chemistry A* 102, 646-648.

Jacob, D. J., 2000. Heterogeneous chemistry and tropospheric ozone, *Atmospheric Environment*, 34, 2131-2159.

Kim, Y. P., Seinfeld, J. H., Saxena, P., 1993. Atmospheric gas-aerosol equilibrium I. Thermodynamic model, *Aerosol Science and Technology*, 19, 157-181.

Knipping, E. M., Lakin, M. J., Foster, K. L., Jungwirth, P., Tobias, D. J., Gerber, R.B., Dabdub, D., Finlayson-Pitts, B. J., 2000. Experiments and simulations of ion-enhanced interfacial chemistry on aqueous NaCl aerosols, *Science* 288, 301-306.

Kolb, C. E., Jayne, J. T., Worsnop, D. R., Davidovits, P., 1997. Solubility data requirements and new experimental methods in atmospheric aerosol research. *Pure and Applied Chemistry* 69, 959-968.

Kwok, E. S. C., Atkinson, R., 1995. Estimation of hydroxyl radical reaction rate constants for gas-phase organic compounds using a structure-reactivity relationship: an update. *Atmospheric Environment* 29, 1685-1695.

Li, S. N., 1999. Field and laboratory evaluation of six inhalable aerosol samplers and two impactors. *Ph. D. Thesis*, University of Florida, Gainesville, FL.

Li, S. N., Lundgren, D. A., 1997. Effect of clean air core geometry on fine particle contamination and calibration of a virtual impactor. *Aerosol Science and Technology* 27, 625-635.

Lurmann, F. W., Main, H. H., 1992. *Analysis of the Ambient VOC Data Collected in the Southern California Air Quality Study*; Final Report to the California Air Resources Board Contract A832-130, Sacramento, CA.

National Research Council 1979. *Airborne Particles*, University Park Press, Balitmore, MD.

Martin, S. T., 2000. Phase transition of aqueous atmospheric particles. *Chemical Reviews* 100, 3403-3453.

McMurry, P. H., Rader, D. J., 1985. Aerosol wall losses in electrically charged chamber. *Aerosol Science and Technology* 4, 249-268.

McMurry, P. M., Grosjean, D., 1985. Gas and aerosol wall losses in Teflon film smog chambers. *Environmental Science and Technology* 19, 1176-1182.

Neeb, P., 2000. Structure-reactivity based estimation of the rate constants for hydroxyl radical reaction with hydrocarbons. *Journal of Atmospheric Chemistry* 35, 295-315.

Nelson, L., Rattigan, O., Neavyn, R., Sidebotton, H., Treacy, J., Nielsen, O. J., 1990. Absolute and relative rate constants for the reactions of hydroxyl radicals and chlorine atoms with a series of aliphatic alcohols and ethers at 298K. *International Journal of Chemical Kinetics* 22, 1111-1126.

Odum, J. R., Jungkamp, T. P. W., Griffin, R. J., Flagan, R. C., Seinfeld, J. H., 1997. The atmospheric aerosol-forming potential of whole gasoline vapor. *Science* 276, 96-99.

Pandis, S. N., Wexler, A. S., Seinfeld, J. H., 1995. Dynamics of tropospheric aerosols. *Journal of Physical Chemistry* 99, 9646-9659.

Peters, T. M., Chein, H. M., Lundgren, D. A., Berntsen, J., 1994. Submicronmeter aerosol generator development for the U.S. environmental protection agency's human exposure laboratory. *Aerosol Science and Technology* 20, 51-61.

Seinfeld, J. H., 1988. Ozone air quality models: a critical review, *JAPCA-The International Journal of Air Pollution Control and Hazardous Waste Management* 38, 616-645.

Seinfeld, J. H., 2000. Meeting at the interface, *Science* 288, 285.

Seinfeld, J. H., Andino, J. M., Bowman, F. M., Forstner, H. J., Pandis, S., 1994. Tropospheric chemistry. *Advances in Chemical Engineering* 19, 325-407.

Seinfeld, J. H., Pandis, S. N., 1998. *Atmospheric Chemistry and Physics*. John Wiley & Sons: New York.

Shen, T. L., Wooldridge, P. J., Molina, M. J., 1995. Stratospheric pollution and ozone depletion. In: Singh, H. B. (Eds.), *Composition, Chemistry, and Climate of the Atmosphere*. Van Nostrand Reinhold, New York, NY, pp394-442.

Snider, J. R., Dawson, G. A., 1985. Tropospheric light alcohols, carbonyls, and acetonitrile-Concentrations in Southwestern United States and Henry law data. *Journal of Geophysical Research-Atmosphere* 90D, 3797-3805.

Staudinger, J., Roberts, P. V., 1996. A critical review of Henry's law constants for environmental applications. *Critical Reviews in Environmental Science and Technology* 26, 205-297.

Taylor, W. D., Allston, T.D., Moscato, M. J, Fazekas, G. B., Kozlowski, R., Takacs, G. A., 1980. Atmospheric photodissociation lifetimes for nitromethane, methylnitrite, and menthyl nitrate. *International Journal of Chemical Kinetics* 12, 231-240.

Wallington, T. J., Dagaut, P., Liu, R., Kurylo, M. J., 1988. Rate constants for the gas-phase reactions of OH with C5 through C7 aliphatic alcohols and ethers - predicted and experimental values. *International Journal of Chemical Kinetics* 20, 541-547.

Wallington, T. J., Kurylo, M., J., 1987. The gas-phase reactions of hydroxyl radicals with a series of aliphatic alcohols over the temperature range 240-440K. *International Journal of Chemical Kinetics* 19, 1015-1023.

Wang, S. C., Paulson, S. E., Grosjean, D., Flagan, R. C., Seinfeld, J. H., 1992. Aerosol formation and growth in atmospheric organic/NOx systems-I. Outdoor smog chamber studies of C_7- and C_8- hydrocarbons. *Atmospheric Environment* 26A, 403-420.

Warneck, P, Mirabel, P., Salmon, G. A., van Eldik, R., Vinckier, C., Wannowius, K. J., Zetzsch, C., 1996. Review of the activities and achievements of the EUROTRAC subproject HALIPP. In: Warneck, P. (Eds.), *Heterogeneous and Liquid Phase Processes*. Springer, Berlin, pp56-71.

Willeke, K., Whitby, K. T., 1975. Atmospheric aerosols: size distribution interpretation. *Journal of the Air Pollution Control Association* 25, 529-534.

Yaws, C. L., Yang, H. C., 1992. In: Yaws, C. L. (Eds.), *Thermodynamic and Physical Data*. Gulf Publishing Company: Houston, pp181-206.

BIOGRAPHICAL SKETCH

Se Won Oh is originally from Seoul, Korea. He received a B.S. degree in chemical technology from Seoul National University in February 1990. He continued his study in the same department and received a M.S. degree in February 1992. For his master's thesis, he studied the use of oxide sensors for the detection of toxic gases, and the result was published in Sensors and Actuators in 1993. From 1992 to 1997, he worked for Kolon Engineering Inc., a leading company in environmental business in Korea. During this period he was involved with projects dealing with municipal waste incineration, advanced water treatment, and physical coal cleaning for SO_2 emission control. He entered the University of Florida in September 1997 to pursue a Ph. D. degree in Environmental Engineering Sciences.

Se Won Oh received the Axel Hendrickson Scholarship Award for 1999 from the Florida Section of the Air & Waste Management Association. Currently he lives with his wife and daughter in Gainesville, Florida.

I certify that I have read this study and that in my opinion it conforms to acceptable standards of scholarly presentation and is fully adequate, in scope and quality, as a dissertation for the degree of Doctor of Philosophy.

Jean M. Andino, Chairperson
Assistant Professor of Environmental
Engineering Sciences

I certify that I have read this study and that in my opinion it conforms to acceptable standards of scholarly presentation and is fully adequate, in scope and quality, as a dissertation for the degree of Doctor of Philosophy.

Dale A Lundgren

Dale A. Lundgren
Professor Emeritus of Environmental
Engineering Sciences

I certify that I have read this study and that in my opinion it conforms to acceptable standards of scholarly presentation and is fully adequate, in scope and quality, as a dissertation for the degree of Doctor of Philosophy.

Brij M. Moudgil

Brij M. Moudgil
Professor of Materials Science and
Engineering

I certify that I have read this study and that in my opinion it conforms to acceptable standards of scholarly presentation and is fully adequate, in scope and quality, as a dissertation for the degree of Doctor of Philosophy.

Chang-Yu Wu

Chang-Yu Wu
Assistant Professor of Environmental
Engineering Sciences

I certify that I have read this study and that in my opinion it conforms to acceptable standards of scholarly presentation and is fully adequate, in scope and quality, as a dissertation for the degree of Doctor of Philosophy.

Matthew M. Booth
Assistant in Environmental Engineering
Sciences

This dissertation was submitted to the Graduate Faculty of the College of Engineering and to the Graduate School and was accepted as partial fulfillment of the requirements for the degree of Doctor of Philosophy.

May 2001

M. Jack Ohanian
Dean, College of Engineering

Winfred M. Phillips
Dean, Graduate School